

*Control what we can,  
Manage what we cannot.*

**University of Alberta**

**Mechanical Properties of Hexadecane-Water Interfaces  
with Adsorbed Hydrophobic Bacteria**

by

Zhewen Kang

A thesis submitted to the Faculty of Graduate Studies and Research  
in partial fulfillment of the requirements for the degree of

Doctor of Philosophy

in

Chemical Engineering

Department of Chemical & Materials Engineering

©Zhewen Kang

Fall 2009

Edmonton, Alberta

Permission is hereby granted to the University of Alberta Libraries to reproduce single copies of this thesis and to lend or sell such copies for private, scholarly or scientific research purposes only. Where the thesis is converted to, or otherwise made available in digital form, the University of Alberta will advise potential users of the thesis of these terms.

The author reserves all other publication and other rights in association with the copyright in the thesis and, except as herein before provided, neither the thesis nor any substantial portion thereof may be printed or otherwise reproduced in any material form whatsoever without the author's prior written permission.

## **Examining Committee**

Murray R. Gray, Department of Chemical and Mataterials Engineering

Anthony A. Yeung, Department of Chemical and Mataterials Engineering

Julia Foght, Department of Biological Sciences

Qi Liu, Department of Chemical and Mataterials Engineering

James J. Feng, Department of Chemical and Biological Engineering

*For dad and mom*

## Abstract

Certain strains of hydrophobic bacteria are known to play critical roles in petroleum-related applications. The aim of this study was to investigate how hydrophobic bacteria in their stationary phase could adsorb onto the hexadecane-water interface and alter its mechanical properties. The two strains of bacteria used in forming the interfacial films were *Acinetobacter venetianus* RAG-1 (a Gram-negative bacterium) and *Rhodococcus erythropolis* 20S-E1-c (Gram-positive). Experiments at two different length scales (millimetre and micrometre) were conducted and the results were compared. In addition, a simple flow experiment was designed in a constricted channel and the results were related to the intrinsic mechanical properties of bacteria-adsorbed films.

On the millimetre scale, using the pendant drop technique, the film interfacial tension was monitored as the surface area was made to undergo changes. Under static conditions, both types of bacteria showed no significant effect on the interfacial tension. When subjected to transient excitations, the two bacterial films exhibited qualitatively similar, yet quantitative distinct rheological properties (including film elasticities and relaxation times). Under continuous reduction of surface area, the RAG-1 system showed a “paper-like” interface, while the interface of the 20S-E1-c system was “soap film-like.” These macroscopic observations could be explained by the surface ultrastructures of the two cell strains.

On the micrometre scale, using the micropipette technique, colloidal stability of the bacteria-coated oil droplets was examined through direct-contact

experiments. Both types of bacteria were seen to function as effective stabilizers. In addition, the adsorbed bacteria also interacted with one another at the interface, giving rise to higher order 2-D rheological properties. A technique of directly probing the mechanical properties of the emulsion drop surfaces revealed that (a) the films behaved as purely elastic sheets, and (b) with a reduction in cell concentration in the aqueous phase, less oil was emulsified, but the elastic moduli of the adsorbed films remained unchanged. These results are in contrast to the above millimetre-scale study. Therefore the rheological properties of these bacteria-adsorbed films appear to be length scale-dependent.

An oil displacement experiment was designed to investigate the flow behaviour of micron-scale emulsion drops in a constricted channel. The qualitative results can be correlated with the interfacial rheological properties and may have valuable relevance to the study of multiphase flow through constricted channels in porous rocks (e.g. in MEOR operations).

## ACKNOWLEDGEMENTS

There are many people to whom I owe gratitude for making this dissertation what it is today and, more importantly, making me what I am today. Most of all, it is lucky to me that Dr. Murray R. Gray and Dr. Anthony A. Yeung have accepted the responsibility of being my supervisors over the entire course of my graduate study. I am always grateful for their suggestion and guidance for my research program, as well as their warm-hearted encouragement, unbelievable understanding and endless support in these years. Dr. Gray is not only my supervisor, but also my role model. I have learned so much from him on how to be a successful person, in both career and life. I am also able to say that Tony remains one of my best friends in U of A. It has taken much patience and understanding in their part to see me through to the end, although the road has been rough all times.

I really appreciate Dr. Julia Foght for her very helpful suggestions in the biological experiments and her kindness to allow me to use the equipment in the lab. She opened a door to the beautiful microbiological world, which I really enjoy. Great thanks to my other committee members, Dr. Qi Liu and Dr. James J. Feng, who gave me a lot more thoughtful ideas and valuable suggestions to this project.

I would like to express my gratitude to Dr. William McCaffery. He gave me another opportunity and enrolled me in this department after I changed my mind and determined to come to Edmonton. The offer letter signed by Dr.

McCaffery has changed my whole life and provided me with chances to meet so many great people here in U of A.

Great appreciation goes to my husband, Yangang, for his love, support, patience, and everything. Through all the ups and downs, he always stands by my side. I even couldn't complete this degree without him.

I owe my parents for their encouragement and support over the past years. My dad didn't live to today to see my accomplishments, but I am sure he is proud of me.

Special thanks to my friends Loredana, Tuyet, Andrée, Zhenhui, Jihua, Payman, and Yissella, for their great help in courses, experiments and life.

I am proud to finally completed graduate school. The most valuable lessons I have learned here weren't taught to me only by professors. All the people I have named and many, many others I have not mentioned have educated me. Because of them, I will leave here with a truer understanding of the universe than I had ever expected to have. More important than any title or degree are these people with whom I share my life.

# TABLE OF CONTENTS

<b>CHAPTER 1 INTRODUCTION.....</b>	<b>1</b>
1.1 Background.....	1
1.2 Research Approach and Thesis Overview .....	3
<b>CHAPTER 2 LITERATURE REVIEW.....</b>	<b>9</b>
2.1 Bacterial Role in Petroleum-related Processes .....	9
2.1.1 Microbial enhanced oil recovery (MEOR) .....	10
2.1.2 Bioremediation of hydrocarbon-contaminated soil .....	15
2.2 Mechanisms of Mass Transfer .....	19
2.2.1 Direct contact between microorganisms and hydrocarbons .....	20
2.2.2 Formation of emulsions .....	20
2.2.3 Bacterial cell surface properties.....	25
2.3 General Theory of Emulsion.....	34
2.3.1 Type of emulsion and emulsifier .....	35
2.3.2 Stability of emulsion .....	39
2.3.3 Characterization of emulsions.....	49
2.4 General Theory of Interfacial Rheology .....	59
2.4.1 Basic concepts of interfacial rheology.....	60
2.4.2 Previous studies in interfacial rheology of adsorbed molecules at oil/water interfaces.....	68
<b>CHAPTER 3 EXPERIMENTAL APPROACH.....</b>	<b>78</b>
3.1 Microbiological Methods.....	78
3.1.1 Chemicals.....	78
3.1.2 Bacterial strains.....	78
3.1.3 Growth condition .....	79
3.1.4 Growth measurements .....	80
3.1.5 Bacterial staining .....	82
3.2 Physical Methods .....	82
3.2.1 Surface and interfacial tension measurements by Wilhelmy plate .....	82

3.2.2 Pendant drop technique.....	83
3.2.3 Transmission Electron Microscopy (TEM) test.....	83
3.2.4 Emulsion preparation.....	84
3.2.5 Microscope and micropipette technique.....	85

## **CHAPTER 4 INTERFACIAL RHEOLOGY ON THE MILLIMETRE**

### **SCALE: PENDANT DROP TECHNIQUE..... 90**

4.1 Introduction.....	90
4.2 Materials and Methods.....	91
4.2.1 Sample preparation.....	91
4.2.2 Control experiments.....	91
4.2.3 The pendant drop apparatus calibration.....	92
4.2.4 Interfacial tension measurements.....	93
4.3 Results and Discussion.....	95
4.3.1 Results for control experiments.....	95
4.3.2 Results for cell-free interfaces.....	98
4.3.3 Equilibrium tension for interfaces adsorbed with bacterial cells.....	101
4.3.4 Two types of bacterial films and their relation to cell surface properties.....	104
4.3.5 Interfacial rheology revealed by step up/down of area excitations.....	109
4.4 Conclusions.....	121

## **CHAPTER 5 INTERFACIAL RHEOLOGY AT MICROMETRE SCALE:**

### **MICROPIPETTE TECHNIQUE..... 123**

5.1 Introduction.....	123
5.2 Theory.....	125
5.2.1 Capillary instability and the measurement of IFT.....	125
5.2.2 Surface elasticity and the elimination of capillary instability.....	129
5.3 Materials and Methods.....	130
5.3.1 Sample preparation.....	130
5.3.2 Micropipette experiments setup.....	131
5.4 Results and Discussion.....	137
5.4.1 Bacterial films at interfaces.....	137

5.4.2 Behaviour of emulsion drops .....	140
5.4.3 Crumpling test and stability against coalescence.....	143
5.4.4 Elimination of capillary instability with bacteria adsorbed at the interface.....	148
5.4.5 Determination of micron-scale dilational elasticity.....	149
5.4.6 Relation between elastic moduli and cell concentration in buffer .....	156
5.4.7 Geometric analysis of bacterial cells at the interface in emulsion system.....	161
5.5 Conclusions.....	167
<b>CHAPTER 6 PRELIMINARY STUDY ON EMULSION FLOW THROUGH A CONSTRICTED CHANNEL .....</b>	<b>169</b>
6.1 Introduction.....	169
6.2 Materials and Methods.....	170
6.2.1 Sample preparation .....	170
6.2.2 Micropipette experiments setup.....	170
6.3 Preliminary Results .....	171
6.4 Conclusions.....	176
<b>CHAPTER 7 SUMMARY AND RECOMMENDATIONS.....</b>	<b>178</b>
7.1 Summary of contributions.....	178
7.2 Recommendations for future work .....	181
<b>BIBLIOGRAPHY .....</b>	<b>183</b>
<b>APPENDIX A .....</b>	<b>213</b>
<b>APPENDIX B .....</b>	<b>214</b>
<b>APPENDIX C .....</b>	<b>215</b>
<b>APPENDIX D .....</b>	<b>217</b>

## LIST OF TABLES

<b>Table 2.1:</b> Tensides and HLB values .....	52
<b>Table 4.1:</b> Measured IFTs and their literature values.....	93
<b>Table 5.1:</b> Verification of the Geometric Model in the Emulsion System.....	165

## LIST OF FIGURES

<b>Figure 2.1:</b> MEOR involves injection of a solution of microorganisms and nutrients into the reservoirs. ....	15
<b>Figure 2.2:</b> Schematic, generalized representation of a (a) Gram-positive and (b) Gram-negative bacterial cell wall structure.....	33
<b>Figure 2.3:</b> Contact angle of sessile drop on bacterial lawn. ....	33
<b>Figure 2.4:</b> Some surfactant structures.....	39
<b>Figure 2.5:</b> Mechanisms in stabilization of emulsions.....	41
<b>Figure 2.6:</b> A drawing showing how the Gibbs-Marangoni effect can inhibit coalescence by slowing film drainage. ....	45
<b>Figure 2.7:</b> Sketch of processes occurring in an unstable o/w emulsion. ....	48
<b>Figure 2.8:</b> Upper sketches: Position of a small spherical particle at a planar fluid-water interface for a contact angle (measured through the aqueous phase) less than 90° (left), equal to 90° (centre) and greater than 90° (right). Lower sketches: Corresponding positioning of particles at a curved fluid-water interface.....	58
<b>Figure 2.9:</b> The pendant drop geometry.....	63
<b>Figure 2.10:</b> Schematic diagram of the two modes of surface deformation. ....	67
<b>Figure 3.1:</b> A schematic of the Wilhelmy plate apparatus. ....	87
<b>Figure 3.2:</b> Photograph (a) and sketch (b) of the pendant drop apparatus for a water drop suspended in <i>n</i> -hexadecane.....	88
<b>Figure 3.3:</b> Photograph (a) and sketch (b) of the micropipette apparatus for an experiment with oil-in-water emulsions .....	89
<b>Figure 4.1:</b> Photograph of an actual water drop in the pendant drop experiment.....	95
<b>Figure 4.2:</b> Results for control tests. (a) Interfacial tensions (IFTs) between RAG-1 cell-free spent buffer and <i>n</i> -Hexadecane. (b) Interfacial tension between cell-free spent buffer (from RAG-1 suspension) and hexadecane after suspension was agitated in hexadecane for 4 hours.....	97

<b>Figure 4.3:</b> Pendant drop results for interfacial tension (solid line) vs. area (dash line) for cell-free interfaces for cell-free interfaces with (a) static area, (b) step-up area and (c) step-down area.....	101
<b>Figure 4.4:</b> Evolution of the interfacial tension (solid line) as the drop surface area (dash line) was held fixed. The interface was adsorbed with <i>A. venetianus</i> RAG-1 cells (cell concentration in bulk: $2 \times 10^9$ CFU/mL).....	104
<b>Figure 4.5:</b> Bacterial films were formed at the surfaces of the two water drops in n-hexadecane (the needle has a diameter of 0.916 mm). (a) <i>A. venetianus</i> RAG-1 at $2 \times 10^9$ CFU/mL, (b) <i>R. erythropolis</i> 20S-E1-c at $10^9$ CFU/mL .....	107
<b>Figure 4.6:</b> TEM images of negatively stained (a) <i>A. venetianus</i> RAG-1, and (b) <i>R. erythropolis</i> 20S-E1-c. ....	108
<b>Figure 4.7:</b> Responses of interfacial tension to step-strain deformations for interfaces adsorbed with <i>A. venetianus</i> RAG-1 (cell concentration: $2 \times 10^9$ CFU/mL). (a) IFT (solid line) in response to. step-up area (dashed line); (b) IFT (solid line) in response to step-down area (dashed line).....	111
<b>Figure 4.8:</b> Responses of interfacial tension to step-strain deformations for interfaces adsorbed with <i>R. erythropolis</i> 20S-E1-c (cell concentration: $10^9$ CFU/mL). (a) IFT (solid line) in response to step-up area (dashed line); (b) IFT (solid line) in response to step-down area (dashed line).....	112
<b>Figure 4.9:</b> Effect of area perturbation on the interfacial tension for interfaces adsorbed with bacterial cells (cell concentration for <i>A. venetianus</i> RAG-1: $2 \times 10^9$ CFU/mL; for <i>R. erythropolis</i> 20S-E1-c: $10^9$ CFU/mL). (a) Step-up excitations; (b) step-down excitations. ....	114
<b>Figure 4.10:</b> Effect of area perturbation on the relaxation time for interfaces adsorbed with bacterial cells (cell concentration for <i>A. venetianus</i> RAG-1: $2 \times 10^9$ CFU/mL; for <i>R. erythropolis</i> 20S-E1-c: $10^9$ CFU/mL). ....	116
<b>Figure 4.11:</b> Effect of area perturbation and cell concentration on the interfacial tension for surfaces adsorbed with <i>A. venetianus</i> RAG-1 .....	118
<b>Figure 4.12:</b> Effect of area perturbation and cell concentration on the interfacial tension for surfaces adsorbed with <i>R. erythropolis</i> 20S-E1-c.....	119

<b>Figure 4.13:</b> Effect of cell concentration on “apparent elasticity” $E$ of interfaces adsorbed with (a) <i>A. venetianus</i> RAG-1 and (b) <i>R. erythropolis</i> 20S-E1-c. The lowest cell concentration was $5 \times 10^6$ CFU/mL in both plots. ....	120
<b>Figure 5.1:</b> (a) Schematic of a liquid drop being held at the tip of a suction pipette. (b) The suction pressure, as defined in Fig. 5.1a, is plotted as a function of the projection length; the drop surface is characterized by a constant interfacial tension. (c) Same situation as in Fig. 5.1b, but with the drop surface characterized by an interfacial tension and a dilational elasticity. ....	129
<b>Figure 5.2:</b> (a) Micropipette with closed end; (b) sketch of pipette puller setup; (c) truncated micropipette; (d) sketch of the pipette truncating. ....	136
<b>Figure 5.3:</b> A liquid drop held at the tip of a micropipette by suction pressure; the oil-water interface was “clean” (i.e. free of surfactants and adsorbed materials).....	136
<b>Figure 5.4:</b> Oil/water interface adsorbed with <i>A. venetianus</i> RAG-1 .....	139
<b>Figure 5.5:</b> Oil/water interface adsorbed with <i>R. erythropolis</i> 20S-E1-c.. .....	140
<b>Figure 5.6:</b> Observation of oil-in-water emulsion drops using optical microscopy.....	143
<b>Figure 5.7:</b> Deflating an emulsion droplet using micropipette. ....	147
<b>Figure 5.8:</b> Studying colloidal stability through direct-contact experiment .....	148
<b>Figure 5.9:</b> Micropipette deformation of an oil droplet coated with <i>A. venetianus</i> RAG-1 bacteria.....	149
<b>Figure 5.10:</b> Raw data of pipette suction (i.e. applied force) vs. droplet projection into pipette (i.e. resulting deformation). ....	154
<b>Figure 5.11:</b> Fitting theoretical calculations to experimental data taken from Fig. 5.10.....	156
<b>Figure 5.12:</b> Raw data of pipette suction (applied force) vs. droplet projection into pipette (resulting deformation). . ....	159
<b>Figure 5.13:</b> Fitting theoretical calculations to experimental data taken from Fig. 5.12. ....	161
<b>Figure 5.14:</b> A sketch of the emulsion system.....	164
<b>Figure 6.1:</b> The actual experimental system. ....	173

**Figure 6.2:** Behavior of oil drop coated with *A. venetianus* RAG-1 in an “oil displacement” experiment through a constricted channel. .... 174

**Figure 6.3:** Behavior of oil drop coated with *R. erythropolis* 20S-E1-c in an “oil displacement” experiment through a constricted channel. .... 175

# CHAPTER 1 INTRODUCTION

## 1.1 Background

The field of biotechnology in the petroleum industry encompasses: biorefining for the removal of sulphur, nitrogen and metals; upgrading of heavy oils and asphaltenes by bioreactors and biocatalysts; hydrocarbon degradation by whole-cell bioprocesses; and application of biosurfactants and bioemulsifiers in crude oil production and microbially-enhanced oil recovery (MEOR). The potential scope of microorganisms (usually belonging to the basic categories of bacteria and fungi) in MEOR and bioremediation processes can be defined to include all activities which make the hydrocarbon easier to produce and transport, as well as the chemical changes which increase the value of the oil. In MEOR, injection of properly-chosen bacterial strains into oil reservoirs can have the potential to alter the compositions of heavy oils to enable easier pumping and/or selectively plug high-permeability zones to improve sweep efficiency (Khire and Kham, 1994; Yen, 1990). In bioremediation, the bacteria can function as hydrocarbon-degrading agents as they consume the oil contaminants and transform them through enzymatic reactions (Langwaldt and Puhakka, 2000; Holliger *et al.*, 1997; Atlas, 1995). These activities could therefore be applied to *in situ* treatment, production, transportation, and processing of crude oils.

For these processes to be effective, the issue of mass transfer must first be addressed: because the bacteria are invariably cultured and suspended in aqueous media, their contact with liquid hydrocarbon can only occur at the oil/water

interface. To maximize this contact area (and hence improve mass transfer), many bacteria have the ability to emulsify oil/water mixtures, creating either oil-in-water or water-in-oil emulsions (Atlas, 1991; Atlas, 1995). In the literature, formation of such emulsions during bacterial growth on hydrocarbons is often attributed to extracellular compounds—such as biosurfactants and bioemulsifiers which are released from bacteria with the enzymatic breakdown of hydrocarbons (Zosim, 1982; Sar and Rosenberg, 1983; Cooper and Goldenberg, 1987; Bredholt *et al.*, 2002; Lin, 1996). However, experimental results show that certain intact bacterial cells are also able to attach themselves onto the oil/water interfaces as soft colloidal particles (Dorobantu *et al.*, 2004). In such cases, it had been demonstrated that the intact bacterial cells were able to stabilize emulsions without changing the interfacial tension; the assembly of such cells at the interface resulted in a “surface skin” which resisted coalescence of emulsified oil droplets. As such, in addition to the ability to digest oils, an effective strain of bacteria for MEOR applications must also have the capability of altering the *physics* (i.e. mechanical properties) of oil/water interfaces.

In the literature, the molecular surfactants released from bacteria have been studied extensively, including their biosynthetic pathways, chemical structures, and the effects on hydrocarbon uptake by the microorganisms. It has been known that the released biosurfactants are able to alter the interfacial tension between oil and water; however, no evidence has shown that they can also modify *high order* interfacial mechanical properties. These higher-order properties — which include surface viscosities and elasticities — can be strongly influenced by

the interactions between adsorbed bacterial cells which behave as colloidal particles. From an engineering perspective, these mechanical properties are known to be critical to multiphase flows which occur commonly in oil recovery and bioremediation applications. Unfortunately, the basic physics which underlies these operations have not been studied in petroleum research. Therefore, this project is motivated by this very significant industrial problem. For these operations to be optimized in future applications, it is necessary to establish a scientific knowledge base related to the technology. The mechanical properties of cell-coated oil droplets are important components of such a knowledge base. The mechanisms through which bacteria affect interfacial material properties are crucial for understanding the role of bacteria in petroleum production processes which involve large specific oil/water interfacial areas (such as multiphase flows in porous media).

## **1.2 Research Approach and Thesis Overview**

This research project was based on two hypotheses. First, intact bacterial cells that attach onto the oil/water interface cannot change the interfacial tension, but would alter the *higher order* interfacial rheological properties; second, these higher order interfacial properties could be length scale-dependant (i.e. the interfacial mechanical properties may be different on the millimetre and micrometre scales).

The overall goal of this study was to investigate the mechanical properties of the bacterial films formed at oil/water interfaces on the millimetre and

micrometre scales. Here, we will focus only on the effects that resting bacteria (i.e. those that are neither dividing nor secreting biosurfactants and, as such, behave effectively as inanimate colloidal particles) have on oil/water interfacial properties — in the absence of molecular surfactants. In order to understand the properties of different interfacial films, two bacterial strains with different surface properties were selected in this study; these are *Acinetobacter venetianus* RAG-1 and *Rhodococcus erythropolis* 20S-E1-c. These bacterial strains represent two major groups of bacteria: Gram-negative and Gram-positive, which were originally classified on the basis of their cell wall compositions. Gram-negative bacteria (represented in this study by *Acinetobacter venetianus* RAG-1) have structurally and chemically complex cell walls: the outer layer is an asymmetric membrane with amphipathic lipopolysaccharides comprising the outer leaflet. In addition, *A. venetianus* RAG-1 bacteria can synthesize proteinaceous fimbriae (pili) that extend beyond the cell wall. Gram-positive bacteria (represented in this study by *Rhodococcus erythropolis* 20S-E1-c) have less complex cell walls comprising primarily of peptidoglycan and teichoic acids, and lacking fimbriae. *R. erythropolis* 20S-E1-c is a member of the “acid-fast” Gram-positive bacteria that have mycolic acids (comprised of long chain fatty acids) external to the peptidoglycan layer that confer a hydrophobic nature to the cell surface (Dworkin *et al.*, 2006).

In this project, the bacterial cells were repeatedly washed and re-suspended in phosphate buffer to remove the growth medium and halt cell division. Bacterial cells in such a state behaved in essence as stable colloidal

particles over a period of hours or days, and their surface structures and properties were characterized by various physical analyses (presented in Chapter 3). Due to the hydrophobicity of the cell surfaces, the bacteria were able to attach onto the oil/water interfaces and, through self-assembly, formed a “surface skin” which inhibited droplet coalescence; this is much like the phenomenon of emulsion stabilization by solid particles. Since the objective of this study is to investigate the effects of *intact, non-growing* bacterial cells on the oil-water interface, we carefully selected a specific time window of cell exposure to *n*-hexadecane for conducting the experiments, during which it was determined that any modification of interfacial mechanical properties would be due entirely to the intact cells (behaving effectively as inanimate particles) and not to any surface active compounds released from the bacteria. On the millimetre and micrometre scales, mechanical properties of the adsorbed interface were quantified using the techniques of dynamic pendant drop and micropipettes. These intrinsic material properties can then be related to the cell surface ultrastructures (the makeup and conformation of the individual cell) to derive insights into the physics of colloids-adsorbed interfaces, which is crucial in understanding the bacteria-involved two phase flow properties in porous medium. This work was comprised of three phases, with specific objectives as follows:

1. To understand the mechanical properties of interfacial bacterial films on the *millimetre scale* using the dynamic pendant drop technique, and to identify the relation between macroscopic film properties and single cell

surface ultrastructures. The following approach was taken (presented in Chapter 4):

- a. Develop appropriate control experiments with Wilhelmy plate and equilibrium IFT measurements with pendant drop to identify an accurate time window during which the cells would not release extracellular compounds and, as a result, any modification of interfacial mechanical property would be due entirely to the intact cells.
  - b. Show two types of bacterial film at the interface and their relation to cell surface ultrastructures.
  - c. Check whether bacterial cells would affect the equilibrium oil/water interfacial tension (at fixed interfacial area).
  - d. Check whether bacterial cells would affect the higher order surface properties (such as surface elasticity and resistance to in-plan shearing) in response to step area excitations.
  - e. Show whether the cell concentration in the aqueous phase would affect interfacial rheological properties.
  - f. Show how different types of bacterial films could affect the higher order surface rheology (in response to continuous ramping of interfacial area).
2. To explore the behaviour of individual emulsion drops *in situ* and to quantify their mechanical properties on the micrometre scale using the micropipette technique, and to relate these microscopic observations to the

single cell surface ultrastructures, and to show whether these mechanical properties were length scale-dependent by comparing the micrometre-scale and millimetre-scale results. The investigations included (presented in Chapter 5):

- a. Reveal bacterial films at the oil/water interface and the behaviour of bacteria-coated emulsion drops.
  - b. Test the stability of such films against coalescence using two bacteria-coated emulsion drops.
  - c. Demonstrate the existence of added surface elasticity and the elimination of capillary instability by the bacterial films; determine the value of the micron-scale surface elasticity and interfacial tension *in situ* by matching experimental results to theoretical predictions.
  - d. Check whether the concentration of bacteria in the aqueous phase would affect the surface properties of emulsion drops.
  - e. Verify the geometric model in the emulsion system.
3. To investigate the behaviour of emulsion flow in porous medium of the micrometre scale using micropipette as the model device, which would simulate the oil displacement process from porous rocks. The specific approach was the following (presented in Chapter 6):
- a. Attempt the oil displacement experiment in a model constricted channel in which the surface of a hexadecane droplet is adsorbed with bacterial cells and the pipette has deliberately manipulated

surface properties, and correlate these observations to the mechanical properties of bacterial film at interfaces.

## CHAPTER 2 LITERATURE REVIEW

### 2.1 Bacterial Role in Petroleum-related Processes

The history of biotechnology dates back perhaps thousands of years in time. However, it was not until after 1684, when Antoni van Leeuwenhoek first observed microorganisms in a primitive microscope, that biotechnology truly developed and had been seen in various areas of application. From 1863, when Louis Pasteur discovered how to vaccinate against diseases using heat-inactivated organisms, to recent years when the sequence of the human genome was completed, biotechnology is continuously expanding and will play an increasingly important role in future industrial processes. Petroleum biotechnology, which is the focus of this investigation, is a very young and exciting part of such industrial possibilities.

It is well established that petroleum reservoirs contain active and diverse populations of microorganisms (usually belonging to the basic categories of bacteria and fungi). Microbial growth within oil reservoirs has traditionally been associated with biofouling and souring. Furthermore, the potentials for microbial enhanced oil recovery (MEOR) have been investigated for decades and achieved progress in many field tests (Yen, 1990; Khire and Kham, 1994). The technique of bioremediation had been developed in which microorganisms were introduced for curing hydrocarbon contaminations in soil (Langwaldt and Puhakka, 2000; Holliger, *et al.*, 1997; Atlas, 1991). In these processes, the microbes, like all living organisms, consume carbon and nutrients (e.g. nitrogen, phosphorous and

trace metals) as sustenance. In addition, the MEOR and bioremediation processes share another common trait: they both deal with interactions between microorganisms and hydrocarbon at the 1–10  $\mu\text{m}$  scale, which is the typical size of the porous rocks or soil. These bioprocesses have become promising alternatives to conventional methods of remediation due to the fact that they are safer, less costly and more efficient (Atlas and Cerniglia, 1995). We will give a brief review of the studies on using microbes to facilitate oil recovery and the removal of oil spills on land.

### **2.1.1 Microbial enhanced oil recovery (MEOR)**

Conventional oil recovery occurs in three stages: primary, secondary and tertiary. Their processes are described as follows (Sharma and Pandey, 1986; Han *et al.*, 1999; Mahinpey *et al.*, 2007):

1. Primary recovery: It uses the natural pressures of reservoirs which exists within the formation and recovers up to 50% (but typically only 20%) of the original oil in place.
2. Secondary recovery: It involves adding energy to the natural system by injecting water to maintain pressure and displace oil (i.e. waterflood). Typical recoveries are 25-45% oil in place (average 32%) after the primary recovery.
3. Tertiary recovery: This includes all other methods involving chemical or thermal energy. Chemical flooding uses alkaline water flooding, carbon dioxide flooding, and polymer flooding. Thermal recovery includes *in situ*

combustion and the injection of steam. Typical recoveries are 5-20% of the oil in place (average 13%) after primary and secondary recoveries.

The total oil recovered from conventional operations is, in most cases, less than 50% of the oil in place. The hydrocarbon that remains is held firmly within the interstices of the porous rocks by capillary forces, existing as oil “ganglia” (i.e. globules) which are surrounded by water left from the secondary and tertiary recovery phases. At this stage, the configuration of the trapped oil is characterized by very large ratios of interfacial area to hydrocarbon volume; the mobilization of the oil ganglia is controlled predominantly by capillary and interfacial phenomena. Microbial enhanced oil recovery (MEOR), which has been included in the tertiary oil recovery method, can modify the oil/water interfacial properties through introduction of select strains of bacteria into the reservoirs and hence may lead to increased oil production (Janshekar, 1983; Yen, 1990). In MEOR, natural reservoir microorganisms or specially selected bacterial strains, along with appropriate nutrients (to support bacterial growth and for the production of metabolic products), are injected into the porous formation to release the trapped oil (Figure 2.1). In this process, the release of trapped oil within the rocks is believed to be the result of metabolites produced *in situ* by bacterial fermentations, which can be quite complex and involve multiple biochemical processes (Bryant and Burchfield, 1989).

The concept of MEOR was first proposed in 1926 by Beckmann, who suggested that bacterial metabolites could assist in the release and transport of oil in geological structures (Beckman, 1926). Later, people presented a process for

secondary oil recovery *in situ* using an anaerobic, sulphate-reducing bacterial strain called *Desulfovibrio* and even used other types of bacteria to enhance oil recovery in laboratory tests (Cookson, 1994). From then on, researchers had isolated a variety of specific microorganisms which could exist at elevated temperatures and pressures found in many hydrocarbon reservoirs. These important types of microorganisms include (Khire and Kham, 1994): *Pseudomonas* sp., *Rhodococcus* sp., *Bacillus lichiniformis* JF-2, *Bacillus substilis*, *Clostridiuml Thermoaceticum*, *Clostridium Acetobutylicum*, *Desulfovibrio*, *Acinetobacter calcoaceticus*, *Leuconostoc* sp., *Desulfotomaculum*, *Methanohalophilus* sp., and *Thermotoga* sp. In the late 1970s, due to high oil prices and the prospect of declining reserves, great interest in MEOR methods had arisen. Numerous MEOR investigations had been undertaken — from laboratory investigations, coupled with theoretical studies, to field projects throughout the world; many of these studies had led to positive results (Jenneman *et al.*, 1984; Bryant and Burchfield, 1989; Lazar and Donaldson, 1991; Desouky *et al.*, 1995; McInerney *et al.*, 1999).

Despite many successes in the laboratory studies and field trials, MEOR remains a process that is largely empirical. Some possible mechanisms have been proposed, each of which could act individually or in concert with each other:

1. **Splitting heavy fractions.** The two major benefits of splitting heavy hydrocarbons *in situ* are the reduction of oil viscosity, thereby improving flow rate and transportability, and the conversion of crude hydrocarbons

into lower molecular weight products which are lighter and potentially more valuable (Bryant and Burchfield, 1989).

2. **Generation of gases.** Both aerobic and anaerobic microorganisms are capable of producing gases, typically carbon dioxide and methane, and in some cases even nitrogen. The produced gases can enhance oil recovery by lowering oil viscosity (as gas dissolves in oil) and by repressurizing depleted reservoirs (Moses and Springham, 1982).
3. **Production of chemicals.** Both aerobic and anaerobic microorganisms are also capable of producing a broad array of chemical products including surfactants (leading to increased mobilization of residual oil), polymers (improve oil recovery by providing mobility control in high permeability zones), organic acids (improve oil production rates by breaking down carbonates, in essence “acidizing” the formation), and alcohols (Banat, 1995).
4. **Other mechanisms.** In addition to the conventional forms of MEOR, it has been suggested that microorganisms could also plug high permeability zones and lead to a redirection of the flood water in selective plugging processes (Raiders and Knapp, 1989). Another mechanism in MEOR is to biosynthesize surfactants, polymers, and/or hydrocarbon-splitting enzymes under controlled conditions in the ground “bio-reactors” and later to inject these end products, rather than the microorganisms, into the reservoir (Raiders and Knapp, 1989).

The future development of MEOR technologies requires a multidisciplinary effort with researchers in geology, chemistry, microbiology, fluid mechanics, petroleum engineering, environmental engineering, and chemical engineering. Indeed, there has not been a full understanding of the mechanisms behind MEOR processes (Yen, 1990). For example, it has been observed that many microbes could lower the oil-water interfacial tension (IFT) and facilitate liberation of the oil ganglia from the narrow pores through release of biosurfactants with significant surface activities from the cells during their growth phase (Pines *et al.*, 1983; Li *et al.*, 2004). On the other hand, the presence of biosurfactants cannot account for high-permeability zone-plugging phenomena in the reservoirs (thus avoiding “shunting” pressure-driven flows that are intended for oil displacement; Khire and Kham, 1994). Indeed, the reduction of IFT by biosurfactants would have the opposite effect of enhancing multiphase flow through porous media. There is, however, another way in which bacterial cells can modify interfacial properties: provided the cell surfaces are hydrophobic (as is often the case in MEOR applications), the microbes will attach strongly to the oil-water interface, behaving in essence as colloidal particles (Rosenberg and Rosenberg, 1985; Dorobantu *et al.*, 2004) which “rigidify” the oil/water interface. To isolate this phenomenon and understand its role in MEOR, it requires engineering research of microorganisms which focuses on the interactions between these “microbial particles” with one another at the interface, the resulting higher order rheological properties developed at the adsorbed layer, and its relevance to zone-plugging in porous structures.

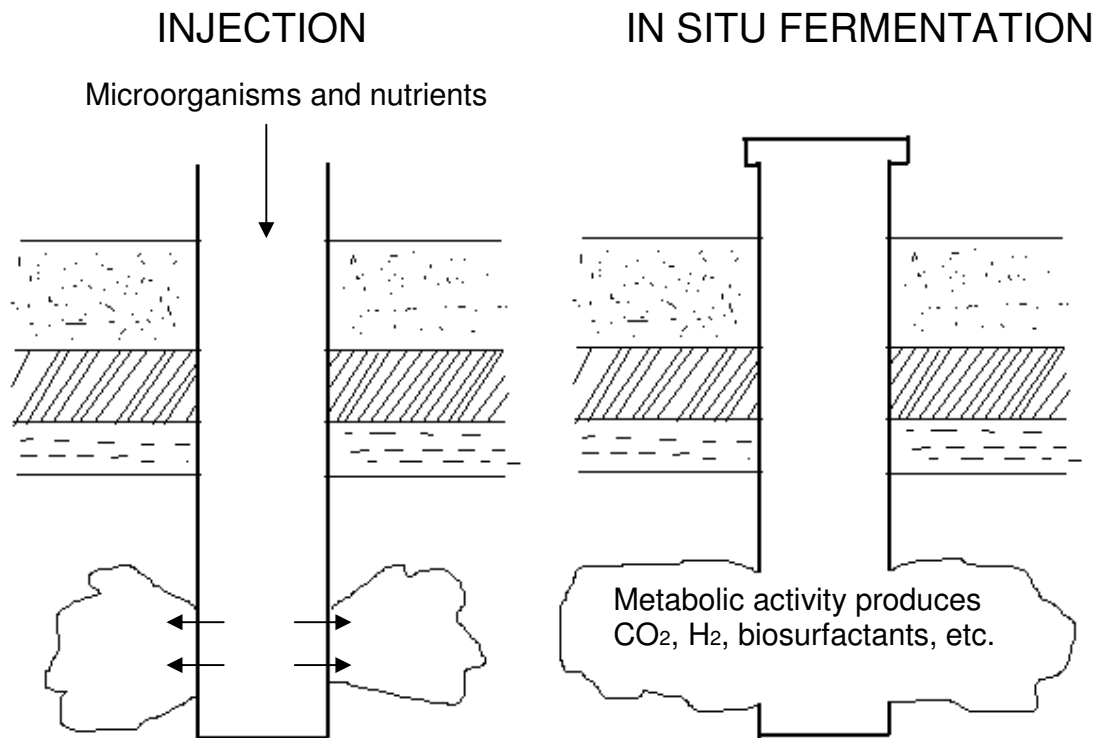


**Figure 2.1:** MEOR involves injection of a solution of microorganisms and nutrients into the reservoirs. The injection well is then shut in for an incubation period, allowing the microorganisms to produce the metabolites that facilitate the release of trapped oil.

### 2.1.2 Bioremediation of hydrocarbon-contaminated soil

In the past decades, hydrocarbon contamination of soil has become a major environmental problem due to the ever-growing demand of oil and the lack of knowledge on safe chemical disposal. The sources of pollution can be due to natural seeps, spills in oil exploration and production sites, sludge and other oily effluents from refinery, spills associated with transportation, condensation from exhausts of gasoline and diesel engines, and runoff from roads and fuelling areas (Atlas and Unterman, 1999). The pollution contains a complex mixture of

different hydrocarbon classes, including alkanes, aliphatic and aromatic compounds, and heteroatomic species. The other components present in contamination are sulfur, nitrogen, oxygen, trace amounts of iron, silicon, and aluminum. The toxicity of crude and refined oil to the environment, and even more importantly to humans, is well-documented (Boesch *et al.*, 1987). It has been proved indisputably that oil pollution presents a serious problem to natural resources and public health.

The conventional remediation approach includes physical and chemical techniques. *In situ* methods include washing with detergent, extraction of topsoil using vacuum/steam/ hot air stripping, and soil solidification (binding hydrocarbon to soil). *Ex situ* methods include excavating the contaminated soil and subjecting it to chemical oxidation, solvent extraction, and adsorption (Doble and Kumar, 2005). Although these conventional cleanup technologies have prevented the contamination problem from spreading, in most cases, they are incapable of restoring water to meet health-based standards in a reasonable time frame and they may transfer contaminants to other sites. In addition, these conventional methods are slow and costly, and tend to create new waste which are often more harmful than the initial substrate. The limitations of conventional technologies have spurred investigations into alternative clean up methods such as bioremediation, which can treat oil pollutants on-site and are much cheaper compared to some chemicals used in conventional technologies.

Biodegradation of the different oil components is well known for many bacterial strains (Atlas and Unterman, 1999; Van Hamme *et al.*, 2003). The most

important mechanism in bioremediation is that microorganisms (mainly bacteria) can be used to destroy hazardous contaminants or transform them into less harmful forms (e.g. CO<sub>2</sub> and biomass). During this process, the microorganisms generate energy and nutrients to generate more cells (Gibson, 1984). Many laboratory studies have been conducted to determine the metabolic pathways for aerobic degradation of these hydrocarbons (the general case for *in situ* bioremediation of hydrocarbon-contaminated soil). Different hydrocarbon classes are metabolized with different microorganism species. The *n*-alkanes are readily degraded by several microorganisms, including *Acinetobacter* sp., *Actinomycetes*, *Arthrobacter*, *Bacillus* sp., *Candida* sp., *Micrococcus* sp., *Planococcus*, *Pseudomonas* sp., and *Streptomyces* (Surzhko, 1995). Branching alkanes are more resistant to biodegradation (Pirnik, 1977) while cycloalkanes are more refractory (Perry, 1977). An *Acinetobacter* sp. isolated from soil was able to mineralize long-chain *n*-paraffins (C<sub>16-36</sub> chain) (Koma *et al.*, 2001). Monoaromatics like benzene, toluene, and xylenes (BTEX) are known to be oxidatively degraded by *Pseudomonas* sp., *Ralstonia* sp., *Rhodococcus* sp., and *Sphingomonas* sp. (Lee and Lee, 2001). Toluene aerobically degrades more rapidly than other BTEX compounds with a wide variety of strains, such as *Pseudomonas putida* mt-2, *P. mendocina*, and *R. picketti* PKO1, and the products could be cresols and benzyl alcohol. Polyaromatics (PAHs) persist in soil and sediment because of their low water solubility and high stability (due to the presence of multiple fused aromatic rings); they can be degraded under a narrow range of conditions, but less readily as the number of condensed aromatic rings

increases. *Burkholderia cepacia* F297 degrades a variety of polycyclic aromatic compounds, including fluorene, methylnaphthalene, phenanthrene, anthracene, and dibenzothiophene (Harayama, 1997). Several microorganisms also have been reported to degrade PAHs, and they include *Rhodococcus* sp., *Alteromonas* sp., *Arthrobacter*, *Bacillus*, *Mycobacterium* sp., *Pseudomonas* sp., and *Phanaerochaete chrysosporium* (Barclay *et al.*, 1995). Other microorganisms, including bacteria and fungi, that are specific for a substrate are described in several reviews (Juhasz and Naidu, 2000; Van Hammer *et al.*, 2003).

The first *in situ* bioremediation system was installed in 1973 to cleanup an oil pipeline spill in Pennsylvania. Since then, bioremediation has become well accepted as an alternative means of cleaning up easily degraded petroleum products on large scales (Atlas and Unterman, 1999). A recent successful project had shown that intrinsic bioremediation achieved a 95% reduction in hydrocarbon concentration within 150 days after the San Jacinto River flood and oil spill in southeast Texas (Mills *et al.*, 2003). Although the technologies for *in situ* bioremediation have been developing rapidly, the manner in which the microbes interact with the oil still requires much study. For example, in the bioremediation process, immiscibility between hydrocarbon and water causes the liquids to separate and form a two-phase system. However, consumption of hydrocarbon by the water-borne microbes poses the challenge of maximizing contact between the two immiscible liquids so that the bacteria can have access to nutrients at the oil/water interface; this leads naturally to the emulsification of one liquid in the other. This suggests that the major problem to be overcome by microorganisms in

degradation is to increase the mass transfer from the hydrocarbon to the cells (Rosenberg *et al.*, 1998).

## **2.2 Mechanisms of Mass Transfer**

A major requirement for effective MEOR or bioremediation is the actual contact of the microorganisms with hydrocarbon substrates. Cell metabolism, which utilizes the hydrocarbons as energy sources, requires the transport of those hydrocarbons to the cells as a first step. If the substrate is water-soluble, it can maintain constant contact with cells. However, since all hydrocarbons in the oil industries are water-immiscible, there should be some means by which those hydrocarbons are transported to the microorganisms to achieve direct contact. Therefore, an effective hydrocarbon-degrading microorganism must have the ability to uptake the water-immiscible hydrocarbons across the cell envelope (Atlas and Cerniglia, 1995).

Studies have been performed on the two possible mechanisms through which hydrocarbons are transported into cells: direct contact of those microorganisms with drops/surfaces of the insoluble oil phase without emulsification, and the formation of either oil-in-water or water-in-oil emulsions which can maximize the interfacial area between insoluble oil and bacterial cells (Beal and Betts, 2000). In the latter mechanism, emulsions can be created either by the release of extracellular compounds from the cells (i.e. biosurfactants or bioemulsifiers) or by certain intact cells (Dorobantu *et al.*, 2004). It has also been noted that different microorganisms may apply either or both mechanism. For

example, it was reported that both mechanisms involved in the growth of *Rhodococcus erythropolis* S+14He on *n*-hexadecane, *n*-octadecane or the branched alkane pristane, and on mixtures of hydrocarbons (Kim *et al.*, 2002).

### **2.2.1 Direct contact between microorganisms and hydrocarbons**

Since the suggestion by Johnson (1964) that bacterial cells were able to grow on high chain liquid *n*-alkanes when they directly contacted the liquid alkane, considerable studies have been conducted to support the hypothesis that direct contact between microbes and hydrocarbons is one of the main mechanisms by which microorganisms interact with hydrocarbons (Neufeld *et al.*, 1983; Bouchez-Naitali *et al.*, 2001). Being one of those hydrophobic microorganisms, the species of *Acinetobacter* sp. has been most carefully studied. Using phase contrast microscopy, it has been observed that exponentially growing cells of *Acinetobacter* sp. are capable of attaching onto the surfaces of alkane drops which are much larger than the cells, and the uptake of hydrocarbon by the cells takes place through diffusion or active transport at contact (Rosenberg *et al.*, 1980).

### **2.2.2 Formation of emulsions**

#### **2.2.2.1 Emulsions created by biosurfactants and bioemulsifiers**

It has long been noted that microbial growth on hydrocarbons is often accompanied by the release of surface active agents (including both biosurfactants and bioemulsifiers), which can lead to the emulsification of the hydrocarbons, rather than by the direct contact of microbial cells and substrate (Rosenberg,

1993). Biosurfactants and bioemulsifiers, which are so named because of their biological source, possess the general properties of surfactants and emulsifiers (a review of general emulsion theory will be given in the next section). The main chemical classes of these compounds are glycolipids, polysaccharide-lipid complexes, lipopeptides, phospholipids, fatty acids and neutral lipids (Zajic and Supplisson, 1972). These surface active agents can be extracellular or cell-associated, and the most commonly isolated extracellular surface active compounds are glycolipids.

Although no studies have been made to determine the ecological distribution of organisms which produce biosurfactants and bioemulsifiers, it still can be assumed that they are rather ubiquitous in the environment since they have been isolated from a variety of sources. Hydrocarbon contaminated materials (including oil polluted soil and water) have yielded many microorganism which produce surface active agents; it has revealed a positive correlation between the existence of biosurfactants/bioemulsifiers and the presence of hydrocarbons (Rapp *et al.*, 1979; Hommel, 1990). For example, *Corynebacterium* sp.PPS11, producer of a biosurfactant, was isolated from sewage sludge enriched with hydrocarbons (Panchal and Zajic, 1978). Another biosurfactant producing strain, *B. licheniformis*, was obtained from an oilfield injection water sample (Jenneman *et al.*, 1983). *A. calcoceticus* RAG-1, which produces a bioemulsifier called emulsan, was isolated from a mixed culture on a marine beach (Reisfeld *et al.*, 1972). However, it has also been demonstrated that a hydrocarbon substrate is not always required for the production of biosurfactants or bioemulsifiers.

Researchers have reported several examples of surface active glycolipids produced on glucose (Cooper *et al.*, 1982; Mulligan *et al.*, 1984). *A. calcoeticus* RAG-1 produces emulsan with a variety of carbon sources including crude oil, pure aliphatic hydrocarbons, alcohols, organic acids, triglycerides, and other alkyl esters (Rosenberg, 1982). The production of biosurfactants by *B. subtilis* is actually inhibited by the presence of hydrocarbons, although hydrocarbons do not affect the growth of the microorganism.

It has also been proposed that surface active compounds function to suspend the hydrocarbon droplets formed, and then make the substrate more accessible to the microorganisms (Gutnick and Rosenberg, 1977). For example, it was suggested that extracellular lipid compounds may facilitate alkane uptake (Finnerty, 1977). Other investigators have noted that the presence of surface active agents markedly stimulate the growth of the organisms on the substrates (Floodgate, 1978). These observations suggest that production of biosurfactants and bioemulsifiers may be related to the presence of hydrocarbons.

The biosurfactant is primarily carbohydrate (e.g. glycolipids) and belongs therefore to the low molecular weight compound (Ron and Rosenberg, 2002). The glycolipids consist of a hydrophilic and a hydrophobic tail, which can facilitate the partition of biosurfactants at the interface between the two fluid phases of different degrees of polarity (e.g. oil/water interface). Therefore, the formation of a molecular film at the interface can reduce the surface and interfacial tension of the fermentation broth. One of the best studied biosurfactants is produced by strains of *Pseudomonas aeruginosa*. Rsan-ver, a

strain of *Pseudomonas aeruginosa*, produces the active compounds identified as rhamnolipids, which reduce the surface and interfacial tension of the medium to 29 and 0.25 dyn/cm, respectively (Guerra-Santos *et al.*, 1984). It was also demonstrated that *P. aeruginosa* P-20 produces a peptidoglycolipid biosurfactant (Koronelli *et al.*, 1983). Another study found that *Pseudomonas* PG 1 produces a peptidoglycolipid which demonstrated hydrocarbon emulsifying and solubilizing properties (Reddy *et al.*, 1983). The emulsifying capability of a glycolipid produced by *Pseudomonas* sp. MUB was also investigated (Wagner *et al.*, 1983).

Bioemulsifiers are high molecular weight products which are composed of proteins, polysaccharides, lipoproteins, lipopolysaccharides or complex mixture of these biopolymers (Ron and Rosenberg, 2002). The best studied bioemulsifier is an extracellular lipopolysaccharide complex called emulsan which is produced by *A. calcoeticus* RAG-1 (Rosenberg and Ron, 1998). Although it has no surfactant properties, it is able to bind very tightly onto droplets of hydrocarbons and strongly stabilize emulsions. Another important bioemulsifier was isolated from *A. calcoeticus* BD413 (Kaplan and Rosenberg, 1982). This lipid-polysaccharide complex has a slightly different chemical composition with emulsan, although the precise composition of either bioemulsifier has not been determined. This bioemulsifier has similar emulsifying capability, but different emulsion hydrocarbon substrate specificity, than emulsan. After testing several strains, Sar and Rosenberg (1983) suggested that production of extracellular emulsifying agent is a general characteristic of this species.

Some strains, such as *A. calcoceticus* 2CA2, cannot produce an extracellular bioemulsifier, but rather had only cell-associated surface activity. It can also reduce surface and interfacial tension and produce an extracellular lipopeptide with good de-emulsifying properties (Neufeld *et al.*, 1983; Neufeld and Zajic, 1984). A strain of *Nocardia amarae* also has shown de-emulsifying capability as well as surfactant activity (Akit *et al.*, 1981), with both of these properties being cell-associated (Cairns *et al.*, 1982; Gray *et al.*, 1984).

Bacteria are not the only microorganisms which can produce biosurfactants and bioemulsifiers. Other classes of microorganisms may also produce surface active compounds through the enzymatic reactions with hydrocarbons. For example, the yeast, *Candida petrophilum*, produced an emulsifying factor composed of protein and lipid (Iguchi *et al.*, 1969) and ten strains of *Candida lipolytica* demonstrated emulsification properties (Illarionova *et al.*, 1984). Roy *et al.* (1979) characterized the active compound produced by *Endomycopsis lipolytica* as being either a peptidolipid or a lipopeptide. A carbohydrate emulsifier was recovered from *C. lipolytica* (Cirigliano and Carman, 1984). Another yeast, *Torulopsis bombicola*, produces a sophorolipid which demonstrates surfactant activity; a potent protein-containing bioemulsifier as well as a glycolipid surfactant were also isolated (Inoue and Ito, 1982; Cooper and Paddock, 1983; Cooper and Paddock, 1984).

In short, biosurfactants and bioemulsifiers can help disperse the oil into droplets as an emulsion, so that the interfacial area between the oil and water is increased or the apparent solubility of the oil in the aqueous phase is increased

(Rosenberg, 1993; Cooper, 1986). As such, hydrocarbon bioavailability to the microorganism is greatly enhanced.

#### **2.2.2.2 Emulsions created by intact bacterial cells**

While numerous reports have shown that microbial cells can produce extracellular surface active agents during growth, emulsifying capabilities of the intact bacterial cells is not a well-documented phenomenon (Cooper *et al.*, 1982; Neufeld and Zajic, 1984; Allen *et al.*, 1992; Dorobantu, *et al.*, 2004). It has been reported that *A. venetianus* sp. 2CA2 was able to emulsify and stabilize kerosene-water mixtures; this ability was not related to the lowering of interfacial tensions (Neufeld and Zajic, 1984). Recently, Dorobantu *et al.* (2004) also reported that certain intact “resting” bacteria of *Acinetobacter venetianus* RAG-1 and *Rhodococcus erythropolis* 20S-E1-c were capable of stabilizing hexadecane-in-water emulsions without significantly altering the interfacial tension. They also pointed out that the mechanism responsible for emulsion stabilization was steric hindrance to coalescence, which is analogous to the adsorption of insoluble particles such as colloidal silica at the oil/water interface.

#### **2.2.3 Bacterial cell surface properties**

Bacterial cell surfaces are in direct contact with the external environment. Understanding the behaviour of cells at interfaces (e.g. adhesion and aggregation) requires determination of the structure, chemical composition and physicochemical properties of the cell surfaces. Cell surface ultrastructure can be

characterized by transmission electron microscopy, combined with freeze-fracture and surface replica. Cell surface and cell wall chemical composition can be estimated by x-ray photoelectron spectroscopy and Fourier transform infrared spectroscopy, respectively (Stoddart and Brack, 2006). Microbial cell surface hydrophobicity and electrical properties contribute to the cell's interactions with hydrocarbons; they can be assessed using Bacterial Adhesion to Hydrocarbon (BATH) test (refer to Section 2.2.3.2), contact angle and electrophoretic mobility techniques, respectively.

#### **2.2.3.1 Bacterial surface structures**

Bacterial surface structures are crucial in conducting mass transfer process between cells and the surrounding environment. The bacterial surface does not have homogeneous compositions. Instead, it consists of a range of heterogeneous molecules with different functions. These materials include the cell wall, the composition of which varies considerably in Gram-positive and Gram-negative bacteria (Wicken, 1985; Hancock, 1991). The structures external to the cell wall include extracellular polymeric substances or S-layers, fimbriae or conjugative pili, fibrils, and flagella, which play a mediating role as surfaces approach one another and in the bacterial adhesion processes. The combination of these structures determines the characteristic physicochemical properties of any particular bacterial strain. Such surface characteristics are not fixed; they vary considerably with changes in the external environment and growth phase (Stoddart and Brack, 2006).

### ***The Bacterial Cell Wall***

As shown in Figure 2.2a, and described by Madigan *et al.* (2000), the cell wall of Gram-positive bacteria consists of a thick, rigid layer of peptidoglycan on top of a phospholipid-rich cytoplasmic membrane. The peptidoglycan layer, which can constitute as much as 90% of the cell wall, provides considerable mechanical strength to the cell. Peptidoglycan is composed of two sugar derivatives, N-acetylglucosamine and N-acetylmuramic acid, as well as a small group of amino acids that are connected to form a repeating structure, the glycan tetrapeptide. Other polymers located in the cell wall include the highly antigenic teichoic acids (linear polymers of glycerol phosphate, or ribitol phosphate with attached sugar or amino acids) and teichuronic acids (less well-defined acidic polysaccharides containing uronic acids and other sugars) (Hancock, 1991; Madigan *et al.*, 2000). These polymers are affected by the composition of growth medium and are important to bacterial physico-chemistry. As well as these anionic structures, Gram-positive bacterial cells also contain neutral polysaccharide wall polymers (e.g. lipoteichoic acids or LTAs) (Hancock, 1991; Madigan *et al.*, 2000). Frequently detected within the peptidoglycan layer, LTAs have been found to be involved in hydrophobic interactions (Hancock, 1991).

Gram-negative bacterial strains have a much thinner peptidoglycan layer than that for Gram-positive strains (Figure 2.2b). However, they have an additional wall layer made of lipopolysaccharide (LPS), which consists of polysaccharide and protein and effectively forms a second lipid bilayer (Madigan *et al.*, 2000). With the lipid and polysaccharide intimately linked to form the

specific structure, the LPS layer is also commonly referred to as the outer membrane (Caroff and Karibian, 2003).

### ***Surface Components Outside of the Cell Wall***

**Extracellular Polymeric Substances and S-layers:** Extracellular polymeric substances (EPS) and glycocalyx are often used interchangeably to describe the complex mixture of macromolecular polyelectrolytes external to the cell wall that includes polysaccharides, proteins and nucleic acids (Suci *et al.*, 1995; Sutherland, 2001). The structure is referred to as a capsule when the layers that contain EPS are organized in a tight matrix that excludes particles; it is referred to as a slime layer when the structure is more easily deformed (Madigan *et al.*, 2000). The structure is important to cell adhesion as it is able to mediate attachment through interfacial processes including covalent or ionic bonding, dipole interactions, steric interactions, and hydrophobic association (Van Loosdrecht *et al.*, 1987; Beveridge and Graham, 1991). In addition to EPS, bacteria may also contain surface layers composed of two-dimensional arrays of protein called S-layers (Madigan *et al.*, 2000). They consist of large amounts of non-covalently bound protein and are the outermost layers of many bacterial strains (Hancock, 1991). The presence of S-layers in Gram-negative bacteria can render the cell surface much more hydrophobic by partially masking the hydrophilic polysaccharide surface of the outer membrane (Hancock, 1991; Beveridge *et al.*, 1997).

**Fimbriae and Conjugative Pili:** Both types of appendages are predominantly observed on Gram-negative bacteria strains, although fimbriae have also been observed on some species of Gram-positive bacteria, such as *Actinomyces* (Duguid and Old, 1980; Busscher *et al.*, 2000). Both fimbriae and pili are made up of organized rod-like arrays of protein subunits, of strain-specific types. Fimbriae contain hair-like and proteinaceous structures typically 0.2-2.0  $\mu\text{m}$  in length and 1-10 nm in diameter. They have a high content of hydrophobic amino acid residues and will generally enhance cell surface hydrophobicity (Busscher *et al.*, 2000). It has been reported that the adherence of *A. calcoaceticus* RAG-1 to hexadecane may be due to the presence of numerous fimbriae on cell surfaces (Rosenberg *et al.*, 1982). However, it cannot be concluded that there is a direct correlation between the presence of the fimbriae and hydrophobicity (Rosenberg *et al.*, 1982).

**Fibrils:** This is another form of cell appendage which is distinct in morphology from fimbriae and pili, being shorter (generally less than 200 nm long) and having no measurable width as they usually appear in clusters (Handley, 1991). They have been observed in oral strains of *Streptococcus* and in several *Bacteroides* species (Handley *et al.*, 1984; 1985). As is the case with fimbriae, fibrils generally increase cell surface hydrophobicity. However, fibrils with known structure have been proved to be glycoproteins, which clearly distinguishes them from fimbriae (Weekamp and Jacobs, 1982; Morris *et al.*, 1987).

**Flagella:** This is the longest cell surface appendage and is most commonly responsible for the mechanisms by which bacteria reach substrate surfaces (motility). The structure is up to 20  $\mu\text{m}$  in length, helical in shape, free at one end and attached to the cell at the other (Brock and Madigan, 1991; Hancock, 1991; Madigan *et al.*, 2000).

### **2.2.3.2 Measurement of surface properties**

#### **Measurement of Cell Surface Hydrophobicity**

Bacterial hydrophobicity is a term used to describe those properties conferred on bacterial cells by their outermost surfaces which facilitate cell adhesion to liquid hydrocarbon during petroleum fermentation (Neufeld *et al.*, 1980). The enormous rise in scientific interest regarding bacterial hydrophobicity is due to its importance in microbial interactions with hydrocarbons (Rosenberg and Doyle, 1990). Here, two common experimental methods for determining bacterial hydrophobicity will be discussed.

#### ***Bacterial Adhesion to Hydrocarbon (BATH) Test***

To quantify bacterial cell surface hydrophobicity, Rosenberg *et al.* (1980) originally described an assay which shows bacterial strains with hydrophobic surface can adhere to liquid hydrocarbons, whereas non-hydrophobic strains cannot. This process can be summarized as follows: a turbid, aqueous suspension of washed bacterial cells is mixed by vortexing in the presence of a test liquid hydrocarbon (usually *n*-hexadecane or toluene) under well-controlled conditions in a glass test tube. The volumes and ratios of the phases employed, and also the

bacterial concentration, should be chosen in such a way that the hydrocarbon phase is not “overloaded.” Following mixing, the two phases are allowed to separate. In the case of a hydrophobic strain, cells from the aqueous phase become bound to the hydrocarbon droplets and rise with these droplets after mixing to form an upper “cream” which consists of cell-coated oil droplets. When hydrophilic, non-adherent bacteria are tested, the phases separate following the mixing procedure, and the cells remain in the aqueous phase. The percentage of cells adhering to the hydrocarbon is used as a measure of cell surface hydrophobicity; it can be determined easily from the decrease in light scattering (i.e., turbidity) of the lower aqueous phase, as compared to the turbidity of a control suspension. One drawback of this technique is the possibility that the cells can be damaged by vortexing in the presence of the liquid hydrocarbon (Rosenberg and Doyle, 1990). However, it has been reported that hexadecane does not damage the integrity of bacterial cells (Pembrey *et al.*, 1999).

Many investigators have modified the original BATH test with respect to the ionic strength, composition, and pH of the buffer (Nesbitt *et al.*, 1982; Rosenberg, 1984; Kozlovsky *et al.*, 1987; Mozes and Rouxhet, 1987). These seemingly small variations can greatly alter the results. For example, when the ionic strength is increased by choosing another type of buffer or addition of salts, the hydrophobicity of the bacteria is enhanced due to the elimination of the influence of electrostatic interactions. In particular, for intermediate or weakly hydrophobic strains, addition of salts to the buffer is a good method to determine the rank order of the hydrophobicity of the strains.

### ***Contact Angle Measurement***

Contact angle represents another measure of surface hydrophobicity (Gould, 1964). It can be measured readily on most solids and are often used simply as a parameter to quantify wettability. This method has been extended to microbial cell surfaces, being considered as the most suitable method in this regard (van der Mei *et al.*, 1991). During contact angle measurement, in order to produce as uniform a surface as possible, it is recommended that bacterial cells (suspended in water) be slowly deposited onto a membrane filter under a negative pressure (van der Mei *et al.*, 1991). These wet membranes with bacterial films can then be attached on sample holders with, for example, double-sided adhesive tape and dried under standardized conditions. The angle of contact between a drop of water placed onto the film and the film surface itself is measured using a traditional goniometer or with the aid of computer-based image analysis software (Figure 2.3).

Many studies have been devoted to measuring the contact angle of microbial cells, although difficulties are often encountered. Van Oss and Gillman (1972) conducted extensive contact angle measurements on phagocytic and other cells, as well as on various bacteria. Contact angles were determined using physiological saline on dried bacterial cells, which has the advantage of simplicity. However, the hydration core around the cell may be lost during the measurements (Rutter and Vincent, 1984), particularly if excessive drying of bacterial films occurred (van der Mei and Busscher, 1990). Thus, contact angles are related to the wettability of a dehydrated surface and reflect the dominant hydrophobic

surface groupings revealed by desiccation. Van Loosdrecht *et al.* (1987) compared the values obtained for a wide range of microbial species using BATH and contact angle measurements and noted that if the contact angle was less than 30°, little if any adherence to the hexadecane interface was observed; for contact angles greater than 30°, adhesion increased concomitantly with the contact angle but the overall correlation was poor.

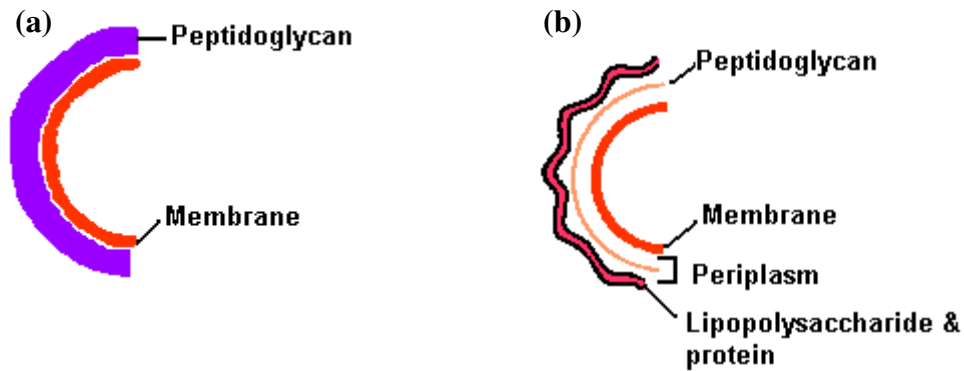


**Figure 2.2:** Schematic, generalized representation of a (a) Gram-positive and (b) Gram-negative bacterial cell wall structure

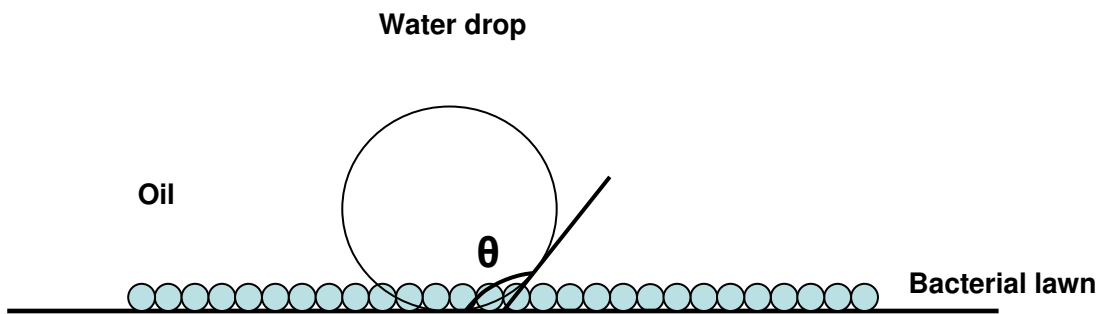


**Figure 2.3:** Contact angle of sessile drop on bacterial lawn.

## 2.3 General Theory of Emulsion

An emulsion is a mixture of two immiscible liquids where one liquid (the internal or dispersed phase) is dispersed within the other liquid (the external or continuous phase) in the presence of emulsifiers (Tadros and Vincent, 1983). The emulsifier helps to form an extended interface by reducing the interfacial tension between the liquids and also helps to stabilize the dispersed droplets against coalescence.

The phenomena of emulsification have been observed and recorded for thousands of years, since the creation of emulsion by beeswax was observed in ancient Greece (Becher, 2001). However, it was not until the beginning of the last century when the basic concepts of emulsion had been established. Emulsions are important because they exist widely in many applications, such as food, petroleum, agriculture products, pharmaceuticals and cosmetics (Chappat, 1994). In many cases, emulsions are desirable. For example, dairy products and cosmetics are emulsions that must be very stable to ensure long shelf life. Microencapsulated drug delivery systems must be stable everywhere except at the target organ where the microemulsion is designed to become unstable and release the drugs. However, in other cases, emulsion stability is undesirable. For example, in the treatment of water-in-crude oil emulsions, it is desirable to break the emulsion in order to achieve rapid phase separation.

Emulsions have been systematically studied for over 100 years and there are a large number of references dealing with diverse scientific areas of this subject. Emulsions are classified as a *macroemulsion* if the droplet size is larger

than about 0.1 $\mu$ m and as a *microemulsion* if the emulsion system contains much smaller structures (usually 5-50 nm) (Hunter, 1995). Generally, most droplet diameters in macroemulsions are larger than 0.1 $\mu$ m, which is of the same order of magnitude as the pore constrictions in enhanced oil recovery. Based on the purpose of our study, all the following discussions, unless otherwise stated, will be focused on the concepts of macroemulsions. The material in the following sections is intended as a brief review and the subjects are discussed in much greater detail in several excellent reviews (Adamson, 1967; Tadros and Vincent, 1983; Israelachvili, 1992; Russel *et al.*, 1989; Ross and Morrison, 1988; Hiemenz, 1986; Hunter, 1995).

### **2.3.1 Type of emulsion and emulsifier**

The two liquids are in general water and oil. Emulsions can be classified depending on the kind of liquid which forms the continuous/dispersed phase: *water-in-oil* (w/o) emulsion for water dispersed in oil or *oil-in-water* (o/w) emulsion for oil dispersed in water; such emulsions are also called simple emulsions. Low molecular weight, hydrophilic emulsifiers induce formation of o/w emulsions, lipophilic emulsifiers favour w/o emulsions. Use of water-soluble macromolecular emulsifiers also results in formation of o/w emulsions (Becher, 2001).

A more complicated situation exists with the presence of an additional phase leading to o/w/o (with dispersed aqueous globules containing smaller oily dispersed droplets) or w/o/w (with dispersed oil globules containing smaller

aqueous dispersed droplets) emulsions, which are considered as double (or multiple) emulsions (Tadros and Vincent, 1983). All the following discussions, unless otherwise stated, will focus on simple emulsions.

An emulsion can be made by the agitation of two immiscible pure liquids with a stirrer, a pump, or flow in a pipeline. Thermodynamically, an emulsion is unstable. Such systems tend to adopt a configuration which minimizes the free energy. For two immiscible liquids, this means minimizing the surface area between the phases. Since one large droplet has less surface area per unit volume than several smaller drops, there is a natural tendency for the smaller droplet to coalesce. At close distances, van der Waals forces attract the droplets towards one another, increasing the number of contacts. The end result of this process is the separation of the emulsion into two homogeneous and distinct phases (i.e. phase separation). To prevent phase separation, the emulsion can be stabilized by addition of adsorbed surfactants, polymers, proteins, finely divided colloidal particles, or their mixture, which can prevent the drops from coalescing (Mittal and Kumar, 2000). These emulsifiers are able to facilitate formation and stabilization of the emulsion through their surface activity, e.g. reducing interfacial tension, and formation of steric barriers at the interface. Generally, four classes of emulsifiers can be distinguished (Hunter, 1995; Mollet and Grubenmann, 2001):

1. **Surfactant:** A surfactant is a dual natured molecule in that part of the molecule, the head group(s), is hydrophilic and the remainder (the tail) is hydrophobic. For example, hexedanol consists of a hydrophobic alkane

tail and a hydrophilic hydroxyl head. A surfactant readily adsorbs on an oil/water interface because the tail(s) can reside in the oil phase and the head(s) in the water phase, as shown in Figure 2.4. A surfactant is either ionic, e.g., a carboxylic acid, or non-ionic, e.g., polyoxyethylenes. Ionic surfactants can be anionic (i.e. surfactants having a hydrophilic group, which carries a negative charge such as a carboxylate, sulfonate, or sulfate group), cationic (i.e. surfactants having a positive charge in their hydrophilic part) or amphoteric (or zwitterionic, i.e. surfactants carrying a positive and a negative charge). The surfactants usually either ionize or attract ions from the aqueous phase so that there is a charge associated with the head group. The charge associated with the surfactant head group can act to stabilize an emulsion or, if the surfactant has a long tail, the tail can also stabilize an emulsion.

2. **Simple inorganic electrolyte:** One example of such a type of emulsifier is potassium thiocyanate (KCNS), which can stabilize (at least temporarily) o/w emulsions by the adsorption of the CNS<sup>-</sup> ions at the interface. The electrical double layer which results from the adsorption of ions at the interface can stabilize the system, although the surface charge density is usually small.
3. **Macromolecular emulsifier:** This includes proteins, polysaccharides (gums, starches and their derivatives) and some synthetic polymers (e.g. polyvinyl alcohol). They are able to produce very stable emulsions (e.g. milk is stabilized by proteins).

4. **Finely divided solid particle:** These particles can produce emulsions by adhering to the interface due to surface energy effect. Adhesion of a particle to a liquid drop is determined by the surface properties of the particle (rather than its bulk properties). The size of these solid particles roughly lies in the range of 1 -1000 nm (i.e. 10Å to 1 µm), which includes a wide variety of organic solids or mineral powders. These solid particles can be spherical, blocks, rod or irregular shapes. They play a very important role in petroleum-related processes, e.g. in the oil agglomeration process for separating mineral particles (surface oxidation of the mineral particles can drastically affect the adhesion of the mineral to the oil droplet) (Yan *et al.*, 2001). Solids-stabilized emulsions still remain a novel technology and need more investigation on the mechanisms and the behaviour of particles at the interface.

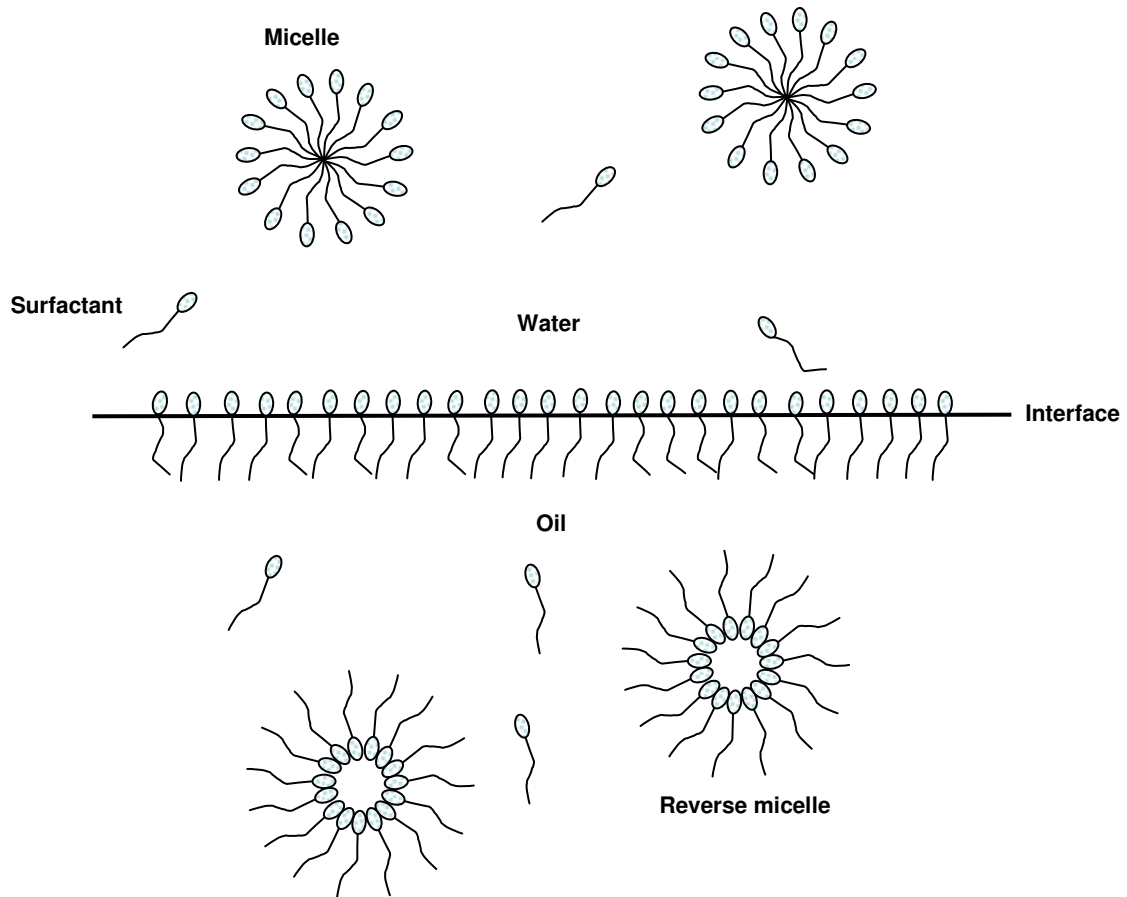


**Figure 2.4:** Some surfactant structures.

### 2.3.2 Stability of emulsion

In order to understand the mechanisms of emulsion stability, it is necessary to know the forces acting on emulsion droplets. The following forces are important in the interaction between emulsion droplets: dispersion, electrostatic, steric, Brownian, viscous, inertial, and gravitational forces. Dispersion, electrostatic and steric forces act between emulsion droplets. Brownian, viscous, inertial and gravitational forces control the movement of the droplets in the continuous phase. Among all these forces, electrostatic and steric

forces are relatively important in understanding the emulsion stability in this study.

Emulsion can be stabilized against breakdown by one or more mechanisms. Three such mechanisms which occur commonly are: charge or electrical stabilization, steric stabilization or repulsion by physical barriers, and stabilization by adsorbed solid particles at the liquid/liquid interface (Figure 2.5; Tadros and Vincent, 1983).

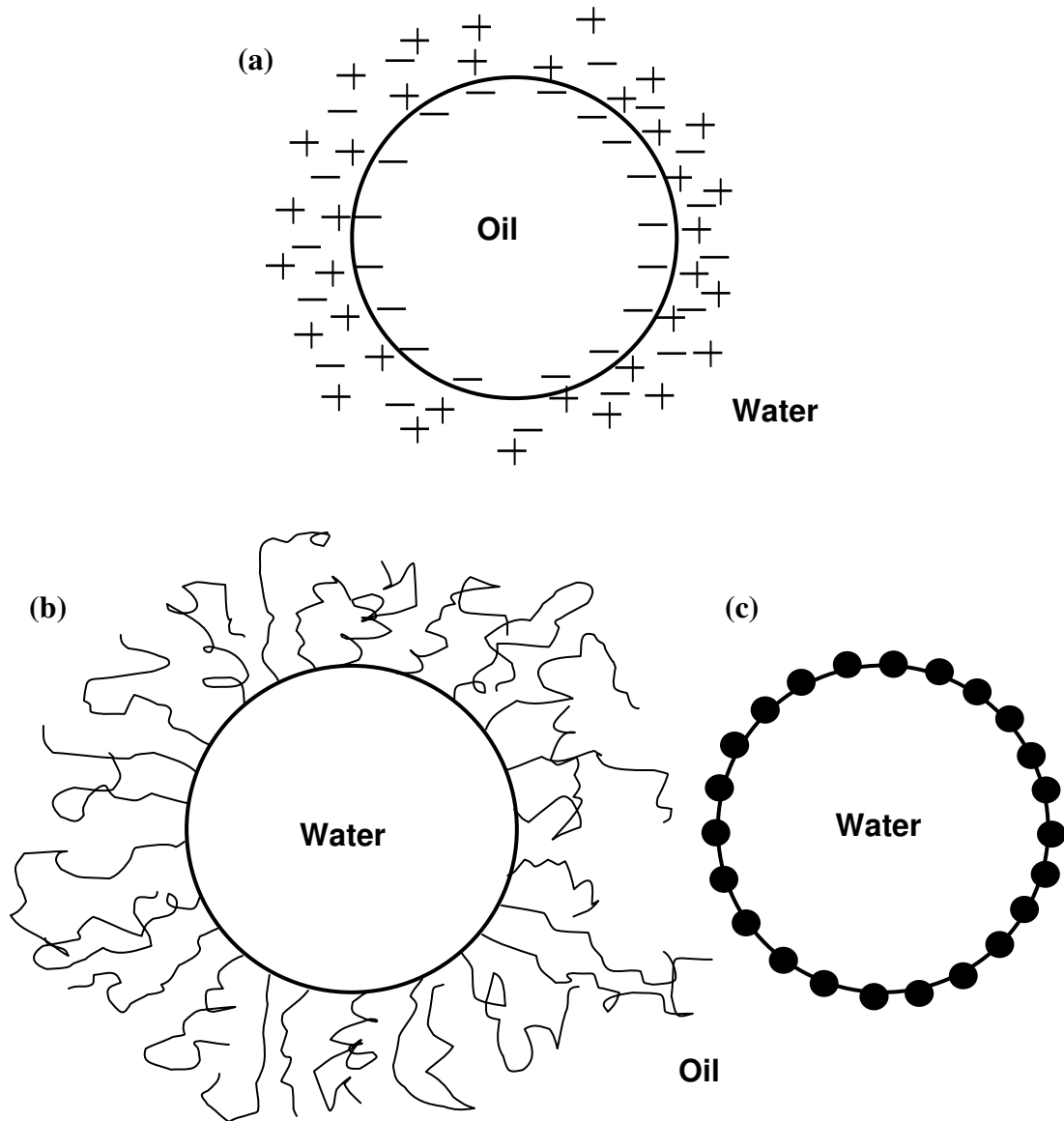


**Figure 2.5:** Mechanisms in stabilization of emulsions. (a) Electrostatic stabilization; (b) Steric stabilization by adsorbed macromolecules; (c) Stabilization by solid particles.

Emulsions usually can be stabilized by the natural presence — or deliberate addition — of an ionic stabilizer (e.g. an ionic surfactant or a polyelectrolyte). The surface charge influences the distribution of nearby ions in the polar medium. Ions of opposite charge (known as counter ions) are drawn near the surface and form an electric double layer. Electrical repulsive forces

arise when two emulsion drops are in close enough proximity that their double layers overlap, resulting in an excess osmotic pressure in the thin gap between the droplets, which in turn leads to a repulsive force. The important factors in charge stabilization are the electrical potential at the droplet surface (known also as the zeta potential) and the thickness of the double layer. If the zeta potential of the emulsion droplets is greater than +30mV or less than -30mV, the emulsion is normally relatively stable and the particles will possess enough surface charge to repel one another. If the absolute value of the zeta potential is less than 30 mV, the emulsion system will often exhibit poor stability (Tadros and Vincent, 1983; Mollet and Grubenmann, 2001).

Adsorption of macromolecules on emulsified drops will give rise to a steric mechanism of stabilization. Many naturally occurring emulsions are stabilized by the presence of macromolecular materials. For the surfactant-stabilized emulsions, steric repulsion between the parts of surfactant in the continuous phase is an important effect (Butt *et al.*, 2003). For a water-in-oil emulsion the hydrocarbon chains are hindered in their thermal movements if two water drops approach closely. For an oil-in-water emulsion, there is an additional effect: the hydrophilic head groups have to be dehydrated before they can come into close contact. The resulting hydration repulsion acts to stabilize the emulsion.

In addition, in the case of geologically occurring emulsion, such as those in oil beds, the presence of solid particles (e.g. silica, bentonite clays) gives rise to the third mechanism of emulsion stabilization. Unravelling the physics of these systems is a complex matter. The mechanism involved in solids-stabilized

emulsions has been the subject of numerous debates in the literature and is at present still far from being understood (Binks, 2002). Depending on the exact system, there are at least two mechanisms by which colloidal particles can stabilize emulsions. In the first mechanism, the particles are required to adsorb at the oil/water interface and form a dense film (monolayer or multilayer) around the dispersed drops to impede coalescence. In the second, additional stabilization arises when the particle-particle interactions are such that a three-dimensional network of particles develops in the continuous phase surrounding the drops. This has been invoked particularly in clay-containing systems in which the oil drops become captured and are more or less immobilized in the array of clay platelets in water (Abend *et al.*, 1998; Lagaly *et al.*, 1999). The effectiveness of solids in stabilizing emulsions depends on particle concentration, size, particle wettability, and interaction between the particles (Binks, 2002).

Both electrical and steric stabilization are due to static forces that are present between the emulsified drops, but there are a number of dynamic effects which are equally important in stabilizing emulsions (Butt *et al.*, 2003). The Gibbs-Marangoni effect is among those important dynamic phenomena in emulsion stability and has been studied extensively (Hunter, 1995). This effect does not occur in pure liquid-liquid systems; they are seen only in emulsion systems which contain adsorbed emulsifiers at the interface. In the dynamic system (e.g. two colliding drops), the Gibbs-Marangoni effect tends to play an important role in preventing the coalescence of emulsion drops. For coalescence to occur, the forces between the drop surfaces must be such that the film of

continuous phase separating them can become sufficiently thin and film rupture becomes possible. In this process, two drops approach each other and their interfaces interact and begin to deform, creating a plane-parallel region between the drops (Figure 2.6). At the same time, the continuous phase between the drops is forced to drain out (in the direction of the large black arrows in Figure 2.6) until a thin film is formed. If the film drains sufficiently, the dispersed phase may break through or bridge the film and initiate coalescence. However, because the adsorbed emulsifier layer is dragged with the continuous phase, an interfacial tension gradient at the drop interface is created. Due to the depletion of the emulsifiers at the centre of the film interface, a diffusion flux is generated towards the thinned spot, opposing the drainage in order to restore the equilibrium interfacial tension (which acts in the direction of the smaller arrows drawn in the drops in Figure 2.6). This diffusion flux increased the rigidity of the interface and impedes fluid drainage. This is known as the Gibbs-Marangoni effect and can prevent coalescence if sufficiently strong. The rate of thinning of the film between dispersed drops and its stability against rupture are among the main factors determining the overall stability of the emulsion. If this film is highly elastic, the Gibbs-Marangoni effect is strong and there is also a strong resistance to any deformation.

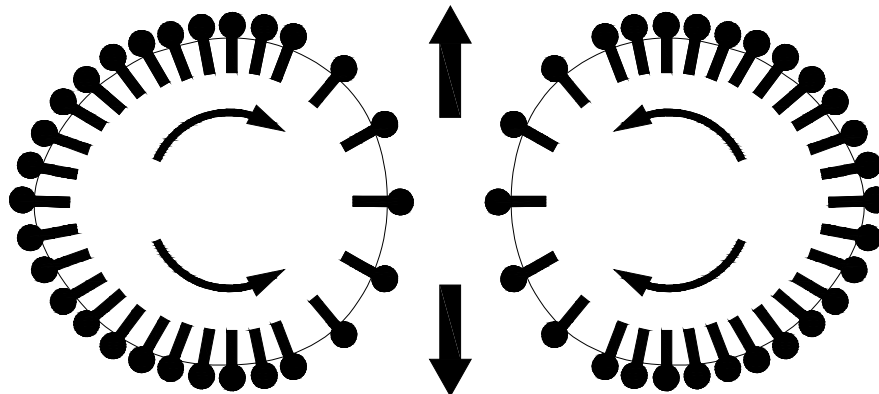


**Figure 2.6:** A drawing showing how the Gibbs-Marangoni effect can inhibit coalescence by slowing film drainage. The large black arrows show the direction that the suspending medium is forced to drain out; the smaller arrows drawn in the drops are the directions for diffusion flux opposing the drainage.

Since emulsions are thermodynamically unstable, the word “stable” is used with reference to emulsion lifetime. Emulsion destabilization may involve a number of processes, among which four important ways should be mentioned; these are: creaming/sedimentation, flocculation, coalescence, and Ostwald ripening (Figure 2.7). Creaming and flocculation affect the dispersion of the droplets in emulsions but not the size distribution of the droplets. By contrast, coalescence and Ostwald ripening result in phase separation in emulsion systems. The form of instability is a function of the forces at different levels (Tadros and Vincent, 1983). For example, in sedimentation and flocculation, the relevant forces are essentially long range, at least relative to forces on the molecular level, such as external field forces (gravity or centrifugal force). In processes such as

coalescence and Ostwald ripening, it is essential to consider short range intermolecular forces.

***Creaming and sedimentation:*** This occurs where there are disparities in density and where gravitational forces are dominant (Tadros and Vincent, 1983). In such situations, the emulsion droplets will rise (sink) and collect at the top (bottom) of the vessel depending on the type of emulsion. The rising or settling droplets are not necessarily associated with aggregation and they can re-disperse. Creaming and sedimentation can take place without any change in the drop size distribution (Binks, 1998).

***Flocculation:*** Flocculation is the aggregation of two or more droplets, with the droplets retaining their original identity without rupture of the stabilizing layer at the interface. It depends on the relative magnitude of the attractive dispersion force and repulsive electrostatic or steric forces existing in the emulsion system. Both forces act on the droplets and arise from an energy potential which is a function of the separation distance (Ross and Morrison, 1988; Sanders and Masliyah, 1990). During flocculation, as long as the individual droplets remain distinct, the emulsion has not been destroyed and the droplets can be re-dispersed.

***Coalescence:*** Coalescence is the process in which two or more emulsion drops fuse together to form a larger drop; such a process is irreversible. When droplets collide and flocculate, the continuous phase between the droplets drains out until a thin film or layer remains between them (Tadros and Vincent, 1983). The film undergoes spontaneous thermal or mechanical fluctuations in thickness,

which can grow or dampen depending on the steric forces and film properties. If the fluctuations dampen, the droplets can remain flocculated but still distinct; if the fluctuations grow, the intervening film ruptures and the droplets coalesce, resulting in a single larger drop. If the coalescence process continues, the two immiscible liquids will phase separate and the emulsion system will be destroyed. It has been noted that the rate-limiting factors in coalescence include the properties of interfacial film (e.g. film elasticity), electrical and steric barriers, viscosity of the dispersion medium, volume ratio of the disperse phase and the dispersion medium, droplet size distribution, and temperature (Mollet and Grubenmann, 2001).

***Ostwald ripening:*** Ostwald ripening is the growth of larger emulsion drops at the expense of small droplets without involving coalescence; it is related to the solubility gradient between the small and large drops. It occurs in emulsions with different drop sizes and leads to further disparities in the drop size distribution. Ostwald ripening is due to mass transfer between droplets of different curvatures, which is inversely related to the surface concentration of the dispersed phase material on the drop surface (Kabalnov and Shchukin, 1992). Thus, compared to a large drop, a small drop has a high surface concentration, which results in a concentration gradient of the dispersed phase material in the continuous liquid. Mass transfer appears along the concentration gradient from small droplets to large droplets (i.e. small droplets shrink and ultimately disappear while large droplets grow, and finally phase separation occurs). It is a slow process and is observed only in emulsions with no coalescence.

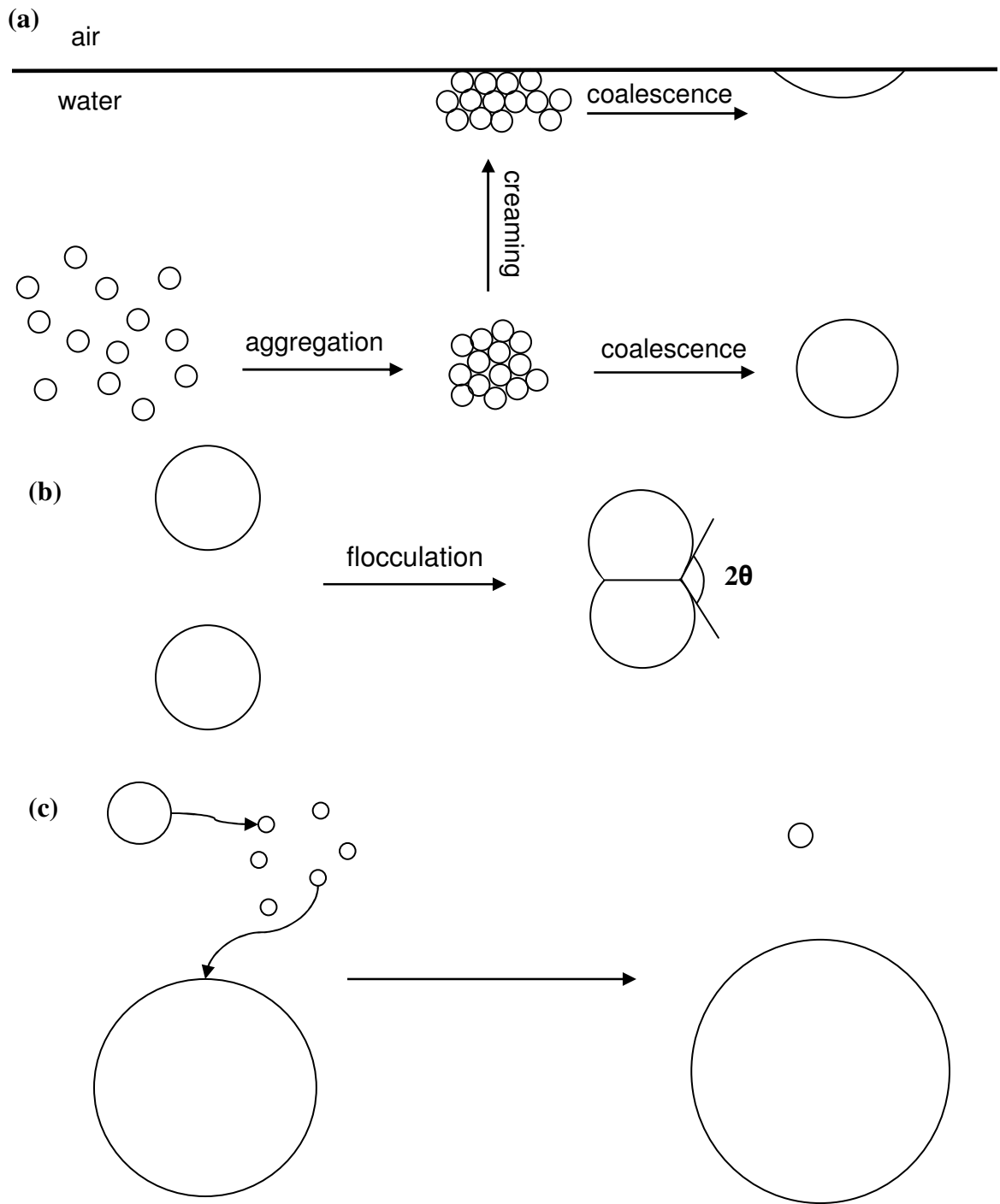


**Figure 2.7:** Sketch of processes occurring in an unstable o/w emulsion. (a) Creaming/ sedimentation and coalescence; (b) flocculation in the aggregation process; (c) Ostwald ripening.

### **2.3.3 Characterization of emulsions**

#### **2.3.3.1 Surfactant-stabilized emulsions**

Surfactant-stabilized emulsions are the most common form of emulsions. Research in this area has taken place over 100 years and there are numerous reference articles and textbooks dealing with their concepts and applications. One characteristic property of surfactants is that they can spontaneously aggregate in solution and form well-defined structures called micelles. This occurs when their concentration in water (or oil) reaches some threshold value called the critical micelle concentration (CMC). Hydrophile-lipophile balance (HLB) and phase inversion temperature (PIT) are two important properties related to surfactant-stabilized emulsions. HLB characterizes the tendency of a surfactant to form water-in-oil or oil-in-water emulsion and is a direct measure of the hydrophilic character of a surfactant: the larger the HLB, the more hydrophilic the surfactant. PIT helps to predict the structure of emulsions stabilized by nonionic surfactants; this concept is based on the idea that the type of emulsion is determined by the preferred curvature of the surfactant film (Butt *et al.*, 2003). These basic concepts of surfactant-stabilized emulsion will be introduced in the following.

#### ***Critical Micelle Concentration (CMC)***

A surfactant is characterized by the critical micelle concentration (CMC), which in effect represents the solubility of a surfactant within an aqueous phase. The micellization process is driven by the same forces that cause surfactants to adsorb onto oil/water interfaces. When surfactants are at low concentration in

water (or oil), the surface tension decreases monotonically with increasing bulk concentration. However, when a certain concentration is reached (the CMC), this decrease in surface tension ceases. Any additional surfactant above the CMC is incorporated into a micelle since the oil/water interface already has a saturated layer of surfactants. Therefore, the interfacial tension does not change with the increase of surfactant concentration. This property is often used to characterize the surface activity of surfactants. Micelles can act as “transport packets” for hydrocarbons or water; these structures are fluid-like and are easily transformed from one state to another since no chemical bonds are formed (Becher, 2001). In water, the surfactant molecules will aggregate in such a way that the polar head groups tend to orient toward the water and the non-polar tails tend to point to the center of the structure away from the aqueous surrounding; this is shown schematically in Figure 2.4. This type of micelle is called “normal phase micelles” (oil-in-water micelles). Inverse micelles have the head groups at the centre, with the tails extending outward (water-in-oil micelle, also shown in Figure 2.4). Micelles can take the forms of spheres, ellipsoids, cylinders, or bilayers. Their shape and size are governed by the molecular geometry of the surfactant molecules and solution conditions (i.e. temperature, pH, surfactant concentration, and ionic strength). With surfactants, the emulsion droplet size typically decreases with concentration until the CMC is reached, after which it remains constant. This decrease in drop size is mainly a result of the lowering of the interfacial tension, which can facilitate drop breakup (Binks, 2002).

Micelles are able to swell, i.e. to retain liquid oil in their internal structures; in the same way, reverse micelles can swell with liquid water accumulating within their interiors. These swollen structures should not be considered as solid particles; instead, it is a microemulsion (usually 5-50nm in drop size; Hunter, 1995). Microemulsions are a second phase and are thermodynamically stable. They are fundamentally different from “standard” emulsions (also called “macroemulsions”). The two types of emulsions can also be distinguished by measuring their interfacial tensions. A “standard” emulsion has a finite oil/water interfacial tension, while the interfacial tension drops to nearly zero in microemulsion systems.

### ***Hydrophile-Lipophile Balance (HLB)***

The first quantitative measure of the balance between the hydrophilic and hydrophobic moieties within a particular surfactant was made in 1949 when Griffin introduced the semi-empirical concept of hydrophile-lipophile balance, or HLB (Griffin, 1949). This is the ratio of the hydrophilic to lipophilic groups in the molecule; it is a way of predicting emulsion type from surfactant molecular composition. The concept has been widely used for correlating the behaviour of non-ionic surfactants in different situations. It has been shown that HLB is the most important parameter in determining whether the surfactants tend to reside in the water or the oil phase (Hunter, 1995). The HLB value determines the tendency of the surfactant monolayer to curve towards water or oil, or remain effectively planar, so that the type of emulsion (o/w or w/o) is determined.

For more lipophilic surfactants, i.e. surfactants with low HLB values (~4) (e.g. non-ionics with low degrees of ethoxylation), the area per chain is larger than that of the head group and the monolayer will curve toward the water phase, resulting in water-in-oil (w/o) emulsions. For hydrophilic surfactants i.e. surfactants with high HLB values (~20) (non-ionics with a high degree of ethoxylation), the area per head group exceeds that of the chain and oil becomes the dispersed phase, resulting in oil-in-water (o/w) emulsions. The surfactants with intermediate HLB values (~10) are considered to be balanced hydrophilically-lipophilically. The HLB values and their corresponding applications are summarized in Table 2.1 (Tadros and Vincent, 1983).

**Table 2.1:** Tensides and HLB values

	HLB value	Application
Lipophilic ↓ Hydrophilic	0-3	defoamers
	3-8	w/o emulsions
	7-9	wetting agents
	8-18	o/w emulsions
	11-15	detergents
	15-18	solubilizers

In general, HLB values have been recorded for non-ionic emulsifiers and are between 0 and 20. If the HLB concept is applied to ionic tensides, additional dissociation effects can lead to HLB values over 20. For example, sodium dodecyl sulfate has an HLB value of 40 (Mollet and Grubenmann, 2001).

It has also been observed that some conditions of the solution can modify the geometry of the surfactant and hence affect the value of HLB; some examples are temperature, electrolyte concentration, oil type and chain length, and cosurfactant concentration. As a result, the curvature of the surfactant monolayer

is changed, which in turn affects the preferred emulsion type (Graciaa *et al.*, 1989; Davis, 1994).

### ***Phase Inversion Temperature (PIT)***

Phase inversion is the changing of an o/w emulsion into a w/o emulsion or vice versa. It can be one of two types: transitional inversion is induced by changing factors which affect the HLB of the system (e.g. temperature or electrolyte concentration); catastrophic inversion is induced by increasing the fraction of the dispersed phase and has the characteristics of a “catastrophe” (i.e. a sudden change in behaviour of the system as a result of gradually changing conditions). Catastrophic inversion is known to be irreversible (i.e. the value of the water:oil ratio at the transition point when oil is added to water is not the same as that when water is added to oil) and is accompanied by dramatic changes in properties of the emulsion — such as viscosity and drop size. The inversion point depends on the intensity of agitation and on the rate of liquid addition to the emulsion. Brooks and Richmond (1994) had made a detailed study on the dynamics of both transitional and catastrophic phase inversions stabilized by nonionic surfactants. In the former, the inversion was caused by changing the system HLB at constant temperature using a combination of surfactants. In emulsions stabilized by only one type of surfactant, inversion did not occur (Binks, 2002). It was also noted that emulsions formed by transitional inversion were finer and required less energy than those produced by direct emulsification.

It is now well known that the choice of emulsification conditions is an important consideration in determining the stability of emulsions. When the temperature is raised, the degree of hydration of the hydrophilic groups of the surfactant declines and the surfactant becomes less hydrophilic and hence its HLB value decreases. Therefore, if an emulsion is of o/w type at lower temperature, it can invert to a w/o emulsion as the temperature is increased. Similarly, a w/o emulsion created at high temperature can invert to an o/w type when the temperature drops. The temperature at which this inversion occurs is called the phase inversion temperature (PIT); it is the point at which the hydrophilic and hydrophobic properties of the emulsifiers are balanced. Shinoda and Saito (1969) were the first to demonstrate the effects of PIT on emulsion systems using nonionic surfactants. Since then, various researchers have confirmed the existence of PIT in various emulsion systems and the influencing factors for PIT (Enever, 1976; Lehnert *et al.*, 1994).

#### **2.3.3.2 Solid particle-stabilized emulsions (Pickering emulsions)**

It has long been observed that finely divided solid particles can also function as emulsifying agents, in ways similar to surfactants in emulsion formation and stabilization (Berkman and Egloff, 1941). At the beginning of the last century, Pickering made the pioneering studies investigating solids-stabilized emulsions (hence this type of emulsion is often called “Pickering emulsion”; Pickering, 1907). He noted that particles which were wetted more by water than by oil, if residing at the interface, acted as emulsifiers for o/w emulsions. Later,

in 1923, Finkle *et al.* (1923) recognized the relationship between the type of solid and emulsions (o/w or w/o). Many studies have shown that the solid particles, which are insoluble in either phase, can create emulsions without affecting the interfacial tension (Berkman and Egloff, 1941). Today, solid particles have been applied in emulsion formation in various areas, including food, paint, agrochemical, pharmaceutical and the oil industry. Among the studies in this field, research groups of Tambe and Sharma (1994), Yan and Masliyah (1995), Zhai and Efrima (1996), Midmore (1998; 1999), and Lagaly and colleagues (Abend *et al.*, 1998; Lagaly *et al.*, 1999) have made particularly important contributions to understanding the particle-stabilized emulsions, frequently in the presence of surfactants or polymers.

It has been noted that there are two requirements which must be met for the emulsion to be stabilized by solid particles: (a) the particle size must be much smaller than the emulsion drop size, and (b) the particle surface must be partially wetted by both oil and water (Levine *et al.*, 1989). During the process of creating a solid-particle stabilized emulsion, three stages were observed: (a) approach of solid particles to the droplet surface; (b) entrainment of particles at the oil/water interface; (c) formation of particle network at the interface. The effectiveness of this process depends on particle wettability, concentration, size, and interactions between the particles.

Many methods are applied to synthesize small, monodisperse particles of different shapes and surface coatings. If the coating (e.g. alkylsilane) is homogeneous over the particle surface, such particles are surface-active but are

not amphiphilic (unlike surfactants). If the coating can be restricted to a particular area of the surface only, the particle will become both surface-active and amphiphilic, i.e. the particle has a specific area which is water-liking and a specific area which is oil-liking. The surface coating controls the contact angle  $\theta$  made by the oil/water interface on the surface of the particle (particle wettability), which is the key parameter for solid particles to adsorb at the oil/water interface and stabilize emulsions. In surfactant systems, the HLB is an important parameter in determining whether aggregated surfactant (micelles) resides in water, oil or a third phase. In the case of solid particles, the relevant parameter which plays a similar role as the HLB is the contact angle  $\theta$  made by the particle with the interface (Binks, 2002).

The contact angle is defined generally as the angle at which a fluid/fluid interface intersects a solid surface (Figure 2.8). Where water is involved, the angle is often identified as the one that is through the aqueous phase. For hydrophilic particles (e.g., metal oxides, bentonite), a larger part of the particle surface resides in water than in oil and the contact angle  $\theta$  is normally  $< 90^\circ$ ; for hydrophobic particles (e.g. specially treated silica, carbon black), a larger fraction of the particle surface resides in oil than in water and the contact angle  $\theta$  is normally  $> 90^\circ$ . By analogy with surfactant molecules, it has been shown that for particles with contact angles greater than  $90^\circ$ , monolayers formed by the solid particles on an interface will curve such that the larger area of the particle surface remains on the oil side and water-in-oil emulsions are formed; conversely, in the case of solid particles with contact angles less than  $90^\circ$ , they stabilize oil-in-water

emulsions. The most stable emulsions occur when the contact angle is close to  $90^\circ$  (Yan *et al.*, 2001). These observations have also been supported by a theoretical study which showed that particle wettability has a major influence on the ability of particles of different hydrophobicity to stabilize emulsions (Levine *et al.*, 1989). For  $\theta$  near far from  $90^\circ$ , the energy required to remove even nanoparticles from this interface can be extremely large and hence the adsorption is effectively irreversible.

Aveyard *et al.* (2003) had shown that the emulsion drop size is set initially by silica particle concentration until a limiting size is reached, after which an excess of particles in the continuous phase appears; this is unlike emulsions stabilized by a single surfactant type (Binks, 2002). All emulsions were stable to coalescence, but the stability to creaming decreased progressively with decreasing particle concentration, along with the increase in average drop size. An added bonus of using relatively high concentrations of silica particles is that the excess remaining causes gelation of the continuous phase, thus retarding or preventing complete creaming of oil drops or sedimentation of water drops (Binks and Lumsdon, 2000).

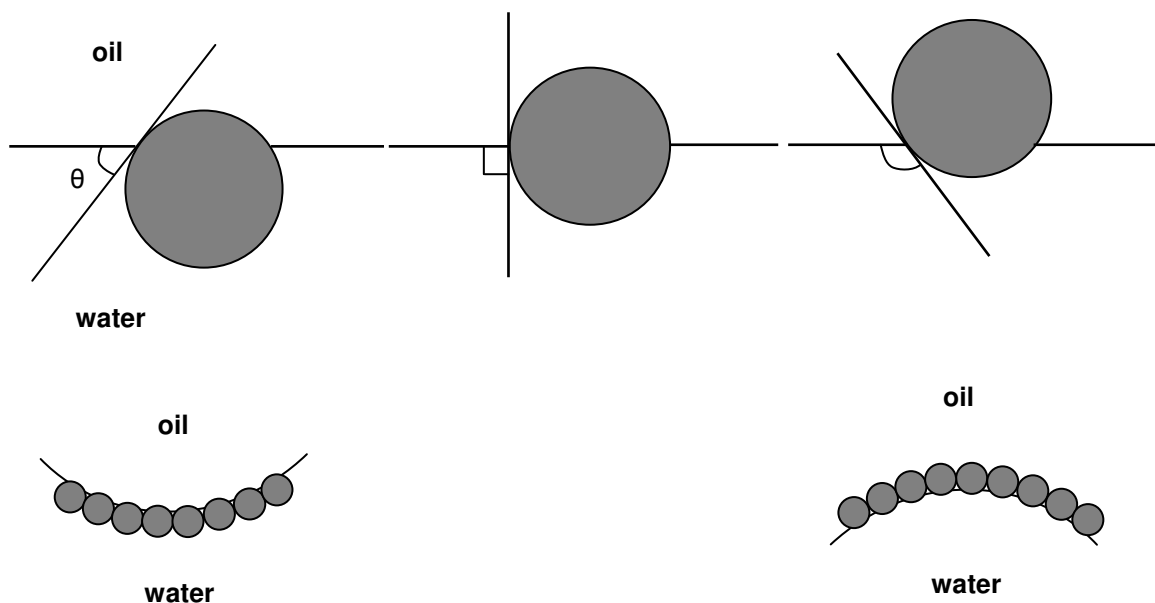


**Figure 2.8:** Upper sketches: Position of a small spherical particle at a planar fluid-water interface for a contact angle (measured through the aqueous phase) less than  $90^\circ$  (left), equal to  $90^\circ$  (centre) and greater than  $90^\circ$  (right). Lower sketches: Corresponding positioning of particles at a curved fluid-water interface. For  $\theta < 90^\circ$ , solid-stabilized o/w emulsions will form (left); for  $\theta > 90^\circ$ , solid-stabilized w/o emulsions may form (right).

Particle size is one of the most important factors that affect the effectiveness of colloidal particles in stabilizing emulsions because it determines the ability of the particles to remain on the oil/water interface (Mollet and Grubenmann, 2001). It is necessary that the particle size be much smaller than the size of emulsion drops (Tambe and Sharma, 1994; Levine *et al.*, 1989). In addition, the high energy of attachment of particles to interfaces means that the particles, once at the interface, can be considered as effectively irreversibly adsorbed; this is in sharp contrast to surfactant molecules which adsorb and desorb at a relatively rapid rate.

It has also been suggested that the interaction between particles is an important factor in stabilizing emulsions. The integrity of the film created at

emulsion drop surfaces by solid particles is a function of the strength of interparticle interactions (Menon and Wasan, 1988). The coalescence of two emulsion droplets is more difficult when particles at the interface can cross-link or strongly associate with one another.

As in the case for surfactants, solids-stabilized emulsions can also exhibit phase inversion phenomena, including catastrophic inversion and transitional inversion (Binks, 2002; Aveyard *et al.*, 2003). Experiments have shown that emulsions formed from small particles can be inverted from w/o to o/w simply by increasing the volume fraction of water. Emulsions stabilized by particles are most stable near this inversion point. Interestingly, these results are in contrast to those for emulsions stabilized by surfactants. The volume fraction of water needed for phase inversion depends on the particle wettability and on the type of oil. Freeze fracture SEM images show that in most Pickering emulsions, the oil/water interface is completely covered with a layer of particles. There is evidence that in some systems, weak flocculation of the particles improves the emulsion stability.

## **2.4 General Theory of Interfacial Rheology**

Interfacial rheology is the study of the relationship between deformation of a fluid surface (e.g. the oil/water interface) and the accompanying forces, often involving time-dependent effects. The simplest physical property for a fluid surface is the interfacial tension (IFT). Higher order interfacial rheology appears due to two types of surface deformations: (a) dilational deformation, which is the

change in area of the liquid interface at constant shape, and (b) shear deformation, which is the change in shape of the interface at constant area. In the following, we will give a brief review of the basic concepts of interfacial rheology and the previous studies which have been made on the interfacial rheology of adsorbed molecules at oil/water interfaces.

## **2.4.1 Basic concepts of interfacial rheology**

### **2.4.1.1 Interfacial tension (IFT)**

The most fundamental physical property at any liquid-liquid interface is the interfacial tension (IFT). It is defined as the reversible work needed to create a unit of interfacial area between two immiscible fluids. Alternatively, it can be viewed as a force per unit length resisting such an area increase (Hunter, 1986). In general, when surfactants are present at the interface, they build up a surface pressure  $\pi$  which lowers the interfacial tension. The surface pressure is directly related to the concentration of surfactants at the interface (much like pressure-volume relations for bulk fluids). For curved interfaces, such as those of emulsion drops, Young (1805) and Laplace (1805) described the pressure difference between the liquid phases and the tension at the interfacial surface through the Young-Laplace equation:

$$\Delta P = \gamma \left( \frac{1}{R_1} + \frac{1}{R_2} \right) \quad (2.1)$$

In the above equation,  $\Delta P$  is the pressure difference across a curved interface and  $\gamma$  is the interfacial tension. The term in the parentheses is referred

to as the mean curvature, with  $R_1$  and  $R_2$  being the principal radii of curvature (Adamson, 1976). When dealing with spherical drops (e.g. emulsion droplets), the mean curvature is simplified to  $2/R_d$ , where  $R_d$  is the drop radius. Assuming that the equilibrium interfacial tension is the only surface mechanical property, deformability of emulsion drops may be described by the Young-Laplace equation (Walstra, 1993).

### ***Techniques of measuring interfacial tensions***

Numerous techniques of measuring interfacial tensions have been developed in the past; some can be dated back more than a century and have withstood the scrutiny of time. Such established techniques include, but are not limited to: the drop volume and maximum bubble pressure method, which is based on the balance of gravity force against capillary forces; the Wilhelmy plate and Du Noüy ring, which measure the force needed to traverse an object through an interface; the sessile drop and pendant drop, which involves analysis of gravity-distorted drop shapes (Adamson, 1976; Tadros and Vincent, 1983; Hunter, 1986). Among these methods, the dynamic pendant drop is an important and widely used technique in determining interfacial tension and other surface material properties (Susnar *et al.*, 1993; 1996). All of these methods require sample sizes of millimetres or larger and are incapable of dealing with individual emulsion drops. At the micrometer scale, a micropipette technique was developed to measure the *in situ* interfacial tension of micron-sized water drops in non-polar media (Yeung *et al.*, 1998). Here we give only a brief overview of the

dynamic pendant drop and micropipette techniques as they will be applied in this study.

### *Pendant drop technique*

In the pendant drop method, a small liquid drop is formed at a capillary tip in a second immiscible fluid; the measurement is performed on the millimetre scale (Figure 3.2). The liquid drop is made large enough that it is appreciably distorted by gravity so that the Young-Laplace equation can be applied for IFT determination; it is noted that tensions cannot be determined for a spherical drop (i.e. one unaffected by gravity). Therefore the length of the drop must be enough for the pressure difference between the top and bottom to distort the drop. This is ensured by using a dispensing tip large enough to support the needed drop size. Lower surface tensions require even larger tips to support the required volume. The principal assumptions for this technique are:

- The drop is axisymmetric about a central vertical axis, which means it is insensitive to the direction from which the drop is viewed.
- The drop is “quiescent” in a sense that viscous and inertial forces do not play a role in determining the drop shape; interfacial tension and gravity are therefore the only two effects which govern the drop shape.

Unfortunately, the Young-Laplace equation cannot be solved analytically for the general case. Therefore, the solution method must rely on numerical techniques and interpolations. The classic solution to the Young-Laplace

equation was called the Bashforth-Adams equation, which relates the drop profile to the interfacial tension through a nonlinear differential equation given below:

$$\frac{1}{\frac{R_1}{a}} + \frac{\sin \phi}{\frac{x}{a}} = -B \frac{z}{a} + 2 \quad (2.2)$$

Where B is given by:

$$B = \frac{a^2 g \Delta \rho}{\gamma} \quad (2.3)$$

Here,  $\Delta \rho$  is the difference between the densities of the two immiscible liquids,  $g$  is the gravitational constant,  $\gamma$  is the interfacial tension,  $a$  is the radius of curvature at the apex of the drop,  $x$ ,  $z$ ,  $\Phi$  are the coordinates defined as in Figure 2.9, and  $R_1$  is the radius of curvature of the meridional section.

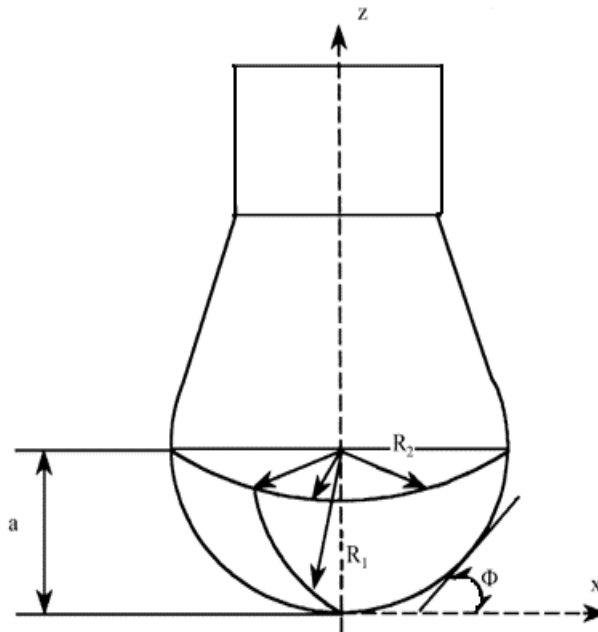


**Figure 2.9:** The pendant drop geometry.

Through simple geometric relations,  $R_1$  and  $\phi$  are given by:

$$\sin \phi = \frac{\frac{dz}{dx}}{\left[1 + \left(\frac{dz}{dx}\right)^2\right]^{1/2}} \quad (2.4)$$

$$R_1 = \frac{ds}{d\phi} = \frac{\left[1 + \left(\frac{dz}{dx}\right)^2\right]^{3/2}}{\frac{d^2z}{dx^2}} \quad (2.5)$$

In 1882, Bashforth and Adams derived the theoretical form of a pendant drop and calculated tables of drop contours; these shapes could be used to determine the interfacial tension by fitting the experimentally measured drop contour to the theoretical curve. Photographs of the evolving drop could be taken as a function of time for comparison. However, this procedure was very tedious. To simplify the procedure, the following empirical relationship was proposed by Andreas (1938):

$$\gamma = \frac{gD_e^2\Delta\rho}{H} \quad (2.6)$$

Here  $\gamma$  is the interfacial tension,  $\Delta\rho$  is the density difference,  $D_e$  is the equatorial diameter of the drop,  $H$  is a correction factor which is related to the shape factor of the pendant drop, and  $S$  is defined as:

$$S = \frac{D_s}{D_e} \quad (2.7)$$

In the above relation,  $D_s$  is the drop diameter measured horizontally at a distance  $D_e$  away from the apex of the drop. Stauffer (1965) and Fordham (1948) obtained the values of  $H$  by solving the Bashforth-Adams equation. The above

techniques have been discussed by Adamson (1976). A more elaborate method was proposed by Roe *et al.* (1967) which involves a series of  $S$  values,  $S_n$ , where:

$$S_n = \frac{D_n}{D_e} \quad (2.8)$$

Here,  $D_n$  is the horizontal drop diameter measured at a distance  $D_{\text{exn}}/10$ , (with  $n$  being an integer) from the apex of the drop.

Recent progress in image analysis and data acquisition systems has made it possible to obtain direct digitization of drop images with the aid of video frame grabbers and digital cameras (Girault *et al.*, 1982). The digital signals are analyzed, based again on the Young-Laplace equation, using different algorithms to determine the interfacial tension from the drop shape (Rotenberg *et al.*, 1983; Skinner *et al.*, 1989; Ramos *et al.*, 1993; Lin *et al.*, 1994).

#### *Micropipette method*

Recently, the micropipette technique was introduced to measure micron-scale interfacial tensions of individual emulsion droplets by exploiting the phenomenon of capillary instability (see Figure 5.1a; Yeung *et al.*, 1998). A single oil droplet in a water-continuous emulsion, with a diameter on the order of  $\sim 10 \mu\text{m}$ , is held at the tip of a micropipette by suction pressure through a connected syringe. As the suction pressure slowly increases, the projection of the drop,  $L$ , into the pipette (and hence the curvature of the oil/water interface) grows, until it eventually becomes a hemispherical cap of radius  $R_p$  and the maximum suction pressure  $P_{\text{max}}$  is reached; this is known as the point of capillary instability

( $L = R_p$ ). It is noted that  $P_{\max}$  is a direct measure of the oil-water interfacial tension and is obtained by the following equation (Evans and Needham, 1987; Yeung *et al.*, 1998):

$$P_{\max} = \frac{2\gamma_o}{R_p} \left( 1 - \frac{R_p}{R_o} \right) \quad (2.9)$$

From the hemispherical shape, if the suction pressure were to increase by even the slightest amount, the entire droplet would be drawn into the pipette over a very short time (typically of order microseconds); this is characteristic of a phenomenon known as capillary instability.

Interfacial tension (IFT) is the simplest rheological property of a fluid surface. All too often, this IFT is also the *only* property considered by researchers in multiphase flows. This limited view, unfortunately, can lead to incomplete understanding of many important processes, including the immiscible displacement of oil from porous media. For example, when dealing with MEOR systems, the accumulation of biosurfactants and/or bacterial cells at the oil-water interface will almost certainly give rise to *higher order* rheological properties, in addition to the IFT.

#### **2.4.1.2 High-order interfacial rheological properties**

To understand rheological properties that are “higher order” than the interfacial tension, one must first distinguish between the two independent modes of surface deformation: (a) dilation, which is the change in area of an interface at

constant shape, and (b) shear (more precisely, in-plane shear), which is the change in shape of an interface at constant area (Figure 2.10).

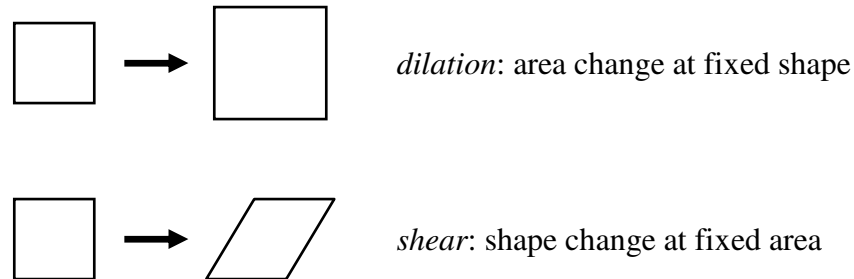


**Figure 2.10:** Schematic diagram of the two modes of surface deformation.

Associated with each mode of deformation are material properties such as elasticity (resistance to deformation) and viscosity (resistance to *rates* of deformation). Interfaces with adsorbed materials may also exhibit combinations of elastic and viscous behaviours, i.e. they can be “viscoelastic” (surface viscoelasticity is often prominent when macromolecules adsorb at the interface). In this study, we classify adsorbed interfaces into the following three general types:

- Type I: Simple interface. This is a surface with only an IFT (e.g. clean oil/water interface); it has negligible surface elasticity and viscosity. As noted above, most researchers who study multiphase flows simply consider this to be the only type of interface.
- Type II: Viscous surface fluid. Also known as the “Boussinesq surface fluid,” this is an interface which possesses an IFT, a dilational viscosity, and a shear viscosity (Plateau, 1869; Boussinesq, 1913). It is described by a two-dimensional analogue to the Newtonian fluid (Scriven, 1960; Evans

and Skalak, 1980; Edwards *et al.*, 1991). A viscous surface deforms at a rate proportional to the applied stress, but has no “memory” of its initial configuration.

- Type III: Elastic sheet. An interface which possesses an IFT, a dilational elasticity, and a shear elasticity (Evans and Skalak, 1980). It is formed when adsorbed materials cross-link or strongly associate with one another at the interface. Like a “Hookean spring,” the deformation of an elastic sheet is proportional to the applied stress.

In addition to these material properties, there are also other possible types of rheological behaviours. For each of the above interfacial material property, “constitutive relations” which relate surface stresses to surface deformations have been developed (Scriven, 1960; Evans and Skalak, 1980; Edwards *et al.*, 1991). These relations, which involve fairly complicated mathematics, are not essential to the present discussion and will not be included here.

#### **2.4.2 Previous studies in interfacial rheology of adsorbed molecules at oil/water interfaces**

Rheological studies of oil/water interfaces had been reported in many references in the literature. This may be due to the important relevance of this subject to technological processes such as enhanced oil recovery, foaming, emulsification, and detergency, and physiological processes such as alveolar stability and the mechanics of biomembranes. A quick reference to general rheological studies on oil/water interfaces is given below.

It is well known that interfacial dilational and shear properties are critical to processes in the oil industry, such as emulsion stability and multiphase flows. Elastic and viscous films have been observed in soluble adsorption layers and insoluble monolayers of surfactants on oil/water interfaces; various techniques have been developed to qualify and quantify the material properties of these surface films. Bartell and Neiderhauser (1949) used the pendant drop technique to observe the so-called “rigid skin” at crude oil-water interfaces upon retraction of an oil droplet in water. They also observed that the rigid skin (interfacial film) formation was accompanied by lowering of the interfacial tension, and thus concluded that the film was formed by an adsorption process. Reisberg and Doscher (1956) employed rigorously controlled anaerobic conditions during crude oil sampling and laboratory measurements to study interfacial film formation of crude oil-water systems. They found that the pH of the aqueous phase had strong effects on rigid film formation. Strassner (1968) further investigated the interfacial films in a crude oil/water emulsion system using the pendant drop technique. He noted that the interfacial film which stabilized the emulsions exhibited three distinct physical behaviours when compressed: rigid, soap-type or minimum film properties. Neustadter *et al.* (1979) demonstrated that the natural surfactants in crude oil could adsorb onto the oil/water interface and the interfacial film gave rise to modification of surface viscosity and elastic mechanical properties. However, using the pendant drop technique, it is very difficult to obtain accurate rheological properties.

The Langmuir film balance was developed to quantify the film pressure of insoluble surfactants as a function of surface area. This technique was applied to many oil/water systems and much useful information was obtained. Kimbler *et al.* (1966) studied the compressibility and collapse pressure of interfacial films formed at crude oil/water interfaces; Loglio *et al.* (1977) measured the film pressure of insoluble surfactants as a function of surface area; Jones *et al.* (1978) observed the elastic asphaltene films and quantified their viscoelastic properties; Ese *et al.* (1998) separated asphaltenes and resins from different crude oils, dissolved them in different paraffinic and aromatic solvents, and studied their rheological behaviors; Zhang *et al.* (2003) demonstrated that asphaltene molecules formed nanoaggregates at heptol-water interfaces and they also noted that the presence of demulsifier in the mixed monolayer rendered the adsorbed film more compressible at the heptol-water interface. In addition to the Langmuir film balance, researchers have developed other methods of studying interfacial rheology based on transient interfacial disturbance. Lucassen and van den Temple (1972) measured the dilational surface properties of solutions containing surface-active materials using the Wilhelmy plate method. To compare with van den Temple's results, Fang *et al.* (1995) obtained the modulus of elasticity for adsorbed decanoic acid monolayers from linear compression of the surface, also using the Wilhelmy plate. Based on the drop volume method developed by Gunde *et al.* (1992), Bhardwaj and Hartland (1998) measured the rheological properties of interfaces adsorbed with natural surfactants from crude oil, including the dynamic interfacial tension at the crude oil/water interface and dilational

modulus of such systems. This type of technique utilizes software-driven instruments which allow different types of area changes: step and ramp type, square pulse and sinusoidal area deformation. These methods have greatly improved the rheological studies on oil/water interfaces. However, they still have several drawbacks, such as the requirement of large amounts of surfactants, and it is more difficult to attain good environmental control when compared with some other techniques. (Kwok *et al.*, 1994)

In order to gain more insight into interfacial properties, Dodd (1960) developed an interfacial film viscometer and measured rheological properties of the oil-water interface; many subsequent studies have been conducted based on this work. Eley *et al.* (1987) measured the compressibility of crude oil/water interfaces using Brega, Kuwait and Tia Juana crude oils by the pendant drop method. They also studied the viscoelastic properties of interfaces using a surface rheometer working at low shearing stresses. It has been suggested that thick asphaltene films were responsible for the rapid elastic deformation and slow irrecoverable flow. Mohammed *et al.* (1993) demonstrated the importance of interfacial rheological properties (e.g. dilatational modulus) in determining the stability of water-in-Buchan crude oil emulsions with a biconical bob rheometer. They evaluated the effects of temperature and the presence of surface-active demulsifiers on film characteristics. They also made visual observation of interfacial skins upon compression of the asphaltenic crude oil/water interface which can be correlated with large shear viscosities that grew slowly in time. Mohammed *et al.* (1994) further evaluated the effects of different demulsifiers on

the interfacial rheology and emulsion stability of water-in-crude oil emulsions. Acevedo *et al.* (1998) also observed that ions in the aqueous phase played a significant role in dynamic interfacial tension of heavy crude oil-alkaline systems. The work by Li *et al.* (2002) with an interfacial viscoelastic meter revealed that crude oil fractions such as asphaltenes, resins and waxes gave rise to different rheological properties and affected the stability of emulsions in crude oil. They observed a good correlation between interfacial pressure, interfacial shear viscosity, interfacial primary yield value of the film, and the stability of crude oil emulsions. Spiecker and Kilpatrick (2004) used a biconical bob interfacial shear rheometer to study the mechanical properties of asphaltenic films adsorbed at the oil-water interface. Solutions of asphaltenes isolated from four crude oils were dissolved in a model oil of heptane and toluene and allowed to adsorb and age in contact with water. Their results directly related asphaltene chemistry to adsorption kinetics, adsorbed film mechanical properties, and consolidation kinetics.

More recently, Neumann and coworkers have developed a new approach to studying hydrocarbon-water systems using a motorized syringe system as well as a drop shape technique known as axisymmetric drop shape analysis (ADSA). This allows the dynamic surface tension of both static and oscillating interfaces to be measured with high accuracy (Rotenberg *et al.*, 1983; Boyce *et al.*, 1984; Cheng *et al.*, 1990; Cheng and Neumann., 1992). The ADSA method can produce definite area changes of the drop surface, which can be used to initiate transient relaxation processes. This approach has an additional advantage in that

it is possible to perform periodic area changes of arbitrary size. This is one of the advantages ADSA shares with the film balance. However, unlike the film balance, the ADSA technique has a more compact design and the ability to deal with both soluble as well as insoluble surfactants. This technique has become the most widely used method in exploring the viscoelastic properties of surface films formed at the oil/water interface. Following the work by Neumann and coworkers, many research groups had made similar contributions in this area. Susnar *et al.* (1993; 1996) were the first to investigate the effect of changes in the interfacial area on surface tension response for soluble surfactants. Using the oscillating pendant drop technique, Aske *et al.* (2002) measured the dilatational elastic modulus and dynamic interfacial tension of 21 crude oils and condensates originating from different production fields. They found that the measurements were greatly affected by solvent composition and oil concentration. In addition, both Aske *et al.* (2002) and Freer *et al.* (2003) noted that the dilatational moduli changed more substantially upon interface aging than does the interfacial tension; similar observations were found at the crude oil/water interface using a shear viscometer (Mohammed *et al.*, 1993; 1994). Radke and coworkers applied the oscillating pendant drop with axisymmetric drop shape analysis on different oil/water interfaces. They studied interfacial dilatation rheology to investigate the relaxation mechanisms of various interfaces, including the asphaltene-adsorbed toluene/water interface (Freer and Radke, 2004); this was the first study which showed that most of the surface-active asphaltenic molecules were irreversibly adsorbed from the oil phase. Radke *et al.* also demonstrated the effect of viscous

forces on the measurement of interfacial tension (Freer *et al.*, 2005). Other investigators also made important contributions in understanding the rheological properties of oil/water interfaces. Bouriat *et al.* (2004) investigated the properties of a two-dimensional asphaltene network at the water/cyclohexane interface with a time/temperature superposition principle. It was found that the asphaltene network, which was formed through a universal process of aggregation, exhibited a glass transition zone and behaved as a gel near its gelation point. Yarranton and coworkers (Sztukowski and Yarranton, 2005; Yarranton *et al.* 2007) correlated emulsion stability to interfacial rheological properties (e.g. the elastic and viscous moduli of the interface, surface pressure isotherms) between a dispersed water phase and a continuous phase of asphaltenes, toluene, and heptane using a drop shape analyzer. Yeung and Zhang (2006) also presented a theoretical model on the shear effects in interfacial rheology and their implications on oscillating pendant drop experiments.

Interfacial rheology has also been investigated for oil/water interfaces adsorbed with proteins, polymers, biosurfactants, colloidal particles, and other materials. Ward *et al.* (1980) demonstrated that, for the adsorption of bovine serum albumin (BSA), constant values of interfacial tension were reached after short time scales. Midmore (1998) described a novel method of stabilizing O/W emulsion by colloidal silica (Ludox) flocculated with the homopolymer hydroxypropyl cellulose and determined the rheological properties of the emulsion drops by a rheometer. Beverung *et al.* (1999) showed that the kinetics of adsorption of proteins display three distinct regimes. Freer *et al.* (2004) utilized

interfacial shear and dilatational deformations to study the rheology of several proteins at the hexadecane/water interface. Freer *et al.* (2005) also applied the oscillating drop technique to measure the interfacial dilatational properties of surfactant/polymer-laden fluid/fluid interfaces. Cohen and Exerowa (2007) studied the interaction behaviour and surface properties of microbial rhamnolipid type biosurfactants. A few recent reviews can be found related to this area (Arashiro and Demarquette, 1999; Wilde, 2000; Langevin, 2000, Bos and Vliet, 2001).

Almost all of the above-mentioned studies of interfacial rheology were performed at length scales of millimetres or larger (Edwards *et al.*, 1991; Miller *et al.*, 1996); these are orders of magnitude above the relevant length scale of emulsion drops. This has tremendous consequences when the specific surface area (i.e. surface area-to-volume ratio) of an emulsion is important. Yeung *et al.* (1998) used a novel micropipette technique, originally developed for the biophysical sciences (Evans *et al.*, 1980), to directly study micro-scale interfacial rheological properties. They had also demonstrated that the physical properties of “microinterfaces” can be quite distinct from their macroscopic counterparts (Yeung *et al.*, 1998). Yeung *et al.* (1999) studied the adsorbed layer formed at the surfaces of micrometre-sized emulsion droplets in diluted bitumen. Using the micropipette technique, the interfacial properties were examined, including adsorption, surface mechanical properties, and emulsion stability. Wu (2003), following the work of Yeung *et al.* (1999), investigated the stability mechanism of water-in-diluted bitumen emulsions through isolation and characterisation of the

stabilizing materials at the interface. Recently, Yeung's group applied the micropipette technique to further investigate the rheological properties of emulsified bitumen droplets, including the determination of surface tension and other interfacial properties (e.g. dilational elasticity, viscoplastic properties), and their effects on the stability of emulsified bitumen droplets.

In spite of the large amount of research which has been carried out to understand the role of interfacial rheology in the oil industry, very few papers can be found which relates micro-scale interfacial rheology to the displacement of oil from porous reservoirs. Although it is generally agreed that pore-scale interfacial phenomena are central to the macroscopic transport of oil in porous structures (expressed, for example, in terms of relative permeability and capillary pressure curves), there is as yet no satisfactory theoretical framework which links pore-scale (i.e. microscopic scale) surface rheology to macro-scale oil displacement. The study by Ehrlich (1993) represented an attempt to incorporate surface shear viscosities into highly idealized (and rather unrealistic) flow conditions. Dilational effects were not considered in the analysis, and it is not clear if the predicted relative permeability would be relevant to actual porous flow situations. The studies by Slattery and coworkers (Slattery, 1974; Giordano and Slattery, 1983; Ramamohan and Slattery, 1984) were valiant efforts to predict the dynamics of viscous surface fluids inside irregular pore structures; full constitutive relations were employed in their work. However, due to the complexities and high variabilities of actual pore channels, the authors acknowledged that their analyses were only approximate and qualitative (despite

the very advanced levels of mathematics that were invoked). Slattery had noted that interfacial viscosities had the effect of increasing the resistance to oil displacement, regardless of the wetting conditions (i.e. contact angles); and for oil displacement inside irregular pores, the interfacial dilational effects were likely much more important than its shear counterpart (Slattery, 1990). However, not enough studies have been performed to relate the elastic interfacial properties to the efficiency of oil displacement.

With this background knowledge, our study endeavours to (a) discern the interfacial rheology of hexadecane-water interfaces adsorbed with hydrophobic bacteria (being treated as solid particles) at millimetre scale (using pendant drop) and at micrometer scale (using micropipette), (b) relate the interfacial rheological properties to the nanometre bacterial cell surface properties, (c) present evidence of elastic interfacial properties in pore structure which appears in MEOR-related systems, and (d) correlate the properties of bacterial film at interfaces to the two-phase flow properties in porous medium .

## CHAPTER 3 EXPERIMENTAL APPROACH

### 3.1 Microbiological Methods

#### 3.1.1 Chemicals

*n*-Hexadecane (99% pure) was purchased from Sigma Chemical (St. Louis, MO) and was used as the oil phase for all the experiments in this study. All other chemicals were reagent grade, unless stated, and purchased from Fisher Scientific (Ontario, Canada).

#### 3.1.2 Bacterial strains

The hydrocarbon-degrading bacterial strains employed in this study were *Acinetobacter venetianus* RAG-1 and *Rhodococcus erythropolis* 20S-E1-c. *A. venetianus* RAG-1 (ATCC 31012), a Gram-negative bacterium, was originally isolated from a marine beach for growth on crude oil (Reisfeld *et al.*, 1972). It was initially identified as a member of the genus *Arthrobacter*, named *Acinetobacter calcoaceticus* and subsequently renamed as *A. venetianus* (Vaneechoutte, 1999). *R. erythropolis* 20S-E1-c is a Gram-positive bacterium and was isolated from marine sediment (Foght, 1999). Both bacterial strains are strictly aerobic and non-motile. In addition, they are metabolically versatile and can grow on a variety of carbon sources, including crude oil, aliphatic hydrocarbons, alcohols, organic acids, and other alkyl esters.

### 3.1.3 Growth condition

During our experiments, all the bacterial cultures were grown in Trypticase Soy Broth (TSB) from Difco Laboratories (Difco, Sparks, MD) which contains 17 g/L pancreatic digest of casein, 3 g/L papaic digest of soybean meal, 5 g/l sodium chloride, 2.5 g/L dipotassium phosphate, and dextrose. All growth media used in this study were prepared in distilled water, purified on a Milli-Q<sup>plus</sup> apparatus (Millipore) to a resistivity higher than  $18.2 \text{ M cm}^{-1}$ . Thirty grams of TSB was dissolved in 1 L of Milli-Q water and the solution was distributed in 250-mL Erlenmeyer flasks (100 ml each). To ensure that the prepared TSB was sterilized, all the flasks were plugged with cotton wool and autoclaved at  $120^{\circ}\text{C}$  and 15 psi for 15 min.

To prepare the bacterial cultures, the first step was to streak each bacterial strain which was suspended in glycerol in the freezer at  $-80^{\circ}\text{C}$  on the plate of Trypticase Soy Agar (TSA) from Difco Laboratories (Difco, Sparks, MD). The streaked plates were then incubated at  $28^{\circ}\text{C}$  for 3 days. They were stored in the refrigerator at  $4^{\circ}\text{C}$  and can be kept for 30 days.

Using a stainless steel loop, a vial of bacteria was then transferred from prepared agar plate to the autoclaved flasks. The flasks were then put in the incubator shaker (Innove 4000, New Brunswick Scientific) at  $28^{\circ}\text{C}$  under gyratory shaking at 200 rpm. Each culture was grown to its early stationary phase (i.e. no net increase or decrease in cell numbers occurs; Madigan and Martinko, 2006) which had been determined in preliminary tests. (Here, the incubating time was 18 h for *A. venetianus* RAG-1 and 50 h for *R. erythropolis* 20S-E1-c; the

growth curves for the two bacterial strain are shown in Appendix A.) The cells were harvested by centrifugation (IEC\* Multi and Multi RF\* High-Performance Centrifuge, Thermo Electron, Benchtop Centrifuges) at 6000×g for 2 min and washed twice with 0.01M phosphate buffer (pH 7). The harvested and washed cells were then re-suspended in 0.01M phosphate buffer (pH 7). Methods to determine the cell concentrations of the washed resting cells in buffer are given in the following sections. The fresh suspension was used immediately as the aqueous phase in subsequent experiments.

### **3.1.4 Growth measurements**

#### **3.1.4.1 Optical density**

Relative growth in culture tubes was monitored by measuring the optical density at wavelength of 600 nm ( $OD_{600}$ ) using a spectrophotometer (SPECTRA max PLUS<sup>384</sup>, Molecular Devices, Sunnyvale, CA) without diluting directly in the tubes. Growth data measured in this way are reported as “qualitative  $OD_{600}$ ” and are only compared within an experiment for a single bacterial strain. Before performing the experiments, the instrument was calibrated using 0.01M phosphate buffer (pH 7) as a blank reference. Since the cell concentration does not always increase linearly with the value of  $OD_{600}$  (especially when the cell concentration is high), this method can only be considered as a rough estimate of cell concentrations.

### 3.1.4.2 Dilution series

To determine the actual size of the bacterial population, the technique of dilution series was employed. The principle behind the dilution series is to dilute the concentration of bacteria per millilitre (mL) to a reasonable number (e.g. 200 – 2000 cells/mL; usually around 300 cells/mL). The experimenter then plates and counts the colonies (each colony represents one bacterium in the original population). Based on the number of colonies that are counted, the size of the original population can be calculated.

To create a dilution series, a group of test tubes (10mm outside diameter) containing 9 mL of 0.01M phosphate buffers (pH 7) were autoclaved. One mL of the cell broth was drawn up by a sterile 1 mL glass pipette and put into tube #1 containing the buffer. To have the solution well mixed, the tube was vortexed for approximately 5 seconds. Using the same method as stated previously, 1mL of the solution in tube #1 was removed into tube #2. This process was continued as needed until the bacterial solution reached the desired dilution level. Once the last buffer solution was created, only the solutions (0.1 mL) in tubes within the predicted colony range (usually the last two) were spread onto the TSA plates (triplicates). The colonies on the plates were counted after the plates were incubated overnight. The total number of bacterial cells in the original bacterial suspension could be calculated and expressed in terms of “colony-forming units” or CFU per mL (correlations between OD<sub>600</sub> and CFU/mL of bacterial cell suspension are shown in Appendix B).

### **3.1.5 Bacterial staining**

Individual bacterial cells are difficult to see, partly because they are small, but also because they are almost transparent. To make the bacterial cells clear under the optical microscope, we used a modified Gram stain method (a method to stain the cell by Crystal Violet and Iodine; Pierce and Leboffe, 1999) after the bacteria had been cultured to the early stationary phase as described above. First, a loopful of Crystal Violet was mixed with 2-3 loopfuls of broth culture and left for 1 min in a 1-mL tube. The cells were then separated by centrifugation at 6000×g for 2 min to remove the stain and then mixed with a loopful of Iodine for another 1 min. Finally, the cells were separated through centrifugation, rinsed with distilled water and allowed to re-suspend in phosphate buffer (0.01M, pH 7). After the staining procedures, the cells appeared to be deep purple in colour and were easily distinguishable under the microscope.

## **3.2 Physical Methods**

### **3.2.1 Surface and interfacial tension measurements by Wilhelmy plate**

The Wilhelmy plate method (Krüss K100) was used to measure the interfacial tension between *n*-hexadecane and spent buffer in the control tests. The plate consists of a thin rectangular piece of platinum of known perimeter (usually on the order of a few centimeters); the surface of the platinum plate is often roughened to ensure complete wetting. The plate is cleaned thoroughly by flaming and is attached to a scale or balance via a thin metal wire. The force on

the plate due to capillary forces is measured via a tensiometer used to calculate the surface tension (Figure 3.1).

### **3.2.2 Pendant drop technique**

A dynamic pendant drop device (First Ten Ångströms, Portsmouth, VA) was used to measure the hydrocarbon-water interfacial tension in response to area changes at room temperature (23°C). The pendant drop apparatus used in this study consists of three parts: an experimental cell, an illuminating and viewing system to visualize the drop, and a data acquisition system to determine the interfacial tension from the shape of the pendant drop. To minimize noise effects, the entire apparatus is placed on a TMC vibration isolation table and is confined in a plexiglass chamber. Figure 3.2 shows a photograph and a schematic diagram of the apparatus. To accomplish good accuracy during experimentation, it was always ensured that the blunt-end stainless steel syringe needle (20 gauge, i.e. 0.916mm outside diameter, 0.635mm inside diameter; Kontes Inc., NJ), PFTE tubing (0.869mm inside diameter, Action Electronics), and glass cell (Fisher Scientific) were all thoroughly cleaned. Data was recorded only when they were reproducible. The calibration process and the methods of measurement will be discussed in Chapter 4.

### **3.2.3 Transmission Electron Microscopy (TEM) test**

An accurate, rapid imaging technique for observation of microorganisms with nm resolution was developed by Albert Prebus and James Hillier at the University of Toronto in 1938 using concepts developed earlier by Max Knoll and

Ernst Ruska (Gunning and Calomeni, 2000). Using transmission electron microscopy (TEM), a beam of electrons is transmitted through a specimen. An image is then formed, magnified and directed to appear either on a fluorescent screen or layer of photographic film, or to be detected by a sensor such as a CCD camera.

In this study, the surface structures of bacterial cells that were grown as described above were examined using Philips/FEI (Morgagni) transmission electron microscopy with a CCD camera (TEM-CCD) at an acceleration voltage of 70 kV. Drops of cell suspension were allowed to settle on a 200-400 mesh on formvar-coated copper grids for 5 min until dried; the excess liquid did not need to be wicked off. Following this, the grids were negatively stained with 2% phosphotungstic acid (pH 6.8) for 1 min. After the grid was placed into the TEM, it was allowed to sit for a few minutes so that the sample could be vacuum dried before irradiation. The sample was then ready for viewing and images could be recorded. Observations of the two bacterial strains with TEM showed fundamental difference in the cell surface structures at the nanometre scale, which in turn would explain their different behaviours on the millimetre and micrometre scales (see discussion in Section 4.3.4).

### **3.2.4 Emulsion preparation**

In this study, the aqueous phase comprised suspensions of bacterial cells (either type of bacterial strains as described above) in phosphate buffer; *n*-hexadecane (99% pure; Sigma Chemical Co.) was used as the oil phase. Oil-in-

water emulsions were prepared with low shear agitation by simply shaking 4 mL of the aqueous phase with 1 mL of *n*-hexadecane by hand in a test tube for 1 min; emulsions were prepared at both high and low cell concentrations for either bacterial strain. For high cell concentrations, we chose  $2 \times 10^9$  CFU/mL for *A. venetianus* RAG-1, and  $10^9$  CFU/mL for *R. erythropolis* 20S-E1-c, respectively as the aqueous phase. For low cell concentration, a concentration of  $5 \times 10^6$  CFU/mL was used for both bacterial strains. The emulsions were allowed to equilibrate for 5 min before the IFT and dilational rheological properties were examined using the micropipette technique (tests were done on individual emulsion droplets). For the pendant drop study, the equilibration time was chosen such that the duration was sufficiently long for development of bacterial films at the interface, but short enough to avoid reactivation of the absorbed cells (which, with their newfound access to hydrocarbon nutrients, may be reactivated and begin to release biosurfactants); this will be further discussed in Chapter 4.

### **3.2.5 Microscope and micropipette technique**

Using optical microscopy, the oil-water interface can be directly observed. A drop of stained cell suspension was first put on a glass slide; this was then covered entirely with hexadecane to create an oil/water interface. The interface was observed under an inverted microscope (Axiovert 100; Carl Zeiss, North York, Canada) equipped with a 100 $\times$  objective lens. To observe the oil-in-water emulsion, about 20  $\mu$ L of dispersed droplets was put in a small sample cell and was observed with 63 $\times$  or 40 $\times$  objectives.

Originally developed in the field of biophysics for studying blood cells and surfactants membranes, the micropipette technique has been adapted for applications in other areas of colloid science (Moran *et al.*, 1999; Yeung *et al.*, 2000). This technique directly measures interfacial mechanical properties *in situ* on dimensions of micrometres (which are representative of the pore sizes in MEOR applications). The micropipette system consists of an inverted microscope (Axiovert 100; Carl Zeiss Canada) which is connected to a video system (CCD camera, videocassette recorder, and TV monitor) to monitor the micropipette experiment in real time (Figure 3.3). The micropipettes were mounted on and controlled by hydraulic micromanipulators (Narishige, Tokyo, Japan). The manufacturing of micropipettes and the determination of interfacial mechanical properties will be discussed in Chapter 5.

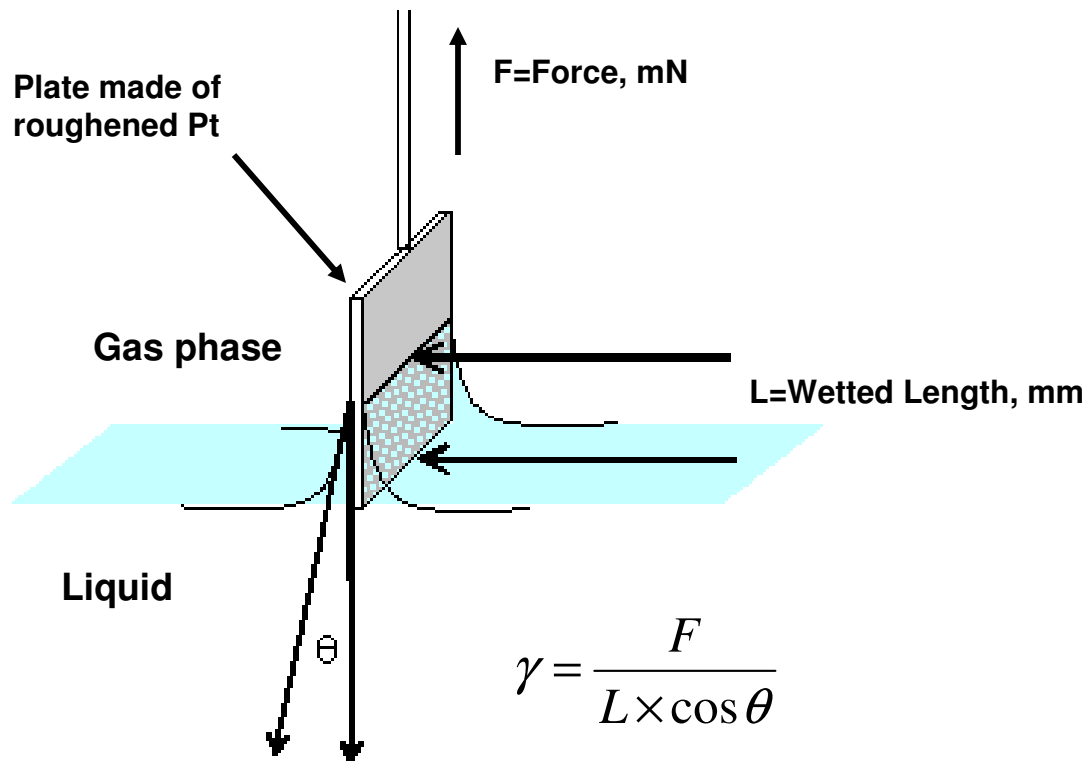


**Figure 3.1:** A schematic of the Wilhelmy plate apparatus.

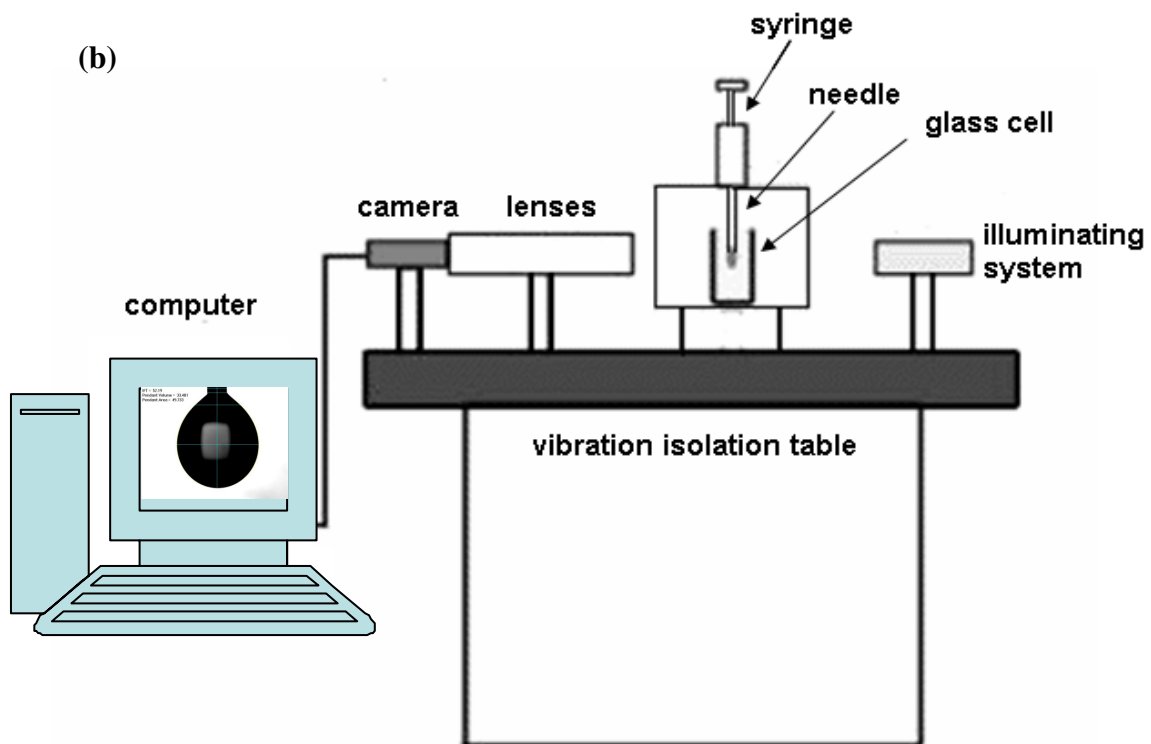


**Figure 3.2:** Photograph (a) and diagram (b) of the pendant drop apparatus for a water drop suspended in *n*-hexadecane. It consists of three parts: an experimental cell, an illuminating and viewing system to visualize the drop, and a data acquisition system to determine the interfacial tension from the shape of the pendant drop.

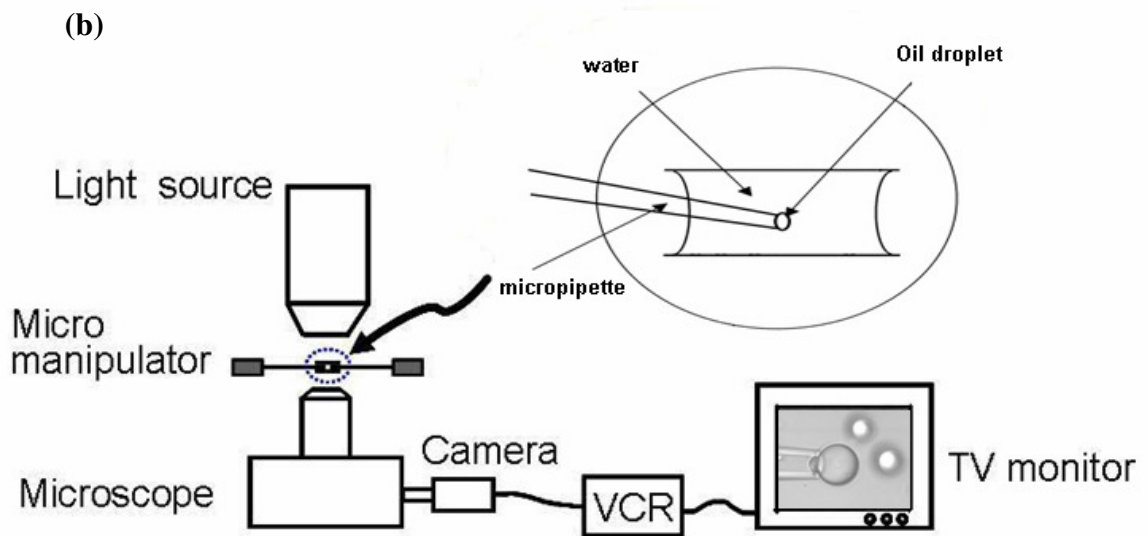
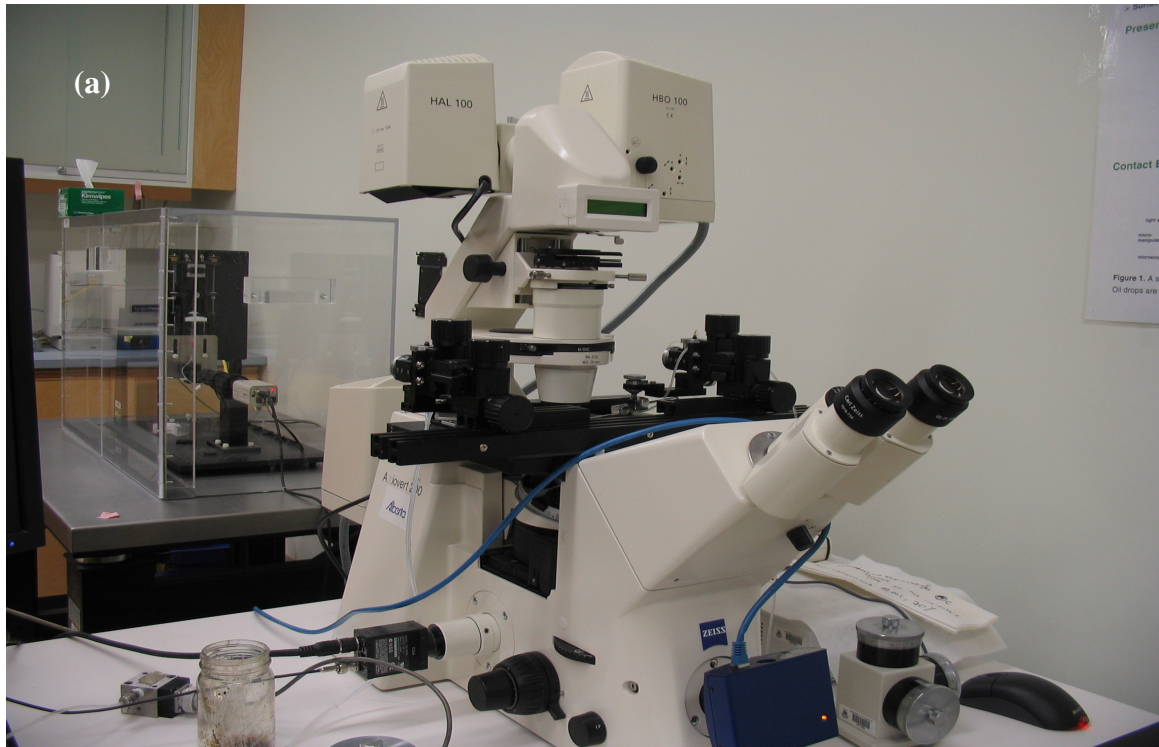


**Figure 3.3:** Photograph (a) and diagram (b) of the micropipette apparatus for an experiment with oil-in-water emulsions. An emulsion sample was placed in a small sample cell. The suction pipette can manipulate individual oil droplets. Using an inverted microscope, the experiment was monitored in real time and recorded on video.

## CHAPTER 4 INTERFACIAL RHEOLOGY ON THE MILLIMETRE SCALE: PENDANT DROP TECHNIQUE\*

### 4.1 Introduction

Certain hydrophobic bacterial strains are known to attach readily onto oil/water interfaces and play important roles in petroleum-related applications such as microbial enhanced oil recovery (MEOR) and bioremediation. Since bacteria can often only grow in the aqueous phase, the only way for them to access the liquid hydrocarbon is at the oil/water interfaces. These bacteria have shown the ability to emulsify oil-water mixtures in order to attain maximum oil/water interfacial area. For this, the microbes must effectively modify interfacial properties so that emulsification would occur and be maintained.

In this chapter, experimental results based on the pendant drop technique will be discussed. The objective of these experiments is to investigate the mechanical properties of hydrocarbon/water interfaces that have been adsorbed with intact resting bacterial cells; the extent of the interfacial area will be on the millimetre scale. As mentioned in Chapter 1, the bacterial strains used in this study (*A. venetianus* RAG-1 and *R. erythropolis* 20S-E1-c) represent two major classes of bacteria — Gram-negative and Gram-positive — which were originally identified on the basis of their 16SrRNA gene sequences shown by cell Gram stain. Here, the cells were repeatedly washed and re-suspended in phosphate buffer to remove the growth medium and halt cell division. Due to the

---

\* Major portion of this chapter has been published: Z. Kang, T. Yeung, J. Foght and M. Gray, "Mechanical properties of oil/water interfaces with adsorbed hydrophobic bacteria," Colloidal & Surface Science B, 62, 273–279, 2008

hydrophobic nature of the cell surface, the bacteria were able to attach to the oil/water interface and self-assemble into a “surface skin.” In this study, the timing was deliberately arranged such that the bacterial cells were in their non-growing state (see Section 3.1). In such a state, the cells behaved in essence as soft, inanimate colloidal particles. Interfacial mechanical properties were examined on the millimetre scale using the dynamic pendant drop technique. In addition, the cell surface ultrastructures were studied using transmission electron microscopy (TEM). The findings have been correlated with macroscopic interfacial properties. Knowledge of interfacial mechanical properties is needed, for example, in the modelling of small oil droplets passing through constricted channels (with relevance to MEOR and bioremediation applications).

## **4.2 Materials and Methods**

### **4.2.1 Sample preparation**

The oil phase in the experiments was chosen to be *n*-hexadecane and the aqueous phase was phosphate buffer with suspended bacterial cells. The method of preparing the aqueous phase was discussed in Section 3.1.3.

### **4.2.2 Control experiments**

Before carrying out pendant drop experiments, two control experiments were performed to determine whether the cells would release extracellular compounds (i.e. biosurfactants) which would affect the oil/water interfacial tension. Our aim is to avoid the added complexity brought on by biosurfactants;

we wish to view the resting cells as passive colloidal particles that are adsorbed at the oil/water interface.

In the first experiment, washed resting cells were kept in buffer for a period of time and the cells were separated by centrifugation in order to obtain the upper spent buffer. Interfacial tension (IFT) between the spent buffer and *n*-hexadecane was measured by the Wilhelmy plate technique (Krüss K100). In the second experiment, *n*-hexadecane and a cell suspension were mixed in a shaker for 4 hours, and the oil and aqueous phases were separated by a funnel. The cells were removed from the aqueous phase by centrifugation to obtain the spent buffer and the IFT between the spent buffer and *n*-hexadecane was measured, again by the Wilhelmy plate technique.

#### **4.2.3 The pendant drop apparatus calibration**

In Section 3.2.2, the photo and sketch of the pendant drop device (First Ten Ångströms, Portsmouth, VA) has been shown. In the following, we will outline the calibration process and discuss the interfacial tension measurements.

The pendant drop apparatus should first be calibrated before actual measurements of interfacial tensions. This is a procedure to determine the accurate magnification of the CCD camera (i.e. the actual size of a captured image must be known). The calibration can be completed in three ways:

1. based on a known linear distance (e.g. diameter of the needle tip);
2. based on a known IFT (e.g. between pure fluids);
3. by directly setting the number of micrometres per pixel.

In this study, calibration was done using the first option — with a needle of known outside diameter. The tip width was measured with a micrometer. Using this known distance, a magnification calibration would be obtained.

After calibration and before the start of actual experimentation, the interfacial tensions of standard fluids (i.e. fluids with known IFT) were tested to verify that the calibration was done correctly. Below are comparisons of measured IFTs and their literature values (experiments were conducted at room temperature).

**Table 4.1:** Measured IFTs and their literature values

Fluid	Measured Value (mN/m)	Literature Value (mN/m)
Water-Air	$73.0 \pm 0.2$	72.8
Toluene-Water	$35.8 \pm 0.1$	36.0
<i>n</i> -Hexadecane-Water	$52.1 \pm 0.1$	52.5

#### 4.2.4 Interfacial tension measurements

The pendant drop apparatus is capable of directly measuring both static and dynamic IFTs (in response to area change) at constant room temperature. The experiment proceeded as follows: A drop of aqueous cell suspension, several millimetres in diameter, was formed at the tip of a blunt-end stainless steel syringe needle (20 gauge) while the entire assembly was immersed in *n*-hexadecane (the lighter phase) (Figure 4.1). Precise control of the drop volume — and hence the interfacial area — was effected through connection of the needle to a computer-controlled syringe pump. Interfacial tension (IFT) was determined from the gravity-distorted drop shape, i.e. by capturing the image of the distorted shape and fitting it to the Young-Laplace equation (equation 2.1). The instrument

functioned as a real-time analyzer, meaning that it could continually capture images of the distorted shape and recall any number of past images after “triggering” (i.e. the switching on of the image recording process). For each captured image, the process of determining the interfacial tension from the gravity-distorted drop shape consists of four steps: (a) capture and digitization of the image of the pendant drop; (b) extraction of the drop shape, determination of the radius of curvature at the apex which is necessary for interfacial tension calculation; (c) smoothing of the extracted shape of the drop using polynomial regression; (d) shape comparison between the theoretical and experimental drop shape, leading to determination of the interfacial tension value as a fitting parameter (the software performs this automatically).

This technique of measuring interfacial tension is applicable in static as well as dynamic situations. Strictly speaking, the IFT thus measured should be termed the *apparent* interfacial tension. This is because the Young-Laplace equation assumes implicitly that the IFT is a scalar quantity, whereas the tension in an adsorbed film may in reality be “tensorial,” i.e. it may exhibit different values in different surface directions (Yeung and Zhang, 2006). For equilibrium measurements, the pendant drop volume was held constant and the drop shape (and hence the interfacial tension) was monitored as a function of time. To study transient responses, it is possible, through programming of the syringe pump, to impose step or other types of changes to the interfacial area (i.e. by subjecting the oil/water interface to sudden or continuous dilation/compression); the resulting time-dependent interfacial tension could, as before, be obtained from drop shape

analysis. These static and dynamic experiments were conducted for both cell-free interfaces (as control experiments) as well as interfaces adsorbed with bacterial cells.

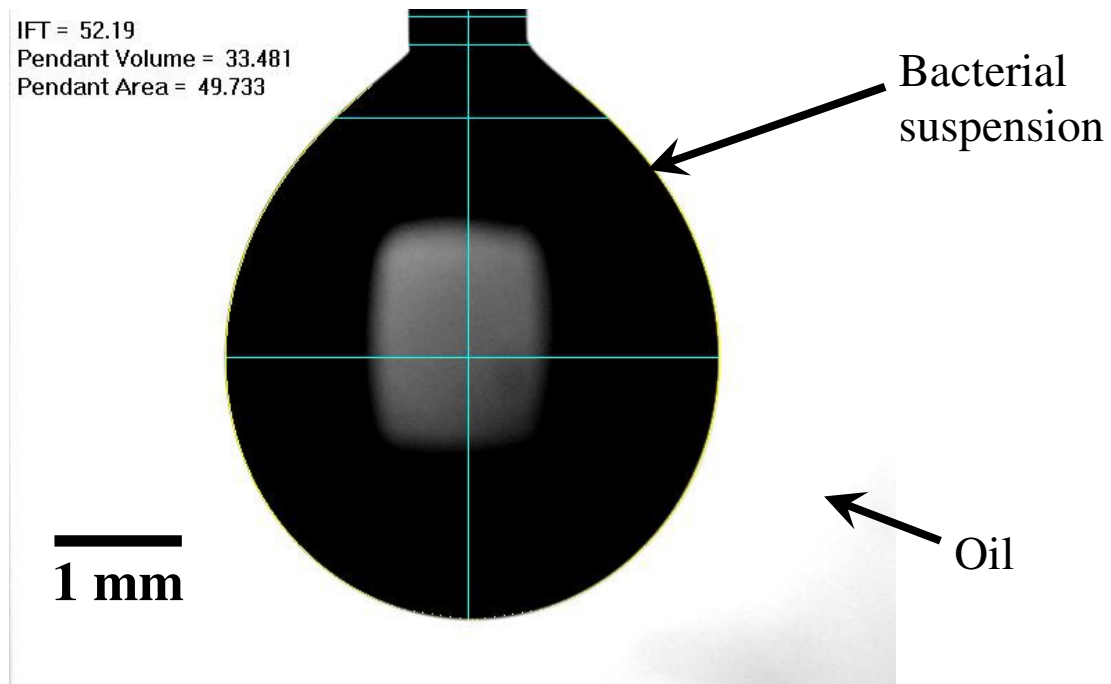


**Figure 4.1:** Photograph of an actual water drop in the pendant drop experiment.

## 4.3 Results and Discussion

### 4.3.1 Results for control experiments

In the first control experiment — the “blank reference” — the interfacial tension between *n*-hexadecane and the phosphate buffer (0.01M, pH 7) was determined to be 48.2mN/m. The results in Figure 4.2a indicated that the washed resting cells did not produce any surfactants in a period of hours. The results for the second control experiment are shown in Figure 4.2b. Here, the cells might

have produced some surfactants to lower the IFT as the cell suspension was in contact with *n*-hexadecane (acting as a carbon source) for a time span of hours. To avoid the influence of surfactants and to understand the behaviour of intact bacterial cells at the interface, all subsequent experiments in this study were conducted within a certain time window; the criterion for this would be established by the pendant drop technique discussed below.

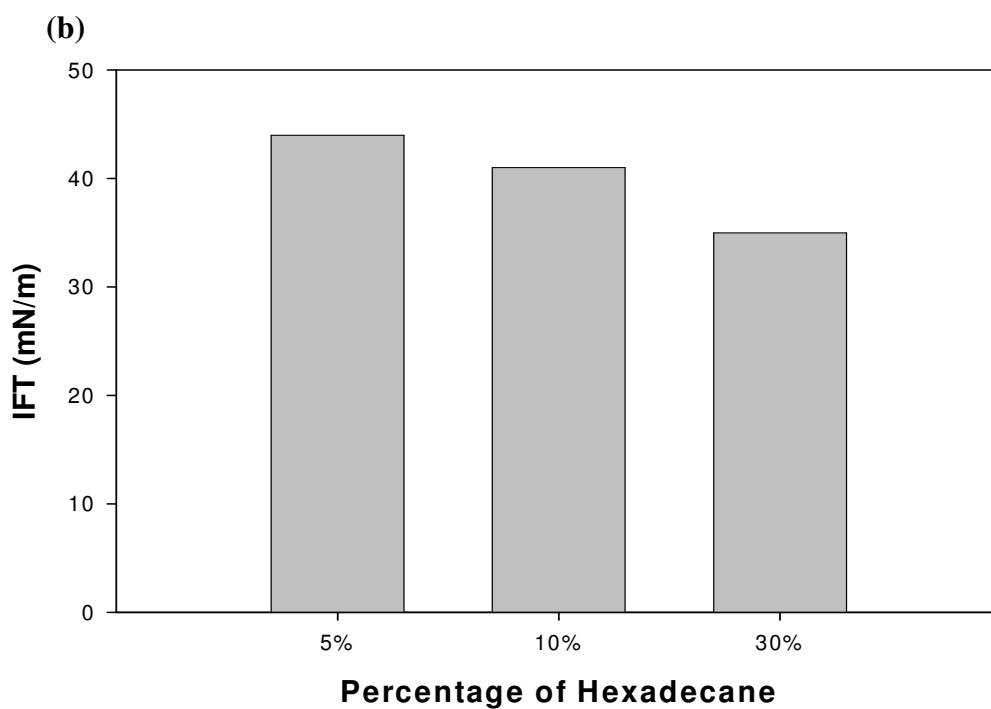
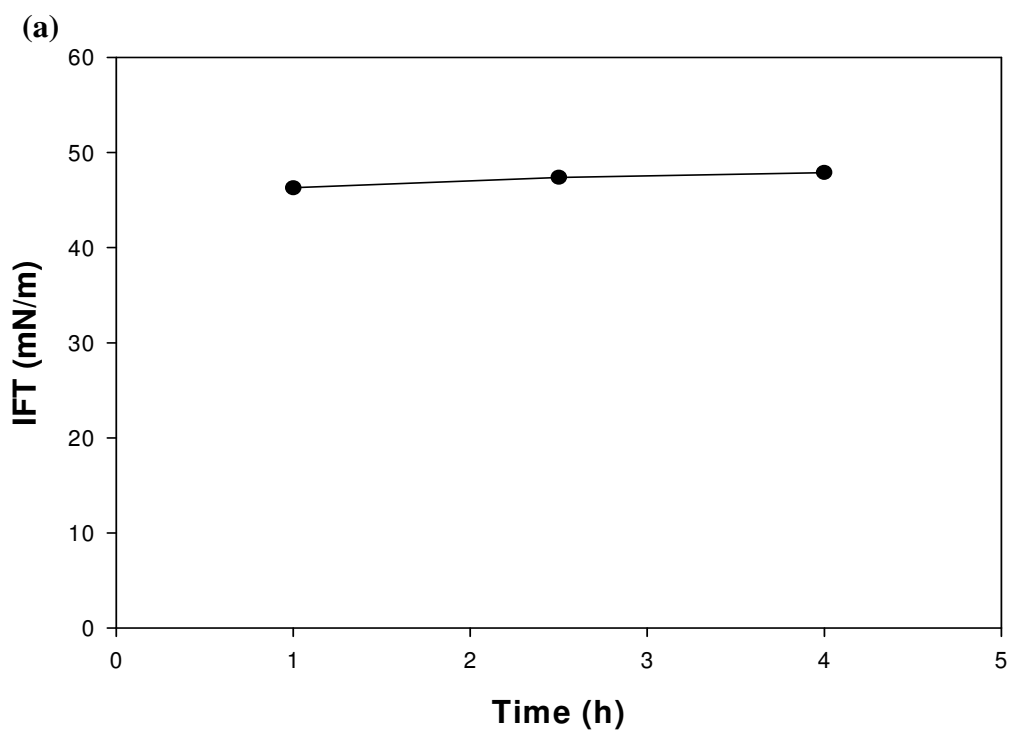


**Figure 4.2:** Results for control tests. (a) Interfacial tensions (IFTs) between RAG-1 cell-free spent buffer and n-Hexadecane. (b) Interfacial tension between cell-free spent buffer (from RAG-1 suspension) and hexadecane after suspension was agitated in hexadecane for 4 hours.

### 4.3.2 Results for cell-free interfaces

Before conducting interfacial tension (IFT) measurements on systems involving actual bacteria, tests were first made on cell-free interfaces. These were surfaces between *n*-hexadecane and a phosphate buffer (0.01M, pH 7), with the hydrocarbon being the continuous phase, and the aqueous buffer forming the pendant drop at the needle tip.

#### *Equilibrium IFT*

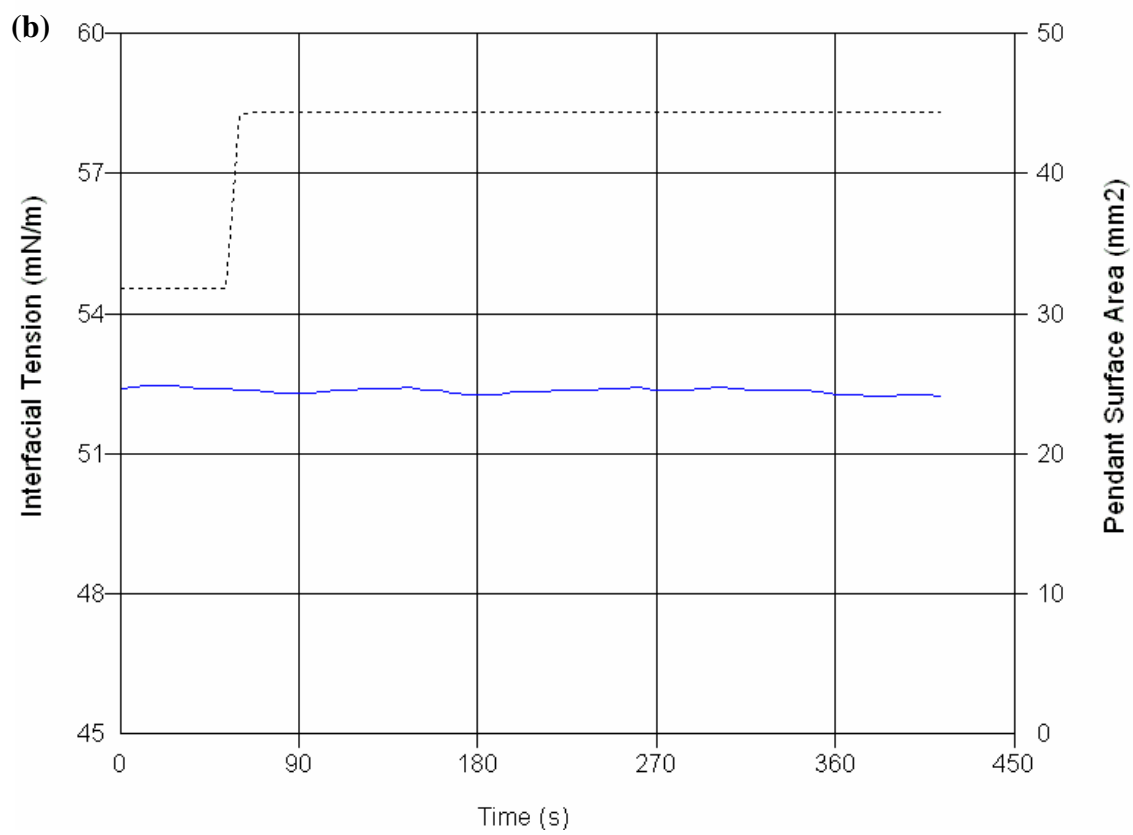
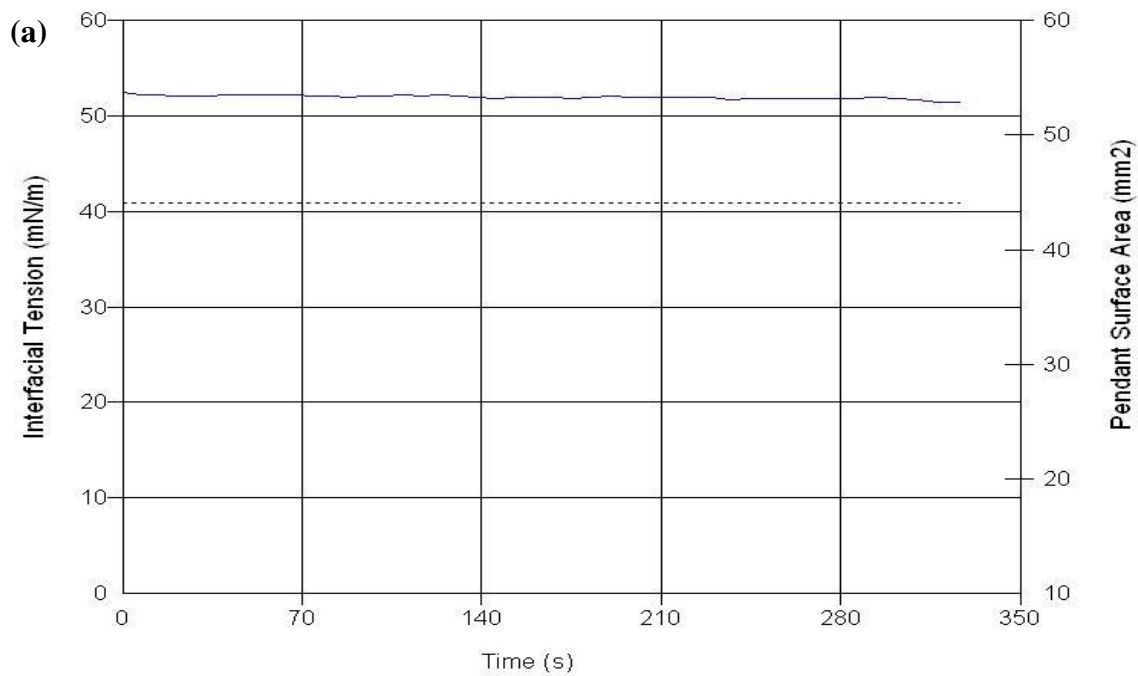
In the absence of suspended cells, the equilibrium interfacial tension was determined to be  $52.0 \pm 0.4$  mN/m (mean  $\pm$  standard deviation,  $n = 3$ ; Figure 4.3a). This value, as expected, was in agreement with published results in the literature (Lee, *et al.*, 2000).

#### *Dynamic IFT*

In addition, Figure 4.3b and 4.3c showed that the IFT was insensitive to both the magnitude and the rate of change of the interfacial area in the cell-free system, which was consistent with expectation and can be the references for the following results for interfaces adsorbed with bacterial cells.

It can be observed that there were small fluctuations of the data shown in Figure 4.3. The fluctuations were most likely the result of vibrations which distort the shape of the drop and noise resulting from mechanical vibration. The equilibrium tensions of the cell-free interfaces showed very slight (almost negligible) decreases over time. This subtle decline in interfacial tension may be

due to the slow buildup of surface-active impurities at the interface (Susnar *et al.*, 1993; Beverung *et al.*, 1999).



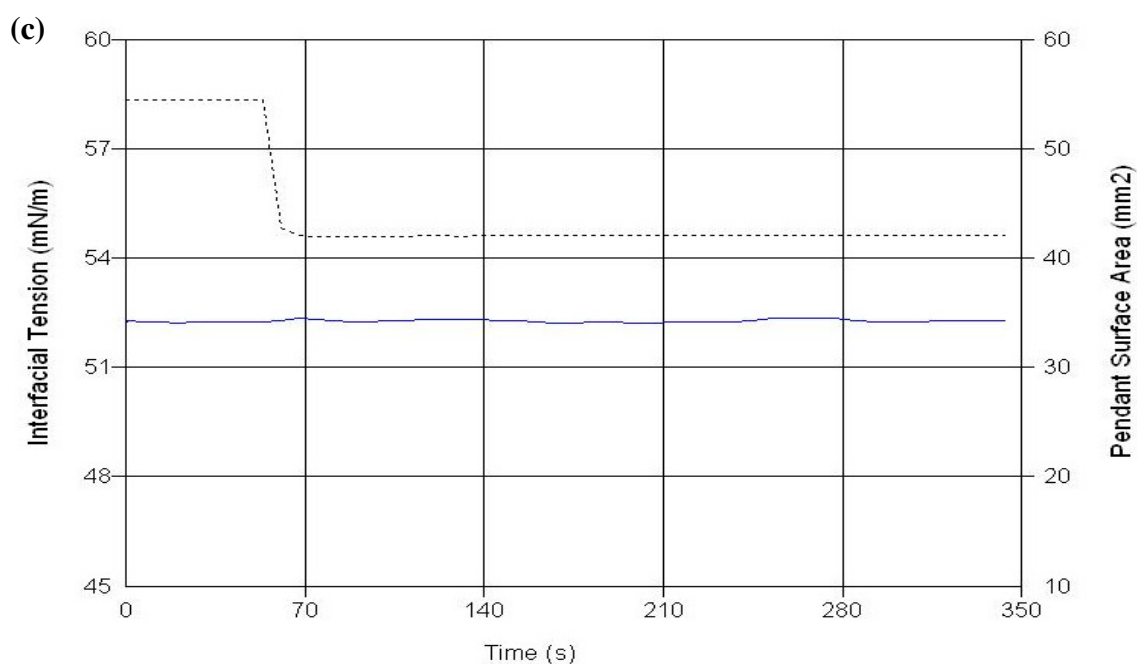


**Figure 4.3:** Pendant drop results for interfacial tension (solid line) vs. area (dashed line) for cell-free interfaces for cell-free interfaces with (a) static area, (b) step-up area and (c) step-down area.

#### 4.3.3 Equilibrium tension for interfaces adsorbed with bacterial cells

We now examine the interfacial tensions of surfaces that are adsorbed with bacteria. Both bacterial strains chosen for this study had the propensity to adhere to the oil-water interface and form a surface film (Dorobantu *et al.*, 2004). The adherence of *A. venetianus* RAG-1 to *n*-hexadecane is due in part to the presence of numerous thin fimbriae on its surface, composed of proteins with high proportions of hydrophobic amino acid residues and lipopolysaccharides (Rosenberg *et al.*, 1982) and, during the exponential growth phase, in part due to a cell-associated bioemulsifier (emulsan) that is sloughed off into the growth medium as the cells enter into stationary phase (Carla *et al.*, 2005). The *R. erythropolis* 20S-E1-c cells are also very hydrophobic because of the aliphatic

chains of mycolic acids covering the surfaces (Bell *et al.*, 1998; Mitani *et al.*, 2005). It has been found that the 20S-E1-c cells have a higher contact angle which suggests they are more hydrophobic, while the RAG-1 cells are more amphipathic due to the cell surface lipopolysaccharides (Rosenberg *et al.*, 1982; Dorobantu *et al.*, 2004).

Figure 4.4 shows the time dependence of the IFT between *n*-hexadecane and an aqueous suspension of *A. venetianus* RAG-1. The interface was formed at time  $t = 0$ , and the drop volume was kept unperturbed throughout the experiment. Although not shown here, similar static experiments involving the *R. erythropolis* 20S-E1-c bacteria resulted in plots that were very similar to Figure 4.4 (in regard to qualitative as well as quantitative features). As seen in Figure 4.4, when the interface was first formed (at  $t = 0$ ), the IFT was equivalent to the value determined in cell-free control experiments (i.e. Figure 3.3a, around 52 mN/m). This indicates that the interface was initially surfactant-free. Indeed, for the first 5 minutes, as the bacteria were allowed to accumulate at the oil-water interface, it is seen that the equilibrium IFT was only slightly lowered. As expected, the adsorption of bacterial cells at the interface, because of their relatively large sizes, did not significantly affect the equilibrium interfacial tensions. (To alter the IFT, there must be at least  $10^6$  adsorbed particles on every square micron of interfacial area; see Appendix C.) After 30 min, the equilibrium IFT was  $49.0 \pm 1.1$  mN/m for interfaces adsorbed with RAG-1, and  $48.5 \pm 1.5$  mN/m for interfaces with 20S-E1-c; these results are consistent with previous measurements on these bacterial strains (Dorobantu *et al.*, 2004; data based on 8 trials in each case). Following an

initial phase of relative invariance in the IFT, the tension began to fall (for  $t > 30$  min in Figure 4.4), suggesting the gradual release of biosurfactants by bacterial cells that were exposed to *n*-hexadecane (Snellman *et al.*, 2002; Leahy *et al.*, 2003). In this study, we wish to focus on the effects that intact, inactive bacterial cells have on the oil-water interface. Therefore, from the data of Figure 4.4 we selected a time window of between 5 min and 30 min of exposure of the cells to *n*-hexadecane for conducting our experiments (between the two bold vertical lines in Figure 4.4). Within this time window, we can safely assume that any modification of interfacial mechanical properties will be due entirely to the intact cells (behaving effectively as inanimate particles) and not to any surface active compounds released from the bacteria.

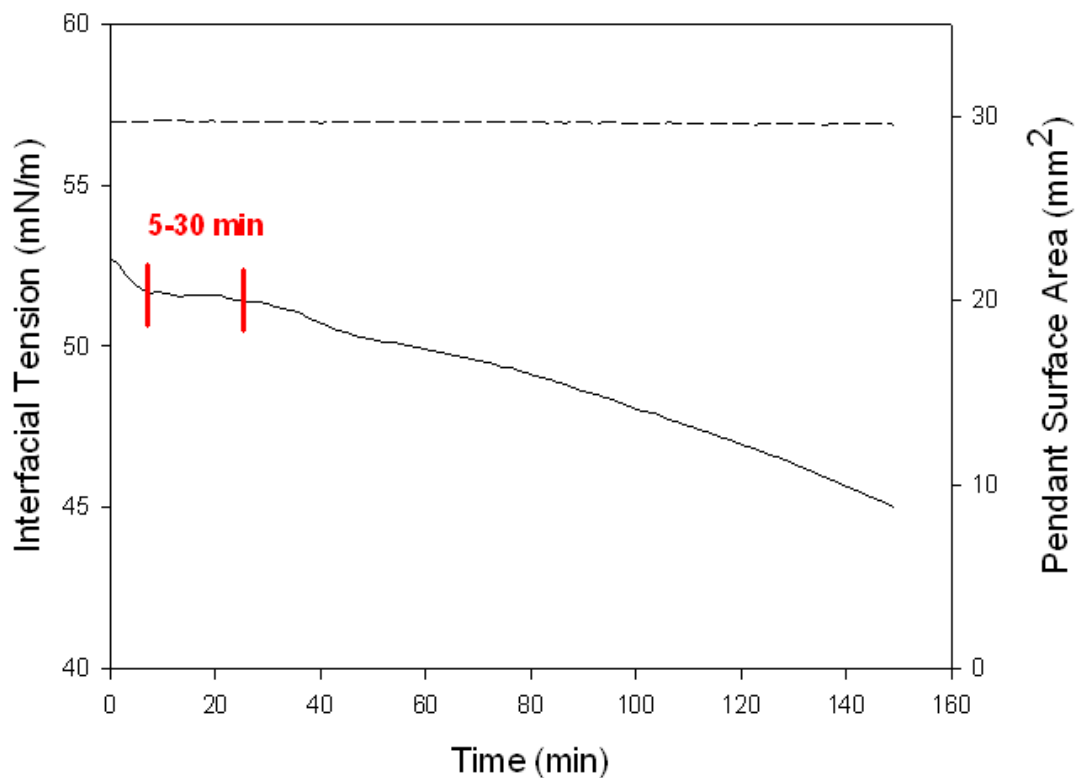


**Figure 4.4:** Evolution of the interfacial tension (solid line) as the drop surface area (dashed line) was held fixed. The interface was adsorbed with *A. venetianus* RAG-1 cells (cell concentration in bulk:  $2 \times 10^9$  CFU/mL).

#### 4.3.4 Two types of bacterial films and their relation to cell surface properties

Contrary to common interpretations, a constant value of IFT with time does not necessarily imply a “clean” oil-water interface. The existence of a bacterial film on the surface of a pendant drop is most clearly demonstrated by observing the drop behaviour during continuous reduction of its interfacial area. The results of such experiments are shown in Figure 4.5, where the volume of a water drop (containing either *A. venetianus* RAG-1 or *R. erythropolis* 20S-E1-c) was reduced while suspended in *n*-hexadecane. For both bacterial strains at relatively high cell concentrations ( $2 \times 10^9$  CFU/mL for *A. venetianus* RAG-1 and  $10^9$  CFU/mL for *R. erythropolis* 20S-E1-c), the cells self-assembled at the oil-

water interface in a closely packed array and formed a “surface skin.” The most striking difference between the two bacterial films was evident as the interfacial area was continuously reduced by withdrawing water back into the capillary. With the *A. venetianus* RAG-1 cells, the oil-water interface crumpled like a sheet of paper (Figure 4.5a). In the case of *R. erythropolis* 20S-E1-c, instead of showing wrinkles, the interface remained smooth throughout the deflation process. As the water droplet was withdrawn, the region near the needle tip grew progressively thinner (Figure 4.5b) until detachment occurred at the “neck.” This very unique phenomenon indicated the following results:

- Even though densely packed, the bacterial film showed no resistance to the “in-plane shearing” (i.e. shape change of the interface within the surface plane);
- The transient interfacial tension decreased precipitously as the surface area was compressed, and became so low that eventually it could not support the weight of the drop. Molecular biosurfactants had no influence in this situation, as all experiments were conducted within the time window illustrated in Figure 4.4. The behaviour in Figure 4.5b, in which the surface did not wrinkle upon in-plane shearing, could be characterized as “soap film-like.”

Whether an oil-water interface is “paper-like” or “soap film-like” would ultimately be determined by the interaction between adsorbed bacterial cells at the interface. Figure 4.6a shows a TEM image of *A. venetianus* RAG-1 with numerous thin fimbriae on the cell surfaces. These fimbriae, which are microns

in length, are remarkably strong in spite of their small diameters; they have been shown to be capable of withstanding forces in excess of 100 pN (Craig *et al.*, 2004). Here, we suggest that the RAG-1 bacteria on the interface could interlink with one another via the fimbriae and form a network which resisted in-plane shearing. As in the case of a sheet of paper, which comprises a network of interlinked wood fibres, any attempt to shear its surface (e.g. from a square into a parallelogram) will result in wrinkling. In contrast, for the 20S-E1-c cells seen in Figure 4.6b, their surfaces appeared much smoother. Here, when the interface was sheared, the smooth surfaces of the 20S-E1-c bacteria would likely facilitate free sliding between adsorbed cells, thus alleviating any buildup of shear strains and avoiding wrinkling. The distinct cell surface properties of two bacterial strains would explain some of the qualitative descriptions in rheological properties.

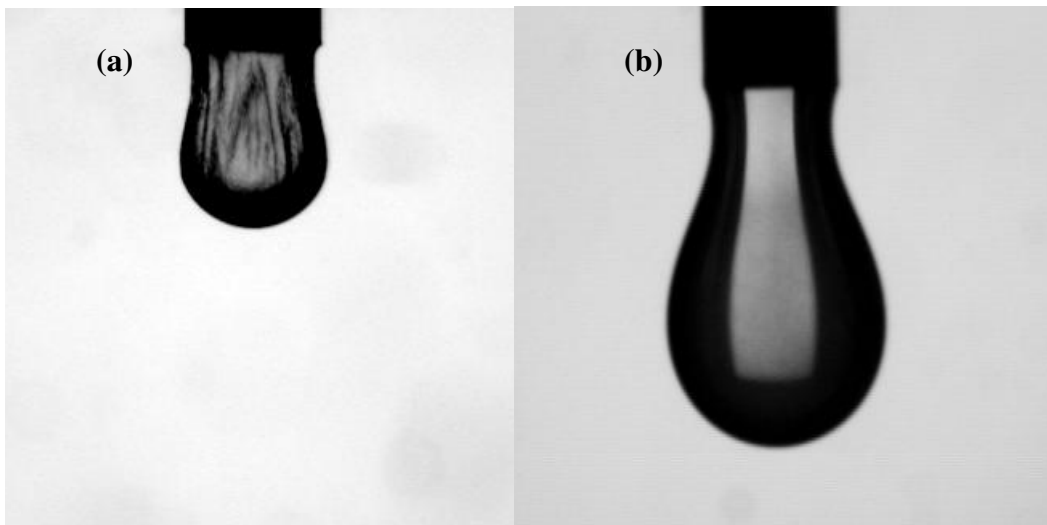


**Figure 4.5:** Bacterial films were formed at the surfaces of the two water drops in *n*-hexadecane (the needle has a diameter of 0.916 mm). (a) *A. venetianus* RAG-1 at  $2 \times 10^9$  CFU/mL, (b) *R. erythropolis* 20S-E1-c at  $10^9$  CFU/mL. The pictures show the observations as the drop volumes were reduced, during which the two surfaces exhibited strikingly different rheological behaviors.

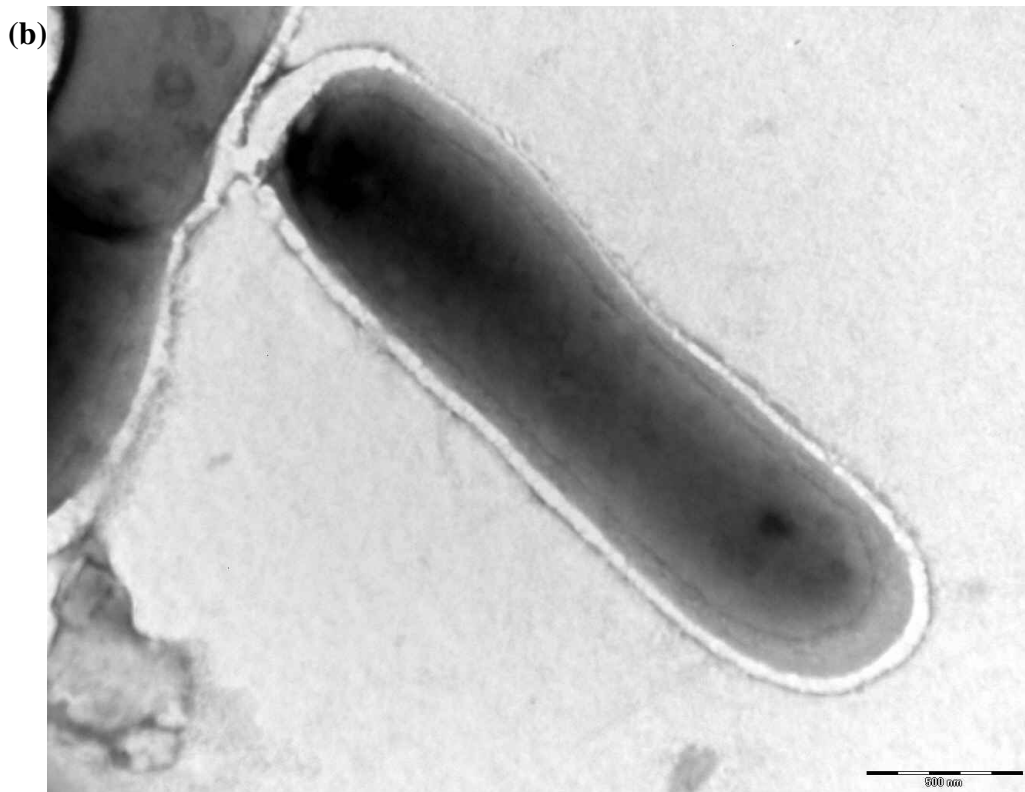
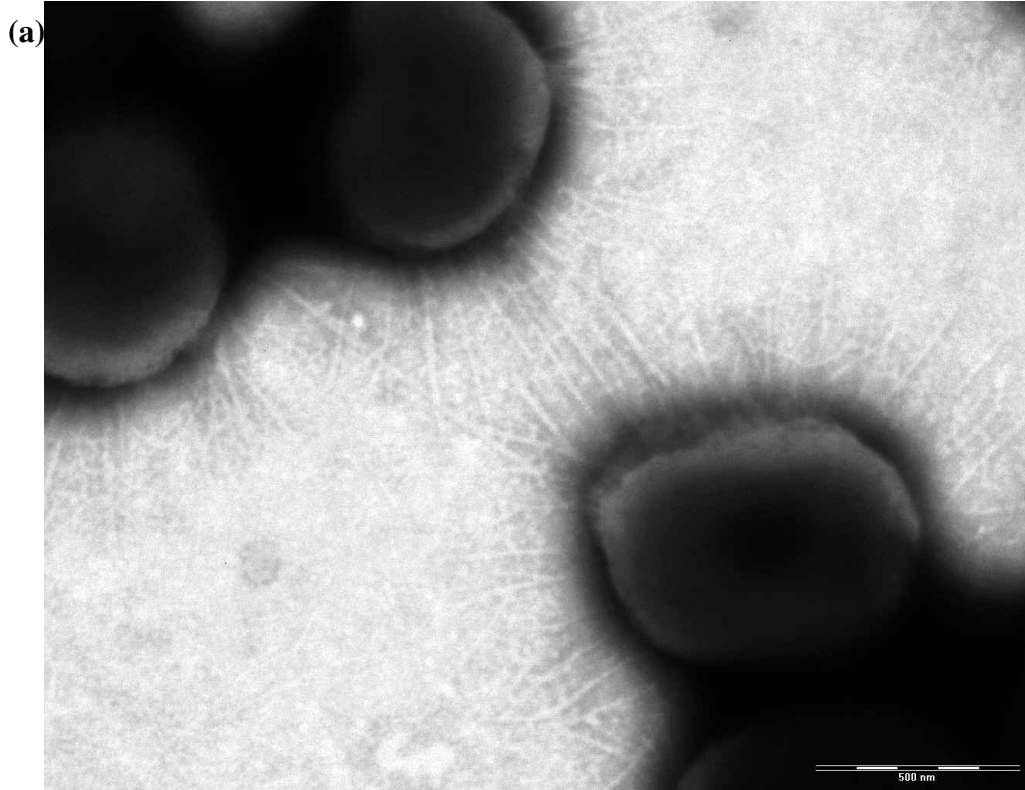


**Figure 4.6:** TEM images of negatively stained (a) *A. venetianus* RAG-1, and (b) *R. erythropolis* 20S-E1-c.

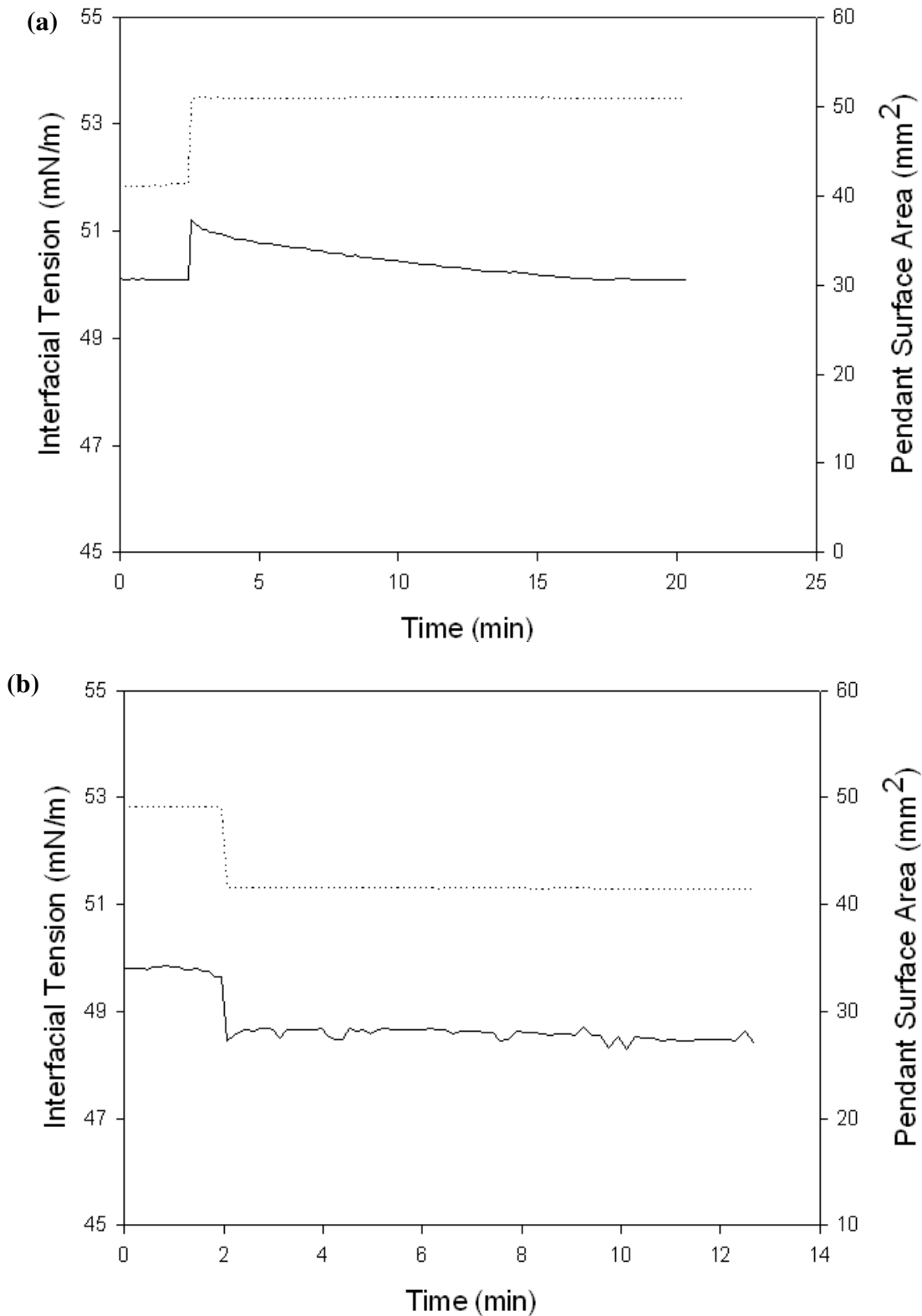
#### 4.3.5 Interfacial rheology revealed by step up/down of area excitations

Figure 4.5 depicts experiments which involved very large and continuous changes in interfacial area (three- to four-fold reduction); the resulting difference in rheological properties between the two strains of bacteria was striking. In contrast, for fractional area changes of about 50% or less, both types of adsorbed films displayed *qualitatively similar* features. Figure 4.7 and 4.8 show the dynamic IFT responses of the *A. venetianus* RAG-1 and *R. erythropolis* 20S-E1-c films to sudden area dilation and compression (the so-called “step-up” and “step-down” excitations) respectively; the droplet phase was the aqueous cell suspension, and the continuous phase was *n*-hexadecane. Upon step-up in area, the interface responded as a viscoelastic surface (specifically, a “Maxwell material,” which is characterized by an instantaneous rise in IFT, followed by a relaxation to its original equilibrium value; see Figure 4.7a and 4.8a). This recovery of IFT was not due to surfactant transfer from the bulk to the interface: as demonstrated earlier, biosurfactants were not important in this situation. When subjected to step-down excitation, the interface behaved as a two-dimensional elastic sheet: the tension decreased simultaneously with the area and remained “frozen” at the lowered value with no sign of recovery (Figure 4.7b and 4.8b).

It appears that, under “small” strains, both types of bacterial film possessed some form of surface elasticity. Moreover, there seems to be a mechanism of tension relaxation or surface rearrangement when the area per cell was suddenly increased. If the IFT recovery in Figure 4.7a (4.8a) were a result of cell transfer from the bulk to the interface (to fill in the empty spaces), it would

imply that the adsorption process is irreversible — since, in Figure 4.7b (4.8b), the IFT showed no sign of recovery upon area reduction (i.e. the cells could not “desorb” as they become more densely packed at the interface). Such a view is of course speculative at this point; more detailed experimentation will be needed to delineate the underlying mechanism(s) which lead to the behaviours in Figures 4.7 and 4.8. As a final note: for both step-up (Figs. 4.7a and 4.8a) and step-down (Figs. 4.7b and 4.8b) experiments, there was a minimum surface strain which must be exceeded before the tension response was repeatable. For surface strains below this level, the IFT response was erratic. The value of this minimum strain was  $\Delta A/A_0 \approx \pm 5\%$  for both bacterial films. This minimum strain suggests the possibility of a surface yield stress that is inherent in bacteria-adsorbed films.

The rheological properties of both types of bacterial film are considered “*non-linear*,” in that their responses to step-up and step-down excitations are not mirror images of one another. For adsorbed interfaces that respond “asymmetrically” to step-up and step-down excitations (Figures 4.7 and 4.8), it would not be appropriate to perform the harmonic tests that are often seen in traditional rheology studies (i.e. subjecting the system to sinusoidal excitations of different frequencies and determining the amplitude and phase responses); such tests are meaningful only for linear materials.



**Figure 4.7:** Responses of interfacial tension to step-strain deformations for interfaces adsorbed with *A. venetianus* RAG-1 (cell concentration:  $2 \times 10^9$  CFU/mL). (a) IFT (solid line) in response to step-up area (dashed line); (b) IFT (solid line) in response to step-down area (dashed line).

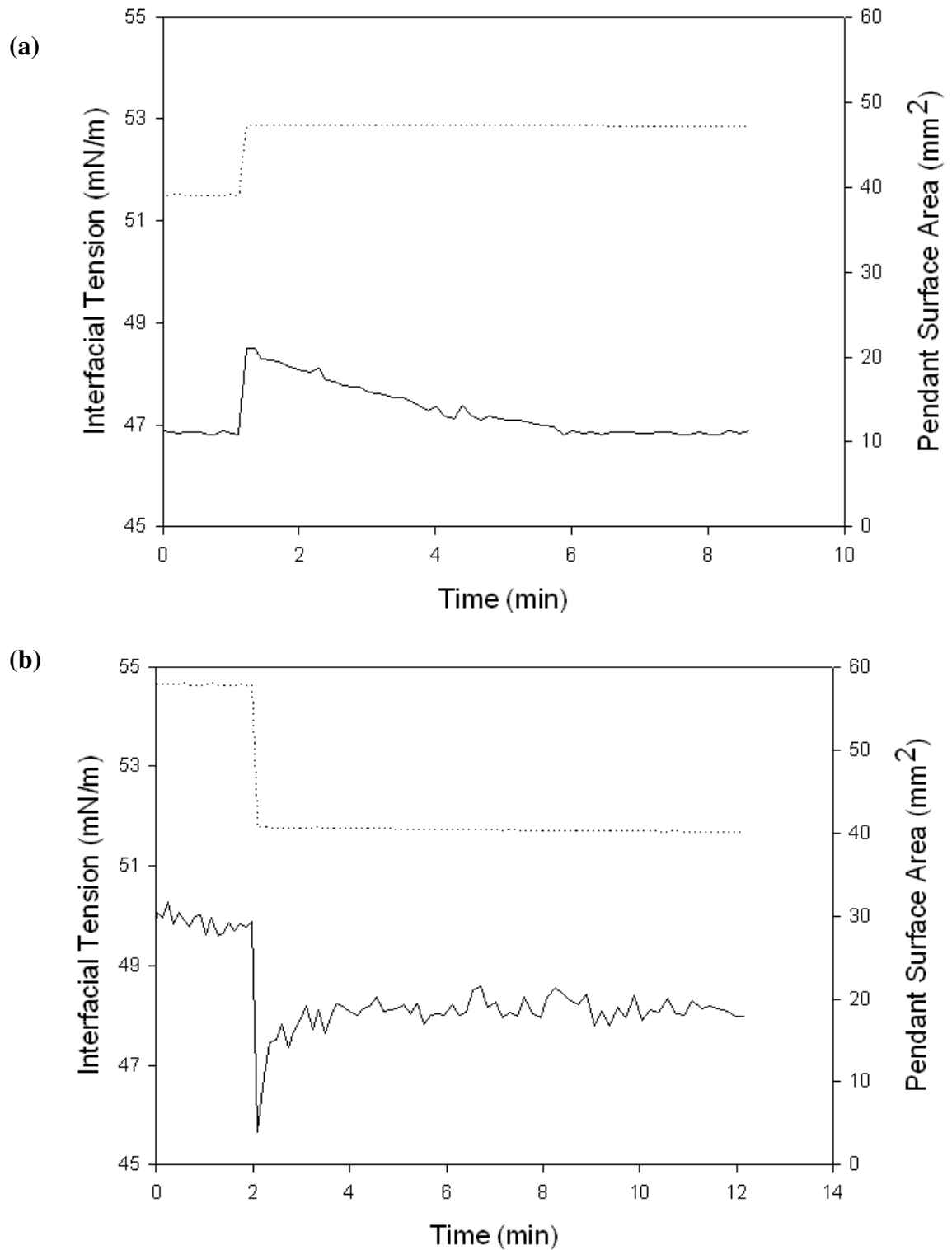


**Figure 4.8:** Responses of interfacial tension to step-strain deformations for interfaces adsorbed with *R. erythropolis* 20S-E1-c (cell concentration:  $10^9$  CFU/mL). (a) IFT (solid line) in response to step-up area (dashed line); (b) IFT (solid line) in response to step-down area (dashed line).

For the above experiments, we will quantify the interfacial mechanical properties based on the tension difference  $\Delta\gamma$  and the relaxation time  $\tau$ ; these quantities are defined as follows: The tension difference  $\Delta\gamma$  is taken as either (a) the instantaneous rise in IFT upon step-up excitation (see Figs 4.7a and 4.8a), or (b) the instantaneous drop in IFT upon step-down excitation (see Figs. 4.7b and 4.8b). Figure 4.9 shows plots of the tension difference  $\Delta\gamma$  versus the fractional area change  $\Delta A/A_0$  for both types of bacterial film ( $A_0$  is the initial area); for clarity, the step-up and step-down responses are plotted separately. All experiments in Figure 4.9a exhibited the behaviour depicted in Figs 4.7a and 4.8a, i.e. a rapid rise in IFT (by an amount  $\Delta\gamma$ ), followed by a relaxation process. Likewise, all experiments in Figure 4.9b exhibited the behaviour depicted in Figure 4.7b and 4.8b, i.e. a rapid drop in IFT (by an amount  $\Delta\gamma$ ) followed by *no recovery*. It is seen from Figs. 4.9a and 4.9b that the tension difference  $\Delta\gamma$  was roughly proportional to the fractional area change  $\Delta A/A_0$  for both bacterial strains. The slopes of these lines, defined as

$$E = \frac{d\gamma}{d\ln A} \quad (4.1)$$

for small strains, can be regarded as the “apparent elasticity” of the film. It is evident from Figure 4.9 that, for each bacterial strain, the elasticity  $E$  was significantly different for step-up and step-down perturbations (step-down excitation gave rise to apparently “stiffer” films). This asymmetry with respect to the two types of perturbations is another demonstration of the “non-linearity” of bacteria-adsorbed films.

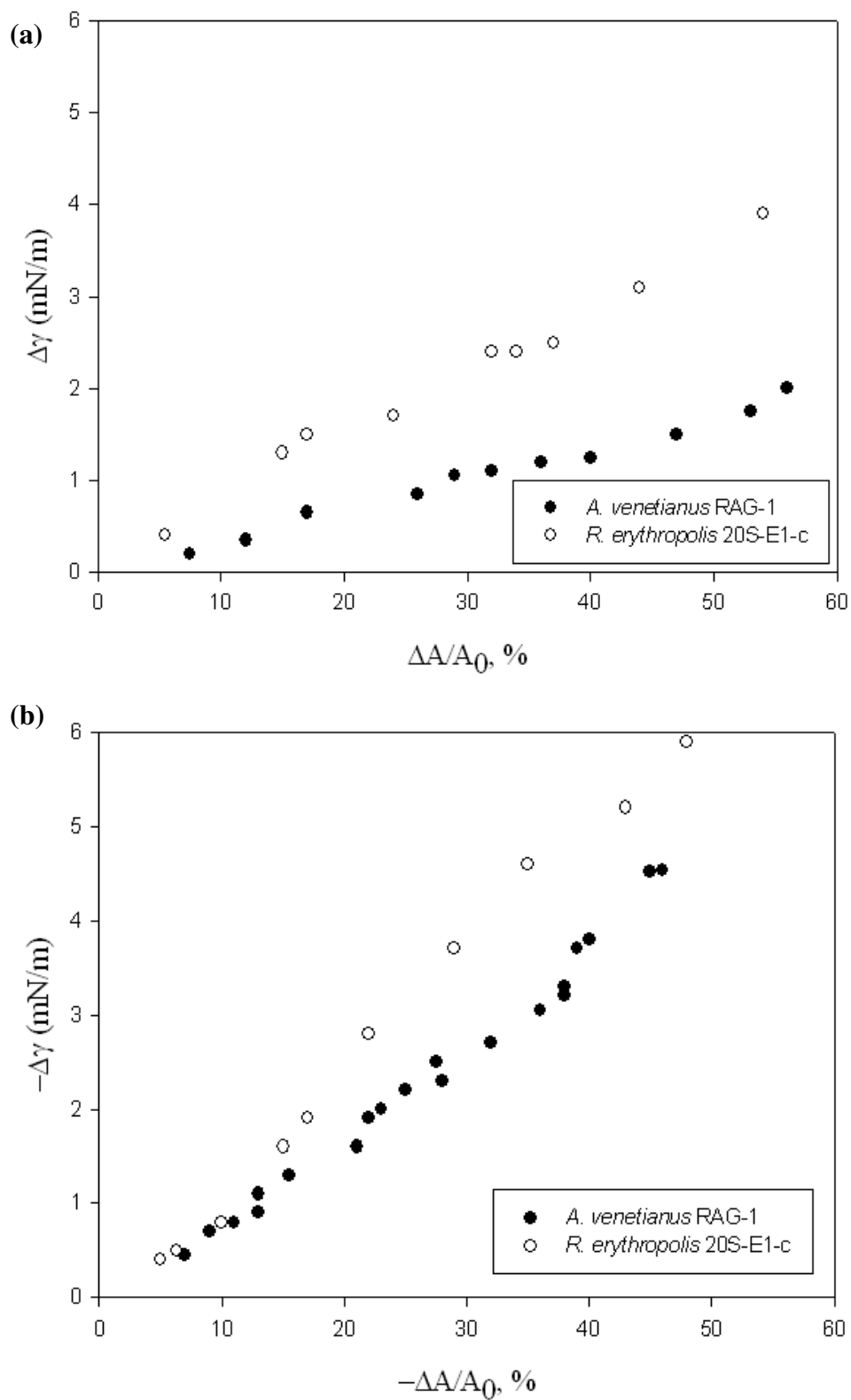


**Figure 4.9:** Effect of area perturbation on the interfacial tension for interfaces adsorbed with bacterial cells (cell concentration for *A. venetianus* RAG-1:  $2 \times 10^9$  CFU/mL; for *R. erythropolis* 20S-E1-c:  $10^9$  CFU/mL). (a) Step-up excitations; (b) Step-down excitations.

As shown in Figure 4.7a (4.8a), a step-up excitation was always followed by a relaxation in IFT. To first order, the process appeared exponential with a relaxation time  $\tau$  defined as:

$$\gamma - \gamma_0 = \Delta\gamma \exp(-t/\tau) \quad (4.2)$$

where  $\gamma$  and  $\gamma_0$  are, respectively, the instantaneous and equilibrium IFT. For each data point in Figure 4.9a, the parameter  $\tau$  was obtained by fitting the relaxation curve (plotted semi-logarithmically) to equation 4.2. The results, shown in Figure 4.10, are quite startling: It is seen that, for each cell type, the relaxation time  $\tau$  was independent of area dilation up to a certain threshold; beyond this threshold (approximate 40% for RAG-1 and 30% for 20S-E1-c), the value of  $\tau$  “jumped” to a different level. Equally intriguing is the trend seen in Figure 4.10: as  $\Delta A/A_0$  was increased, the relaxation time for the RAG-1 films jumped from a higher value to a lower one, while the opposite occurred for the 20S-E1-C films (i.e. from smaller to larger  $\tau$ ). If, for an adsorbed film, the parameter  $\tau$  could be regarded as a “gauge” of its internal mechanism of relaxation, then the discontinuities in Figure 4.10 must be interpreted as fundamental changes in the way internal stresses are relieved. Although intriguing phenomena are clearly occurring, no more conclusions can be drawn at present from the data in Figure 4.10. Further investigation is clearly advisable.

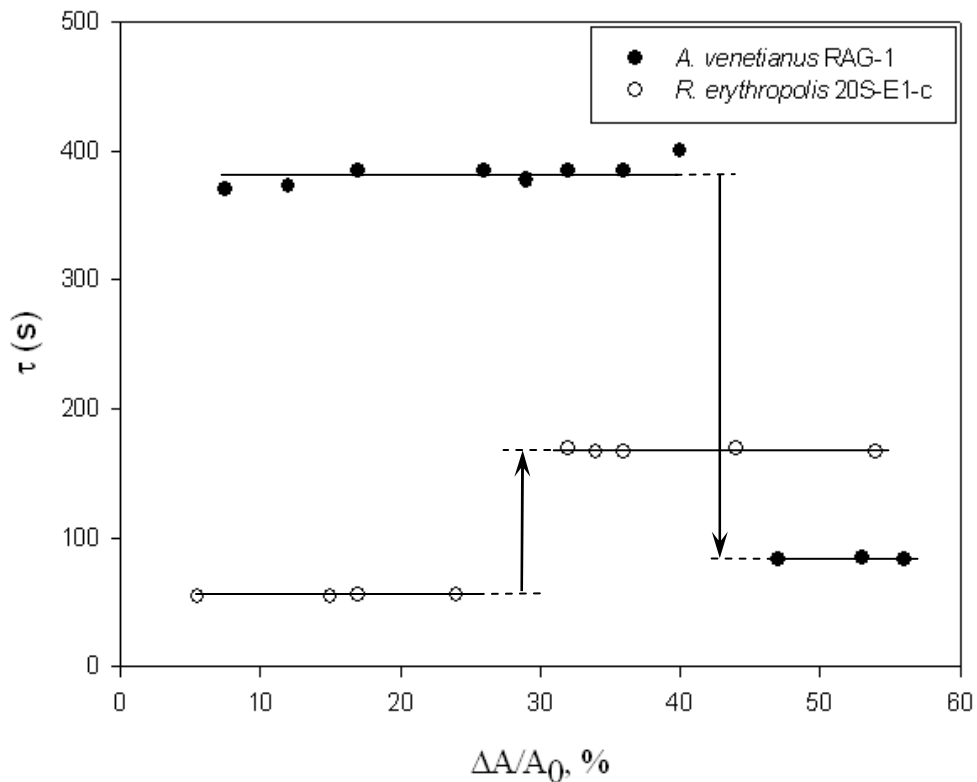


**Figure 4.10:** Effect of area perturbation on the relaxation time for interfaces adsorbed with bacterial cells (cell concentration for *A. venetianus* RAG-1:  $2 \times 10^9$  CFU/mL; for *R. erythropolis* 20S-E1-c:  $10^9$  CFU/mL).

Figures 4.11 and 4.12 show the effects of cell concentration on the apparent film elasticity for interfacial films with *A. venetianus* RAG-1 and *R. erythropolis* 20S-E1-c under step-up and step-down excitations, respectively. Both plots exhibited the same trends. Although not shown, every data point in Figs 4.11 and 4.12 corresponds to an experiment which had the same dynamic behaviour as depicted in Figure 4.7 or 4.8, i.e. a Maxwellian-type response to step-up excitation, and a purely elastic response to step-down excitation. As expected, the apparent film elasticity  $E$  (i.e. the slopes) diminished with cell concentration. The relationship between film elasticity and cell concentration (in the buffer) is summarized in Figure 4.13 for the RAG-1 film and the 20S-E1-c

film. For both step-up and step-down excitations, the elasticity first increases rapidly, then is followed by what appears to be an approach to an asymptotic limit. As pure speculation at this point, the curves in Figure 4.13 appear to resemble a classic Langmuir-type adsorption; this would imply both bacteria-adsorbed films to be comprised of a single layer cells.

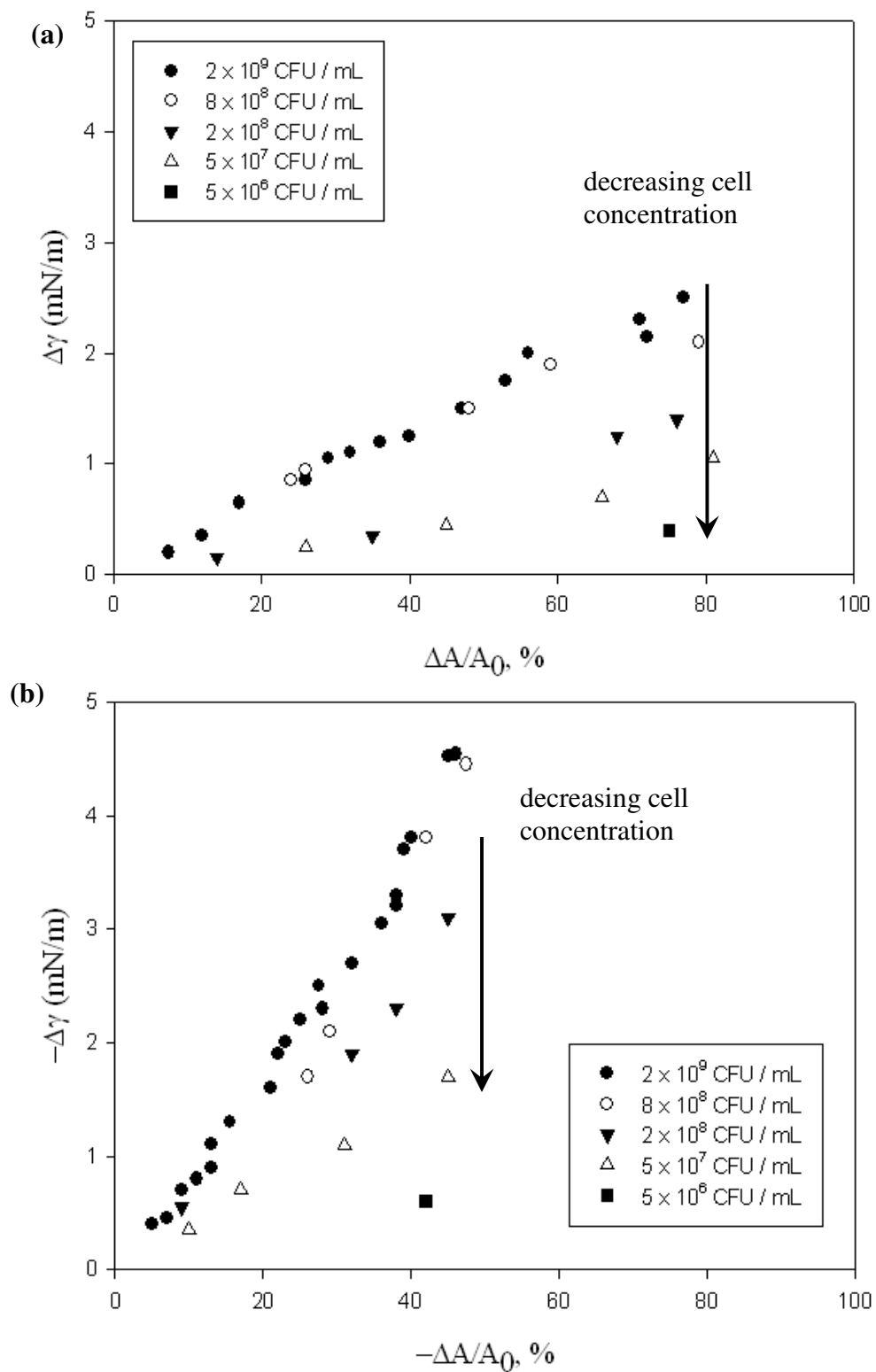


**Figure 4.11:** Effect of area perturbation and cell concentration on the interfacial tension for surfaces adsorbed with *A. venetianus* RAG-1. The trend lines show the decreasing cell concentrations. (a) Step-up excitations; (b) Step-down excitations.

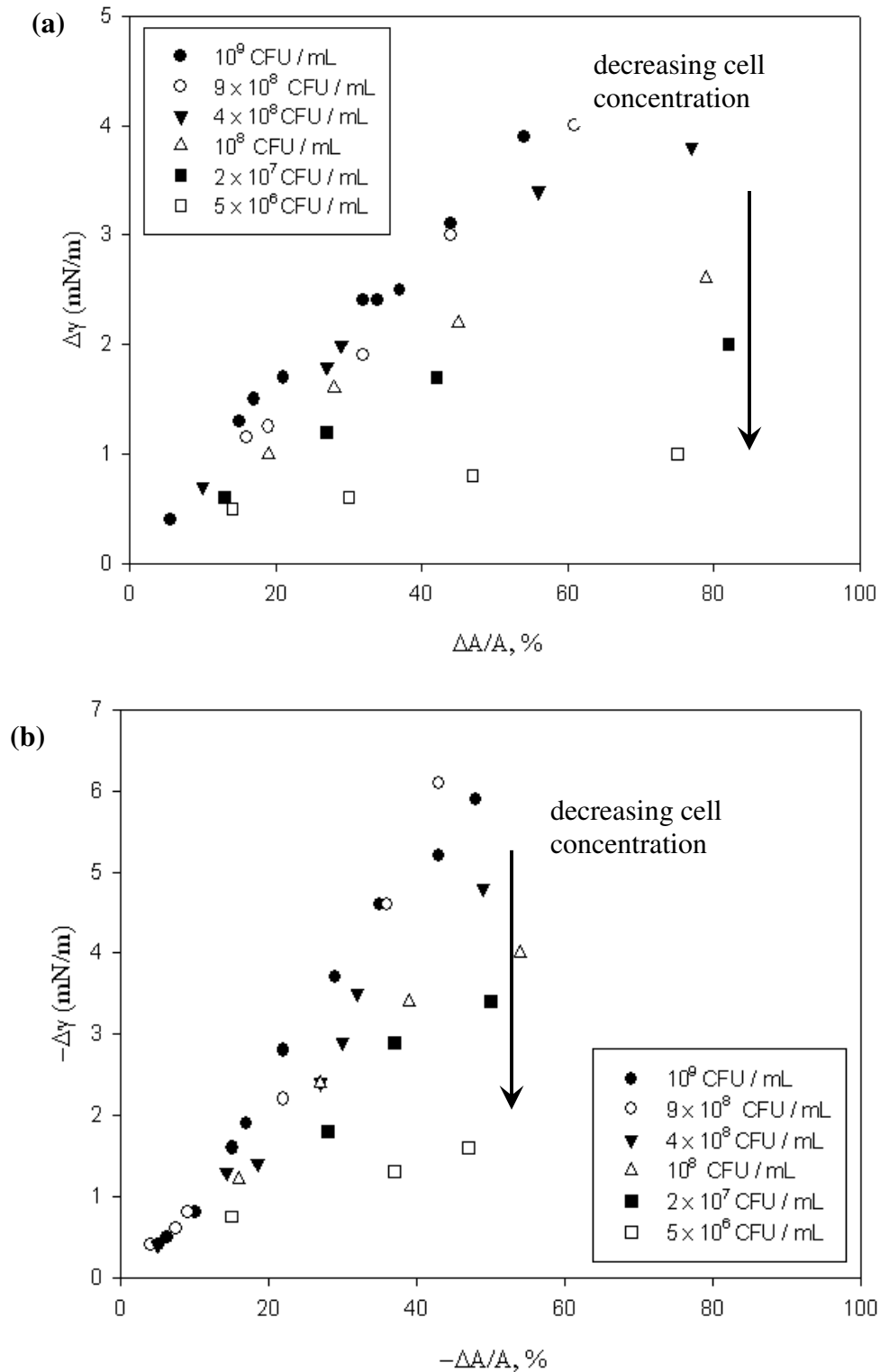


**Figure 4.12:** Effect of area perturbation and cell concentration on the interfacial tension for surfaces adsorbed with *R. erythropolis* 20S-E1-c. The trend lines indicate decreasing cell concentrations. (a) Step-up excitations; (b) Step-down excitations.

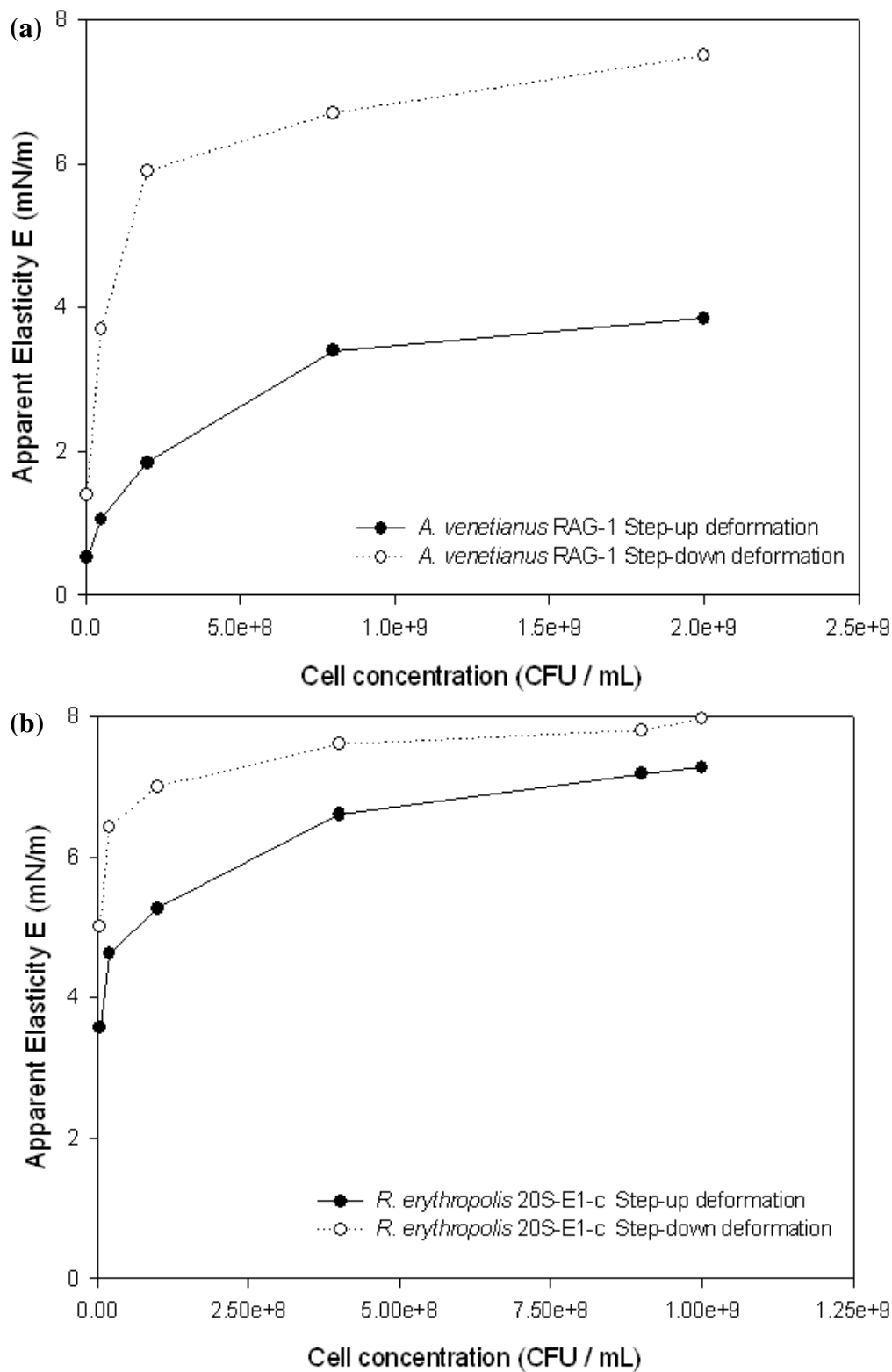


**Figure 4.13:** Effect of cell concentration on “apparent elasticity”  $E$  of interfaces adsorbed with (a) *A. venetianus* RAG-1 and (b) *R. erythropolis* 20S-E1-c. The lowest cell concentration was  $5 \times 10^6$  CFU/mL in both plots.

## 4.4 Conclusions

Adsorption of intact hydrophobic bacteria at the *n*-hexadecane-water interface did not alter the equilibrium interfacial tension. However, *higher order* surface rheological properties, such as dilational film elasticity and internal stress relaxation, were clearly present. Adsorbed films formed from two strains of bacteria (one Gram-negative; the other Gram-positive) exhibited qualitatively similar responses to area perturbations. The film mechanical properties were “non-linear” in that their responses to step-up and step-down excitations were not mirror images of one another (behaving as a Maxwellian material as the interfacial area expanded, and as a purely elastic sheet upon sudden area contraction). On close examination, the two types of adsorbed films exhibited clear quantitative differences: They possessed different dilational elasticities and relaxation times (the corresponding “Maxwell spring constants” were 3.5 mN/m and 7.6 mN/m for RAG-1 and 20S-E1-c films, respectively). More strikingly, the relaxation times were seen to follow opposite trends of discontinuous “jumps” as the area strain was varied (Figure 4.10). Upon continuous area reduction, the Gram-negative system showed a “paper-like” interface, while interfaces associated with Gram-positive cells were “soap film-like.” It is speculated that these two classes of material property are due to differences in cell-cell interactions at the interface (i.e. whether the cells interlock or slide freely past one another on the interfacial plane). TEM images of the surface structures of the bacteria appear to support such a conjecture: the nanoscale fimbriae (i.e. filaments) observed on the surfaces of the *A. venetianus* RAG-1 cells could cause cell

interlocking at the oil-water interface, thus creating a two dimensional network which resisted in-plane shearing. In contrast, the *R. erythropolis* 20S-E1-c cell surfaces appeared smooth, which would likely allow free sliding between the adsorbed cells and thereby alleviating any buildup of in-plane shear strain.

# CHAPTER 5 INTERFACIAL RHEOLOGY AT MICROMETRE SCALE: MICROPIPETTE TECHNIQUE<sup>\*</sup>

## 5.1 Introduction

As was discussed in Chapter 2, any emulsion system must comprise, in addition to the two immiscible liquids, an *emulsifier* whose minimum energy configuration is found at the liquid-liquid interface. The emulsifier may lower the interfacial tension (IFT) and facilitate dispersion of one liquid as small droplets in the other<sup>†</sup>; it must also create repulsive forces between the dispersed droplets and thereby prevent coalescence and subsequent phase separation. If, in addition, the adsorbed substances interact strongly with one another on the interfacial plane (e.g. through inelastic collision or entanglement), higher order rheological properties — such as elastic and/or viscous effects — may arise. These interfacial rheological properties can influence greatly the transport of individual droplets and, in some cases, of entire suspensions (Edwards *et al.*, 1991; Slattery, 1990).

The focus of this part of the present study is on the use of intact, inactive hydrophobic bacteria as emulsifiers to stabilize oil-in-water emulsions. These bacteria, whose dimensions are typically just about a micrometre, can be considered in the present context as “soft colloidal particles.” In regard to their roles in emulsion applications, the microbes share many similarities with the more familiar colloidal solids — such as clays and nanospheres — which are known to produce very stable emulsions (Ramsden, 1903; Pickering, 1907; Yan *et al.*, 2001;

---

<sup>\*</sup> Major portion of this chapter has been published: Z. Kang, T. Yeung, J. Foght and M. Gray, “Hydrophobic bacterial at the hexadecane-water interface: Examination of micrometre-scale interfacial properties,” *Colloidal & Surface Science B*, 67, 59-66, 2008

<sup>†</sup> Only macroemulsions are considered in this section.

Binks, 2002). Both the “soft” and the “hard” colloids are, for example, incapable of lowering IFTs due to their large sizes (see Appendix C); in such cases, relatively high shear rates are required for emulsification. Both types of colloids also tend to attach strongly to the fluid interface — to a point where the adsorption process is effectively irreversible (Binks, 2002; Rosenberg and Rosenberg, 1985). The tenacity of particle attachment to interfaces gives rise to adsorbed layers which behave as strong steric barriers, thus accounting for the remarkable stability of the resulting emulsions. It has been established in a previous study that hydrophobic bacteria, like their solid counterparts, could form stable emulsions without significantly altering the oil-water interfacial tension (Dorobantu *et al.*, 2004).

In Chapter 4, it was stated that, on the macroscopic (i.e. millimetre) scale, bacterial films formed from two strains of microbes exhibited clear signs of higher order rheological properties (such as the dilational film elasticity and the internal rates of stress relaxation); this indicated that the adsorbed microbes interacted strongly with one another at the oil-water interface. These macroscopic rheological properties may not persist on the micrometre scale, i.e. on length scales which are more relevant to the “emulsion world.” Bulk rheological behaviours have been known to be length scale-dependent, especially when the basic unit, or “primary particle,” is not much smaller than the dimensions of the system (Liu *et al.*, 2006; Schmidt *et al.*, 2000). In this section, a micropipette technique was used to probe the mechanical properties of bacteria-adsorbed interfaces at length scales of less than 10 microns. It has been shown that, for

mechanical experiments conducted on the 1–10  $\mu\text{m}$  scale, as in the present application, gravitational body forces and viscous effects are completely negligible. The system of present interest is that of oil drops in water at room temperature, in which the resting (i.e. live but non-dividing) bacteria have attached onto the oil/water interfaces as colloidal stabilizers in the absence of molecular surfactants. As stated in Chapter 4, care was taken to eliminate all influences of biosurfactants, leaving only adsorbed layers of intact living bacterial cells which behave as colloidal particles. This is the first study of the effect of bacterial cells on oil-water interfacial rheology, with the experiments conducted on the micron scale at room temperature over a range of cell concentrations.

## **5.2 Theory**

The following is a brief discussion on the theory of capillary instability and interfacial elasticity; it serves as a supplement to Chapter 2, where the general theory of emulsions was presented. This discussion, which we chose not to present until here in Chapter 5, has direct relevance to the results which immediately follow (in Section 5.4).

### **5.2.1 Capillary instability and the measurement of IFT**

The micropipette technique is a method of directly measuring the IFT of individual emulsion drops; the technique is based on a phenomenon known as *capillary instability*. A sketch of the situation is shown in the Figure 5.1a. A liquid drop of radius  $R_0$  (ca. 10  $\mu\text{m}$ ) is held at the tip of a micropipette by suction

pressure  $\Delta p$ ; the inner radius of the pipette is denoted  $R_p$ . As the suction pressure slowly increases, the projection of the drop into the pipette will grow until it eventually becomes a hemispherical cap of radius  $R_p$  (i.e. when  $L = R_p$ ); this is known to be the point of capillary instability. At this point, even the slightest increase in  $\Delta p$  will cause the entire liquid drop to be drawn into the pipette (over a time scale of microseconds). The critical pressure  $p_{cr}$  at the instability point is given by (Evans and Needham, 1987; Yeung *et al.*, 1998):

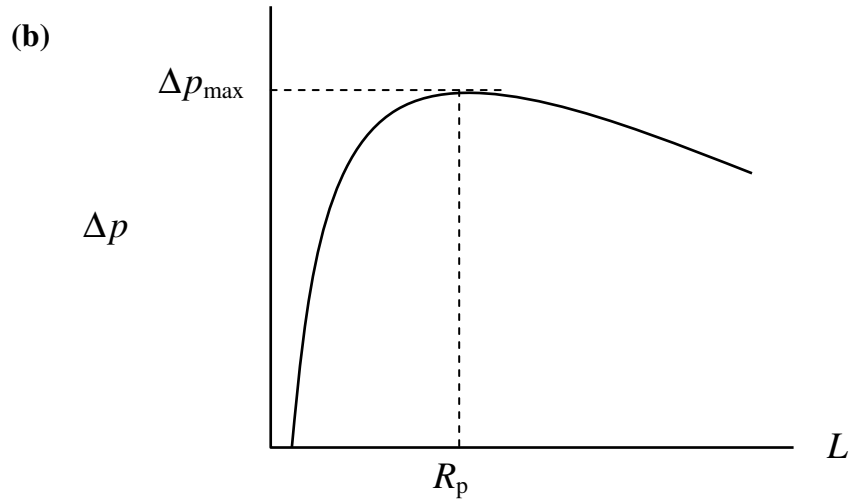
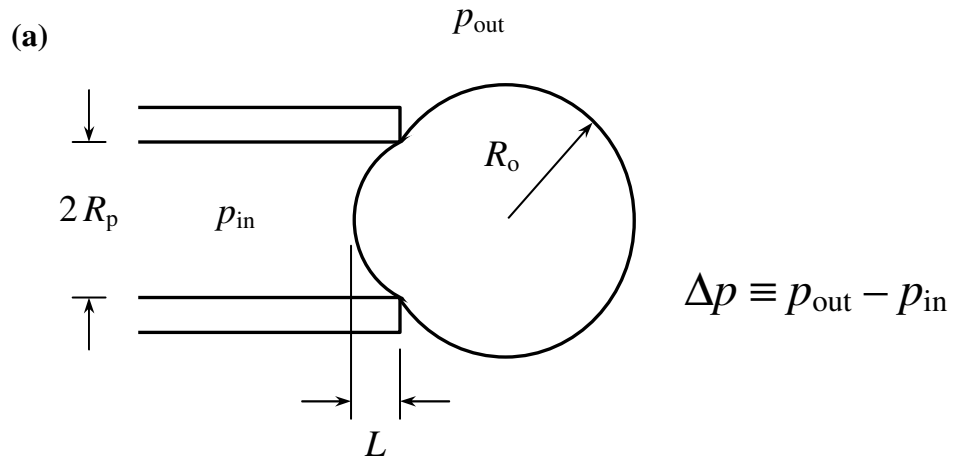
$$p_{cr} = \frac{2\gamma_o}{R_p} \left( 1 - \frac{R_p}{R_o} \right) \quad (5.1)$$

where  $\gamma_o$  is the interfacial tension. In practice, the critical pressure  $p_{cr}$  can easily be measured by connecting the micropipette to a pressure transducer. Knowing  $R_p$  and  $R_o$  from microscope images, the IFT can be calculated accurately using eqn (5.1). This technique of determining *in situ* IFT had been applied successfully to various emulsion systems (Moran *et al.*, 1999; Yeung *et al.*, 1999; Yeung *et al.*, 2000).

The capillary instability phenomenon can be understood through examination of the relation between  $\Delta p$ , the pressure required to maintain *static equilibrium*, and  $L$ , the corresponding projection length. Using the Young-Laplace equation, and assuming: (a) both unsupported surfaces in Figure 5.1a to be spherical segments, (b) uniform IFT, and (c) constant droplet volume, it becomes a straightforward exercise to calculate the  $\Delta p$  vs  $L$  relation. (Such a relation, although straightforward, has no analytical solution and can only be

obtained numerically.) A typical sketch of such a relation is shown in Figure 5.1b. The key feature to note in the figure is that the maximum point, which occurs when  $L = R_p$  and  $\Delta p = p_{cr}$ , is a clear indicator of mechanical instability: as the point of maximum pressure in Figure 5.1c is traversed from the left (i.e. as the projection in the pipette extends beyond a hemisphere), the accumulated suction pressure, which has now reached the peak value  $p_{cr}$ , will exceed the pressure required for mechanical equilibrium (i.e.  $\Delta p$  for  $L > R_p$ ). A pressure differential is thus created which has the effect of drawing the droplet into the pipette. This pressure differential will grow larger as the droplet is drawn further into the tube; mechanical instability therefore ensues.

The relevance of capillary instability to MEOR processes is very clear. As early as 1930, Haines had noted that oil ganglia tended to travel through irregularly shaped pores in an episodic manner — comprising sporadic jumps separated by much slower motions in between; such motions have since been referred to as “Haines jumps” (Ramamohan and Slattery, 1984). Haines jumps can be due to sudden changes in wetting conditions, which are in turn caused by surface imperfections. However, for oil droplets travelling through channels of variable cross sections, capillary instability may in fact be the main cause of the sporadic motions. Conversely, the elimination of capillary instability may lead to profound effects of “zone-plugging”, i.e. the blocking of narrow pore passages by emulsified drops.



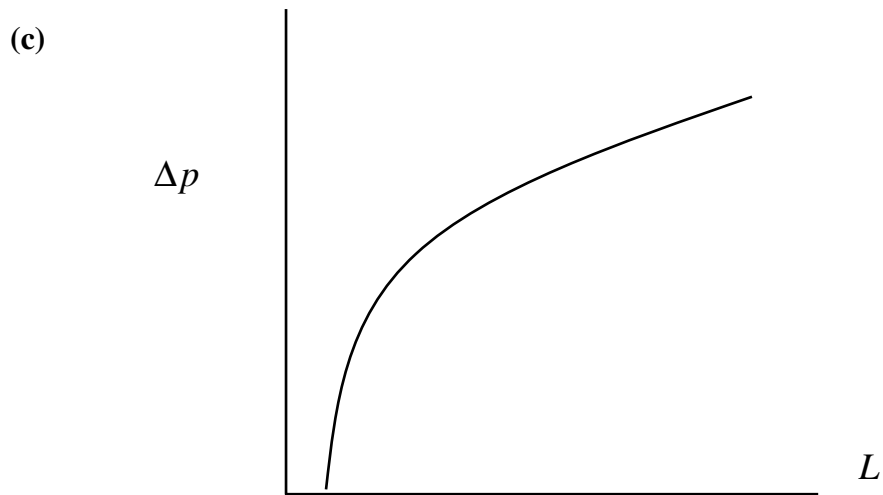


**Figure 5.1:** (a) Schematic of a liquid drop being held at the tip of a suction pipette. (b) The suction pressure, as defined in Fig. 5.1a, is plotted as a function of the projection length; the drop surface is characterized by a constant interfacial tension. (c) Same situation as in Fig. 5.1b, but with the drop surface characterized by an interfacial tension and a dilational elasticity.

### 5.2.2 Surface elasticity and the elimination of capillary instability

The phenomena of capillary instability and the measurement of IFT have been demonstrated in the previous section for constant interfacial tensions  $\gamma_0$ . If, in addition, the adsorbed microbes interlink and form a network at the oil-water interface, an elastic sheet will be created. As a first approximation, this surface elasticity can be modelled according to the relation (Evans and Skalak, 1980)

$$\gamma = \gamma_0 + K \cdot \Delta A / A_0 \quad (5.2)$$

where  $\gamma$  is the effective (or augmented) interfacial tension,  $\gamma_0$  is the intrinsic IFT (i.e. for clean interfaces), and  $K$  is the dilational elasticity of the adsorbed layer. The quantity  $\Delta A / A_0$  is a measure of the dilational strain, with  $\Delta A$  representing the area change and  $A_0$  the surface area of the reference (i.e. stress-free) state.

For elastic adsorbed layers, it is the augmented tension  $\gamma$  that must be used in the Young-Laplace equation to calculate pressure differences across curved surfaces. Following the same procedures as before — that is, assuming spherical segments, uniform (but now strain-dependent)  $\gamma$ , and constant drop volume — the new  $\Delta p$  vs  $L$  relation can, for sufficiently large values of  $K$ , be a *monotonically increasing function* (see Figure 5.1c). This relationship is observed because the surface area must necessarily dilate as the droplet is drawn into the pipette. With the elastic sheet increasingly stretched, progressively larger suction pressures are required to pull in the drop.

The key message from Figure 5.1c is: with the elimination of the maximum suction pressure (as illustrated in Figure 5.1b), the phenomenon of capillary instability disappears. As such, it is possible to observe drop projections inside the pipette which extend *beyond the hemispherical shape* (the previously-unstable point). Thus, equilibrium projection lengths inside the pipette that are longer than  $R_p$  can serve as an unmistakable evidence for the existence of surface elasticity.

## **5.3 Materials and Methods**

### **5.3.1 Sample preparation**

Bacterial culture and staining processes have been introduced in Section 3.1. Emulsion preparation was discussed in Section 3.2; we made emulsions with both high and low cell concentrations for both bacterial strains.

### 5.3.2 Micropipette experiments setup

As stated in Section 3.2.5, the micropipette system consists of an inverted microscope which is connected to a video system; the micropipettes were mounted on and controlled by hydraulic micromanipulators. The following are the detailed micropipette manufacturing process and the descriptions of experiments conducted with micropipettes.

The straight micropipettes (including both closed-ended and open-ended pipettes) were used throughout all the micrometer-scaled experiments in this study. These straight micropipettes were forged in the laboratory prior to their application. The necessary steps in their creation are as follows.

To produce a straight micropipette, the first step is to create a tapered pipette with a closed end (Figure 5.2a). The closed-ended pipette is created using a commercial pipette puller (David Kopf Instruments, Model 730, Tujuvoa, CA; Figure 5.2b) which uses a platinum-iridium wire to heat the middle section of a long glass capillary tube (outside diameter 1 mm, inside diameter 0.7 mm; Borosilicate glass, Kimble Glass Inc.) while pulling on its ends to elongate its centre until it was separated into two tapered pieces. After this pulling, one end of the capillary tube would have a sub-micron opening (or it may be completely closed at the tip).

To be useful in the force-measuring experiments, the closed-ended micropipette must be truncated until the inside diameter of the pipette end reaches several microns, so that the opening can be used to apply suction pressures (Figure 5.2c). The procedure is carried out with a homemade forging device

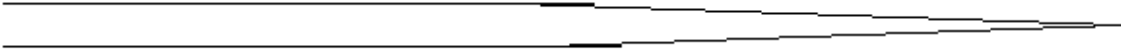
under a Zeiss Axiostar 100 microscope with a 10× objective. The closed-ended micropipette was mounted on a micromanipulator which was capable of controlling the movement of a pipette in three dimensions. A platinum-iridium wire, with a small bead of molten glass suspended at its end, is mounted on a stand; it is heated by conducting an electrical current through it (Figure 5.2d). As the glass bead on the wire melted, the close ended pipette was extended into it; the required pipette and size was controlled by the amount of insertion into the molten glass. When in position, the current through the wire was cut off. As such, the glass bead which was attached onto the wire solidified, and the glass bead and the pipette end which had been inserted into the glass fused into one. From this configuration, the pipette was pulled backwards, thus breaking the micropipette end at the desired position (with an inner diameter of about 5-10  $\mu\text{m}$ ). For accurate determination of the forces involved, it was always ensured that the micropipette tips possess a simple cylindrical geometry with no jagged imperfections. To make a smooth end, the same process is repeated. This time, the situation in the micropipette would be slightly different: As the glass pipette was inserted into the molten glass bead, a small amount of liquid glass (from the molten glass bead) would flow into the open pipette and remain there. When the electrical current is turned off, the molten glass inside the pipette solidified and acted as rigid internal support. As the pipette was pulled back, a clean break of the pipette would occur around the rigid support. As such, a micropipette with a smooth open end at a desired diameter is created; it may then be used in the following experiments.

The micropipette technique can directly measure interfacial mechanical properties on dimensions that are representative of the pore sizes in MEOR applications, i.e. of order 1 to 10 microns. Briefly, the method involves using glass suction pipettes to capture and manipulate individual emulsion drops. By conducting various types of stress-strain experiments on the relevant length scales, *in situ* material properties can be determined. Details of the method have been described elsewhere and are not repeated here (Evans and Needham, 1987; Moran *et al.*, 1999; Yeung *et al.*, 1999; Yeung *et al.*, 2000). As an example of a very simple application, the micropipette technique was used to quantify IFTs directly at the surfaces of individual emulsion drops (Yeung *et al.*, 1998). As shown in Figure 5.3, a liquid drop with a diameter of approximate 15  $\mu\text{m}$  was held at the tip of a pipette under negative (i.e. suction) pressure. The critical pressure required to draw the drop into the pipette can be directly related to the interfacial tension. By measuring this critical suction pressure, the IFT can be determined with high precision (The theory behind this process was discussed in Section 5.2).

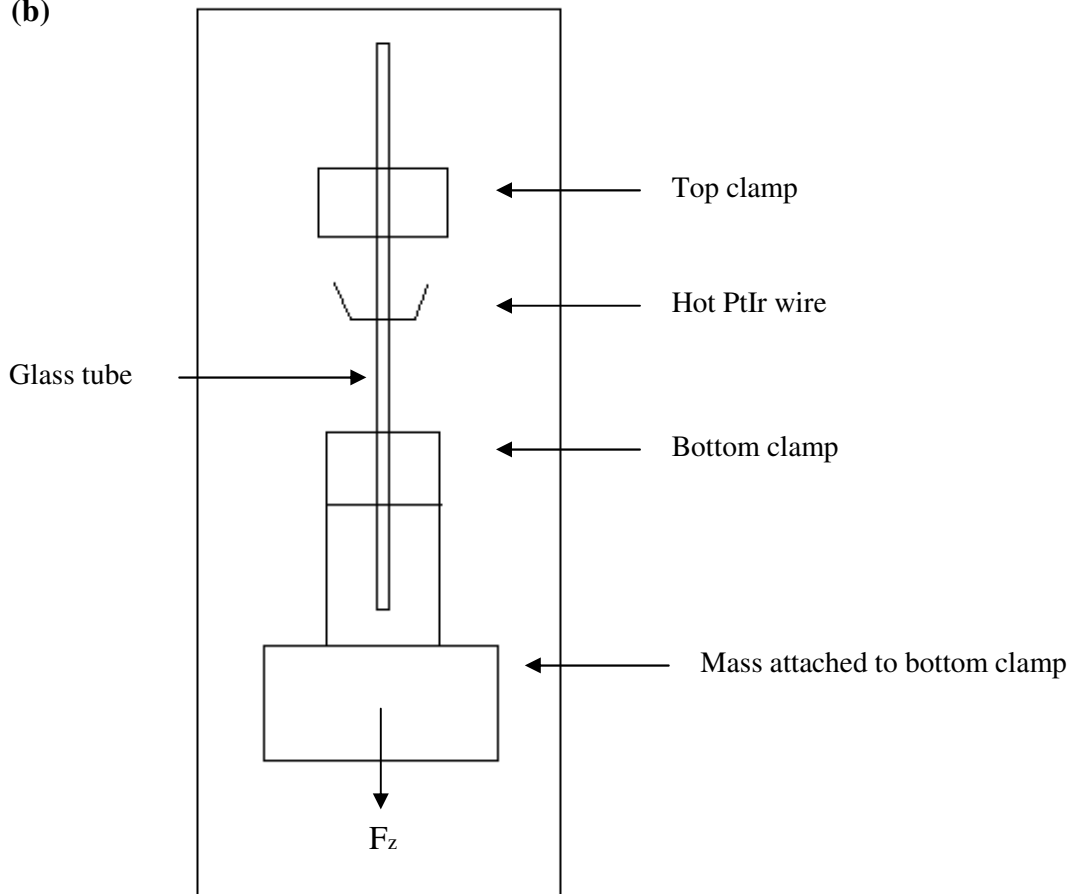
All the force-based experiments were conducted using an open-ended glass micropipette with 5-10  $\mu\text{m}$  inner diameter. Individual micrometre-sized oil-in-water emulsion drops were held at the tip of a micropipette with a suction pressure. About 30  $\mu\text{L}$  of an oil-in-water emulsion was placed in a sample cell. To grasp an emulsion droplet on the pipette tip, an adjustable suction pressure was applied; this was made possible by connecting the untapered (large) end of the pipette to a 100-mL syringe through a flexible tygon tubing. The suction pressure

could be measured accurately using a pressure transducer (Omega Engineering, Stamford, CT) which was connected to the pipette and the syringe with a T-section. By controlling the suction pipette, qualitative experiments could be conducted, including the emulsion drop stability tests described in Section 5.4.3.

(a)



(b)



(c)



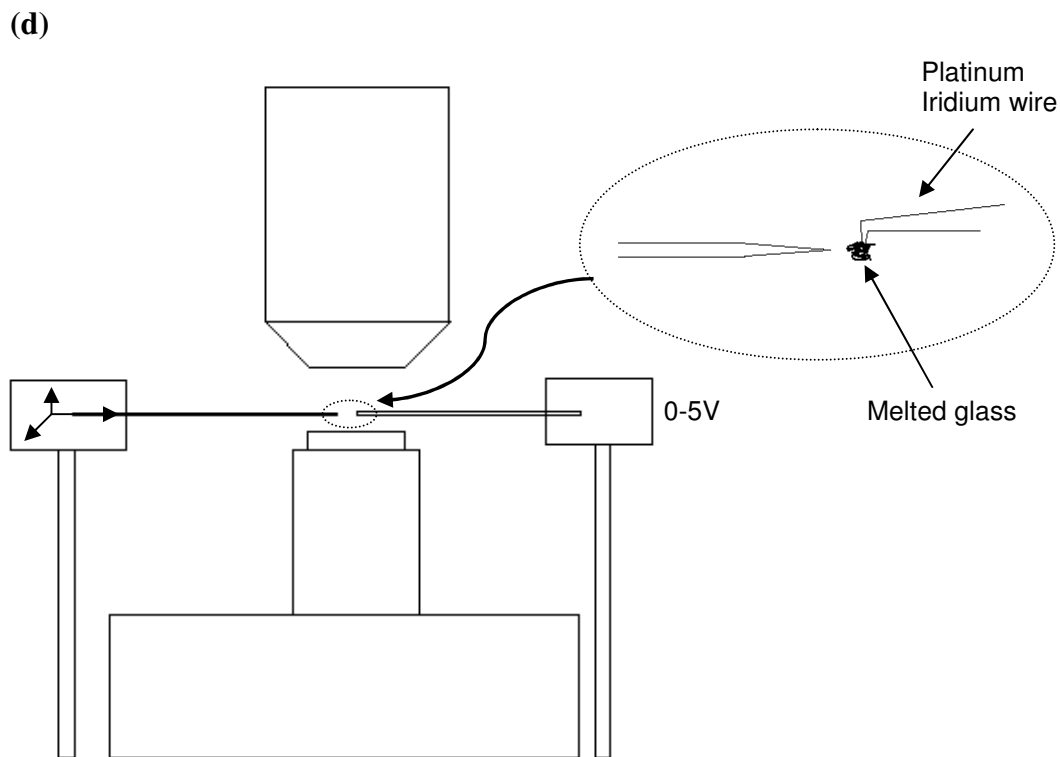
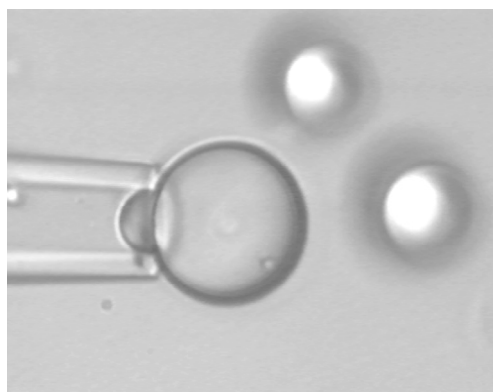


**Figure 5.2:** (a) Micropipette with closed end; (b) sketch of pipette puller setup; (c) truncated micropipette; (d) sketch of the pipette truncating (i.e. the “microforge”) setup.



— 10  $\mu\text{m}$

**Figure 5.3:** A liquid drop held at the tip of a micropipette by suction pressure; the oil-water interface was “clean” (i.e. free of surfactants and adsorbed materials). The projection of the drop inside the pipette was hemispherical, indicating that the system was on the verge of capillary instability.

## 5.4 Results and Discussion

### 5.4.1 Bacterial films at interfaces

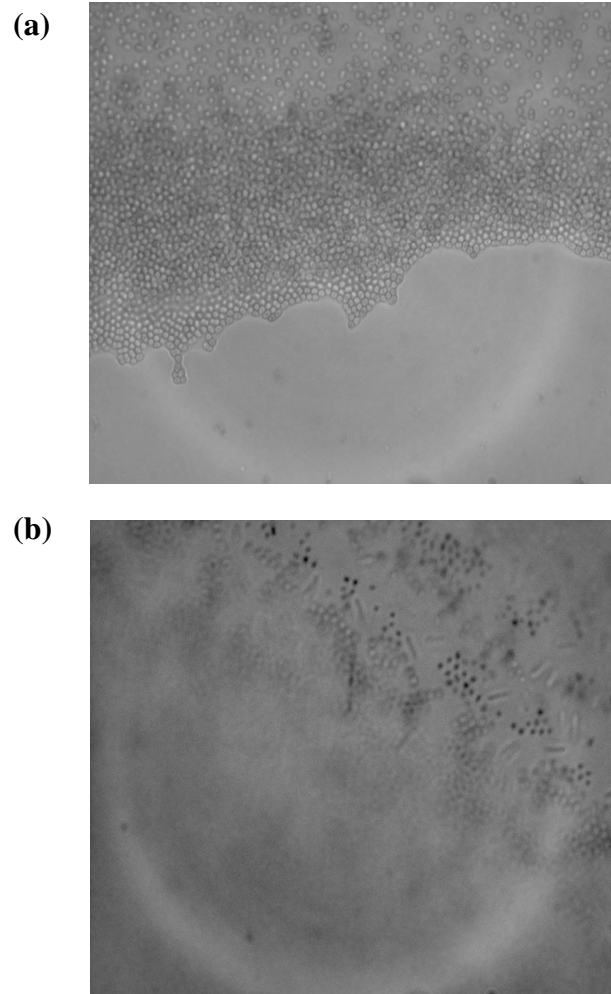
For the oil/water interface with *A. venetianus* RAG-1, when the cell concentration in buffer was high ( $2 \times 10^9$  CFU/mL), the cells on the interface were closely packed and created a film (Figure 5.4); this was consistent with macroscopic observations with the pendant drop (see Figure 4.5). At low cell concentration ( $5 \times 10^7$  CFU/mL), the cells accumulated *in clusters* at the interface, and regions of “uncovered” oil-water interface could be seen between the clusters (Figure 5.4b). The film shown in Figure 5.4a was relatively rigid, i.e. the cells formed a network and interlocked with each other at the interface (thus immobilizing the cells). In contrast, at the lower cell concentration, the cells appeared to move about freely along the interface.

Figure 5.5 depicts situations which involved *R. erythropolis* 20S-E1-c cells at the oil/water interface. For a high cell concentration ( $10^9$  CFU/mL), the cells on the interface were also closely packed and formed a film (Figure 5.5a). However, the rod-shaped cells on the interface were not interlocked, and each cell seemed to move freely within its near vicinity. At a lower cell concentration ( $5 \times 10^7$  CFU/mL), instead of accumulating in clusters at the interface, the cells remained as individuals and could move freely (Figure 5.5b) and this was very different from the *A. venetianus* RAG-1 films.

In addition to the static observations, a dynamic experiment was designed by poking the interface laterally with a blocked pipette. When perturbed, only the *A. venetianus* RAG-1 cells immediately adjacent to the pipette moved while the

others remained stationary. In addition, the cells moved in discrete clumps (or “rafts”) on the interface, which was formed by aggregation of several neighbouring cells. When the pipette withdrew, the moving clusters returned to their original position, suggesting that the bacterial film was elastic (i.e. solid-like). In contrast, when the same experiment was repeated with *R. erythropolis* 20S-E1-c film, the cells moved smoothly past one another when perturbed, and did not show any sign of being locked together.

These visual observations (using optical microscopy) of the two strains of bacteria on the interface were entirely consistent with the interpretation of the distinct surface properties which had been stated in Chapter 4 (Figure 4.6). We suggest that the *A. venetianus* RAG-1 on the interface could interlink with one another via the fimbriae and form a network which resisted in-plane shearing (Figure 4.6a). As in the case of a sheet of paper, which comprises a network of interlinked wood fibres, any attempt to perturb its surface (e.g. by poking the cell network with a close-ended micropipette) will not lead to complete breakage of “bonds” between every *individual* cell-cell interaction; instead, it will only result in the partial breakage where the cell-cell interaction is weaker so that the subunit of cell *clusters* is created and relative movement between these clusters would occur. In contrast, for the *R. erythropolis* 20S-E1-c cells (Figure 4.6b), their surfaces appeared much smoother. Here, if the interface were disturbed by some external forces, the smooth surfaces of the *R. erythropolis* 20S-E1-c would likely facilitate free sliding between neighbouring cells, thus alleviating any buildup of cell clusters.



**Figure 5.4:** Oil/water interface adsorbed with *A. venetianus* RAG-1. The size of each individual cell is around 2  $\mu\text{m}$ . Cell concentrations in buffer were: (a)  $2 \times 10^9$  CFU/mL; (b)  $5 \times 10^7$  CFU/mL

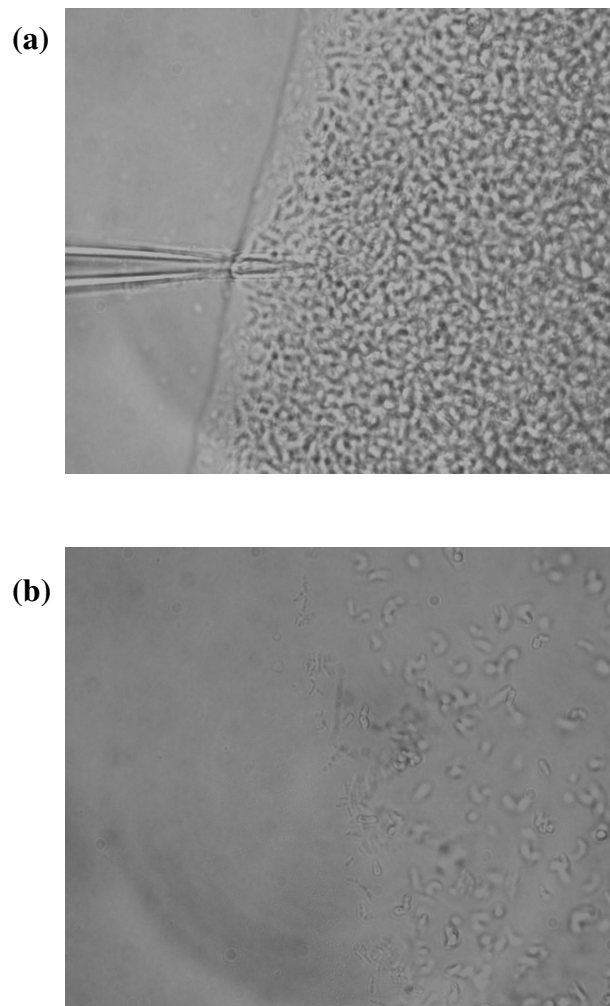


**Figure 5.5:** Oil/water interface adsorbed with *R. erythropolis* 20S-E1-c. The size of each individual cell is around 4  $\mu\text{m}$ . Cell concentrations in buffer were: (a)  $10^9$  CFU/mL; (b)  $5 \times 10^7$  CFU/mL.

#### 5.4.2 Behaviour of emulsion drops

Three types of oil-in-water emulsions were prepared as described above and subsequently viewed first by eye and then under the microscope. The emulsion formed by cell-free phosphate buffer (0.01M, pH 7) and *n*-hexadecane was short-lived and unstable. After agitation for 1 min, it was observed that the individual oil drops in water would quickly float to the top of the water phase until two distinct stable phases were seen. This phase separation process would

occur within minutes. In contrast, stable emulsions were created with either bacterial cells of both high and low cell concentrations. With both bacterial strains at high cell concentration ( $2 \times 10^9$  CFU/mL for *A. venetianus* RAG-1 and  $10^9$  CFU/mL for *R. erythropolis* 20S-E1-c suspension), two layers in the container were observed after the mixture was allowed to settle for 5 min: a top creamy emulsion layer and a bottom water layer (still with suspended bacterial cells, but of a lower concentration). Since all the oil had been emulsified, no oil phase was observed. In contrast, at low bacteria concentrations in buffer ( $5 \times 10^6$  CFU/mL for both bacterial suspensions), three layers were revealed with both bacterial strains: a top oil layer, a middle emulsion layer and a bottom water layer with almost no bacterial cells.

When three types of oil-in-water emulsions were observed under the microscope, it was noted that oil drops emulsified in a phosphate buffer or an aqueous suspension of *A. venetianus* RAG-1/ *R. erythropolis* 20S-E1-c were always spherical in shape. This result was expected since the drops were of micron-sized. Assuming that these oil drops were simple and have non-zero interfacial tensions, they would be spherical as the capillary forces were significantly larger than the body forces (which tended to distort the drops from their spherical shapes). This was made apparent through the Bond number  $Bo = \Delta\rho g R_d^2 / \gamma$ , where  $\Delta\rho$  is the density difference between the two immiscible phases and  $g$  is the gravitational acceleration. In this case,  $Bo$  is of order  $10^{-10}$ .

The “clean” oil drops in water tended to coalesce upon contact with each other. By contrast, oil drops emulsified in buffer containing bacterial cells exhibited markedly different behaviour: The emulsion formed by *A. venetianus* RAG-1 revealed a structure containing both single oil-in-water drops and oil drops surrounded by bacterial films interconnected in a three-dimensional network (Figure 5.6a; Dorobantu *et al.*, 2004). In addition, those interconnected emulsion drops were very rigid, so that the pipette could hardly move them. However, *R. erythropolis* 20S-E1-c only formed single oil-in-water emulsion drops (Figure 5.6b). The above observations applied to emulsions created by both high and low concentrations for the two bacterial strains. The different emulsion behaviours observed under the microscope can also be explained by the different cell surface structures: the fimbriae, which appeared on the *A. venetianus* RAG-1 cell surface, could facilitate drop-drop interactions under agitation when the oil-in-water emulsion was created (Figure 4.6a). In this study, as a first attempt to examine the surface rheology of such emulsion systems, the behaviour of individual drops was investigated in response to mechanical deformation.

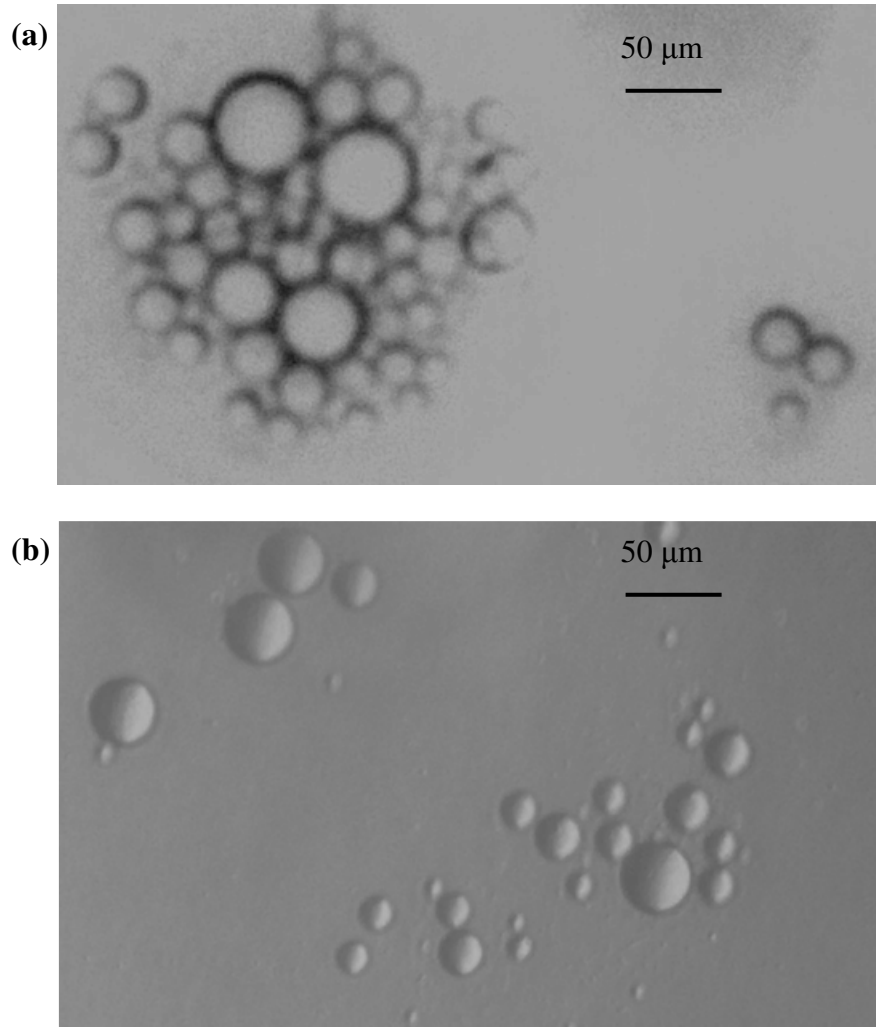


**Figure 5.6:** Observation of oil-in-water emulsion drops using optical microscopy; the surrounding aqueous phases were bacterial suspensions in phosphate buffer. (a) The emulsion formed by *A. venetianus* RAG-1 revealed a structure containing both single oil-in-water drops and oil drops surrounded by bacterial films interconnected in a three-dimensional network. (b) The *R. erythropolis* 20S-E1-c system only formed single oil-in-water emulsion drops.

#### 5.4.3 Crumpling test and stability against coalescence

Owing to the bacteria's hydrophobic character, the cells accumulated at the oil/water interface and formed a skin-like structure (Dorobantu *et al.* 2004).

In addition, the previous millimetre-scale study using the pendant drop technique (Chapter 4) had shown that the disparate cell surface properties had resulted in the formation of distinct bacterial films at oil-water interfaces: “paper-like” film by *A. venetianus* RAG-1 and “soap film-like” surfaces by *R. erythropolis* 20S-E1-c.

Here, the presence of such interfacial films on emulsion drop surfaces can be revealed with the use of micropipettes on the micrometre scale. For this, the following procedure was applied: an open-ended micropipette was inserted into the emulsion and captured a single oil droplet by suction pressure. Then, the suction pressure was increased until the captured droplet was drawn into the pipette. For the clean oil-water interface (no microbes), as a control test, the phenomena of capillary instability appeared and the whole oil drop was sucked into the pipette over time scales of microseconds. For the oil droplet formed with RAG-1 at high cell concentration ( $2 \times 10^9$  CFU/mL), as it was drawn in and its external volume-to-area ratio decreased, the surface resisted the change and crumpled abruptly (Figure 5.7a), revealing a rigid cortical structure. When the same experiment was repeated with droplets created in 20S-E1-c at high cell concentration ( $10^9$  CFU/mL), no such crumpling of the droplet surface was observed and the deflating droplet remained spherical as it shrank (Figure 5.7b). Again, the different behaviours in the deflation process would ultimately be determined by the interaction between adsorbed bacterial cells at the interface; the results were consistent with those obtained by the pendant drop technique (at high bacterial concentrations) on the millimetre scale (see Figure 4.5). An interesting phenomenon was that the same “paper-like” and “soap film-like” behaviours were

observed if tests were done with emulsion drops formed in bacterial suspensions at low cell concentration. These observations were different from pendant drop results, in which the cell concentrations in buffer would greatly affect the creation of bacterial films at the oil-water interface (Figure 4.5).

Using micropipettes, it was possible to directly study emulsion stability between two individual droplets under *in situ* conditions. Therefore, the properties of interfacial bacterial films could be revealed. Emulsion stability, in this context, refers to the ability of micron-sized droplets to resist mutual coalescence and coagulation. Figure 5.8 shows the encounter of two oil droplets in a suspension of *A. venetianus* RAG-1 bacteria. The droplets were captured by suction pipettes and manipulated into direct contact in quiescent aqueous environments. Several observations could be made:

1. Control experiments were first conducted which involved *n*-hexadecane droplets in clean phosphate buffer (in the absence of any microbes). As expected, every pair of oil droplets coalesced immediately on contact.
2. All emulsion drops coated with *A. venetianus* RAG-1 cells remained stable to coalescence even after direct contact for up to 2 min. While in contact, the two drops were pressed together until they were visibly distorted. Upon separation, the drops returned to their spherical shapes without showing any sign of adhesion (forces provided by the cell-cell interactions on the contact point are inadequate).
3. For the oil droplets coated with *R. erythropolis* 20S-E1-c cells, 80% of them remained stable to coalescence when pressed together for up to 2

min; the remaining 20% would coalesce immediately on contact (based on 20 trials).

The observation that oil drops coated with 20S-E1-c were relatively easy to coalesce did not mean that 20S-E1-c were less able to stabilize emulsions. The previous study has shown that the high contact angle of 20S-E1-c films, which was due to the highly hydrophobic mycolic acids covering the cell surface, enables these cells to penetrate deeply into the oil phase. This was not possible for the RAG-1 cells as they were more amphipathic due to the cell surface lipopolysaccharides (Dworkin *et al.*, 2006; Dorobantu *et al.*, 2004). This penetration into the oil phase may explain the above micropipette results: if the cells at the interface entered entirely into the oil phase, the two oil drops would make contact, resulting in coalescence.

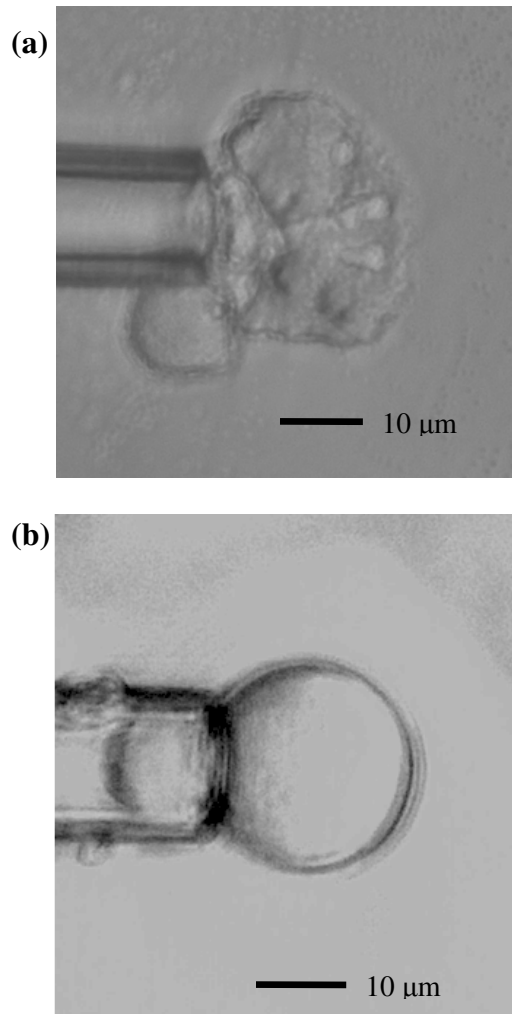


**Figure 5.7:** Deflating an emulsion droplet using micropipette. (a) The droplet was coated with *A. venetianus* RAG-1; the interfacial film was revealed as the droplet area was reduced. (b) The droplet was coated with *R. erythropolis* 20S-E1-c; no crumpling was observed; instead, the deflating oil droplet remained spherical.

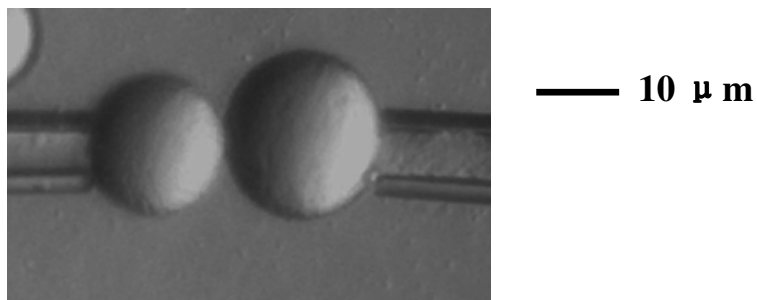


**Figure 5.8:** Studying colloidal stability through direct-contact experiment. Here, two *n*-hexadecane droplets were captured and manipulated into contact using micropipettes. The surrounding aqueous phase was a suspension of *A. venetianus* RAG-1 bacteria.

#### **5.4.4 Elimination of capillary instability with bacteria adsorbed at the interface**

For oil-water interfaces adsorbed with microbes, the elimination of capillary instability has indeed been observed. Figure 5.9 shows an oil droplet dispersed in a suspension of *A. venetianus* RAG-1 cells (oil droplets adsorbed with *R. erythropolis* 20S-E1-c cells showed the same behaviour). When the “suction experiment” was performed on the bacteria-coated drop, it was seen that the instability point had disappeared: the drop projection into the capillary tube had extended well beyond the hemispherical shape, and it was possible to maintain mechanical equilibrium throughout the process.

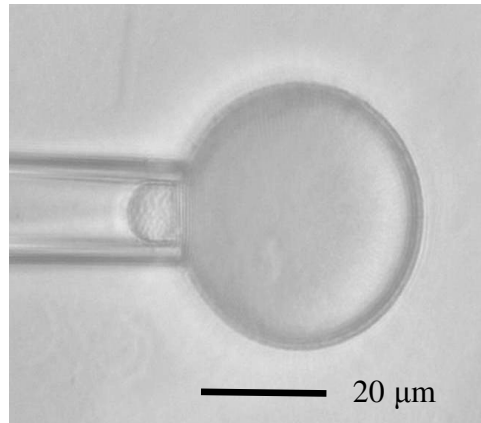


**Figure 5.9:** Micropipette deformation of an oil droplet coated with *A. venetianus* RAG-1 bacteria. The microbes provided added elasticity to the oil-water interface, which resulted in the elimination of capillary instability. The resistance to oil transport through small capillaries was greatly enhanced.

#### 5.4.5 Determination of micron-scale dilational elasticity

In addition to qualitative observations (which had already yielded valuable information), it is also possible to measure the suction pressure  $\Delta p$  as a function of the projection length  $L$ . By fitting this information to theoretical predictions, *in situ* dilational elasticity can be determined (the two-parameter surface elasticity model was described by equation 5.2 and the corresponding MatLab code is given in Appendix D).

A sample of the raw data for a suction experiment is shown in Figure 5.10 (RAG-1 bacterial films in Figure 5.10a, and 20S-E1-c films in Figure 5.10b). Here, the emulsion drops observed were created with bacteria suspension at high concentration ( $2 \times 10^9$  CFU/mL for RAG-1 and  $10^9$  CFU/mL for 20S-E1-c). A few important points about the experimental data are noted below:

- To determine if friction existed between the oil drops and the pipette surface (borosilicate glass), experiments were done with untreated pipettes as well as pipettes that were pre-coated with bovine serum albumen (BSA). Not surprisingly, the RAG-1 films showed much stronger friction against the untreated glass surface in comparison to 20S-E1-c films. (Recall the RAG-1 interface was ‘paper-like’ while the 20S-E1-c interface was ‘soap film-like.’) As friction was not accounted for in the theoretical calculations, only data from BSA-treated pipettes were used in the fitting process.
- To demonstrate that the  $\Delta p$  vs  $L$  relations were truly due to surface elastic (i.e. reversible) effects, the draw-in and push-out paths of each individual drop were carefully followed. Any sign of hysteresis would suggest either the existence of friction against the pipette inner surface, or that the adsorbed layers possessed inelastic (e.g. plastic yield) material properties. As seen in Figure 5.10a and 5.10b, hysteresis with respect to the direction of deformation was virtually non-existent. We can therefore conclude that the  $\Delta p$  vs  $L$  curves in Figure 5.10 represent true (i.e. reversible) elastic material properties.
- The experimental procedures performed on each oil drop required a duration of at least eight minutes. Throughout this time, the adsorbed layer appeared to be perfectly elastic. This result was in direct contrast to the macroscopic (mm-scale) rheological properties of the same adsorbed layers (Chapter 4). On the macroscopic scale, the interfaces appeared

“Maxwellian,” with the IFTs exhibiting relaxation times of 6.5 min for RAG-1 films, and 0.8 min for 20S-E1-c films.

Finally, the data from Figure 5.10 were fitted to theoretical predictions. To begin, the dimensionless suction pressure and projection length are defined as:

$$\text{dimensionless suction pressure} \equiv \Delta p R_p / \gamma_o$$

$$\text{dimensionless projection length} \equiv L / R_p$$

As shown in the last section, with the values of  $R_p$  and  $R_o$  known (from microscope images), the fitting procedure was reduced to two adjustable parameters: the intrinsic interfacial tension  $\gamma_o$  and the dilational elastic modulus  $K$  (the numerical code for the theoretical model will be given in Appendix D). Figure 5.11 shows optimal theoretical fits to the experimental data taken from Figure 5.10. Based on experiments on seven individual hexadecane droplets for each strain of bacteria, the average values of the fitting parameters were:

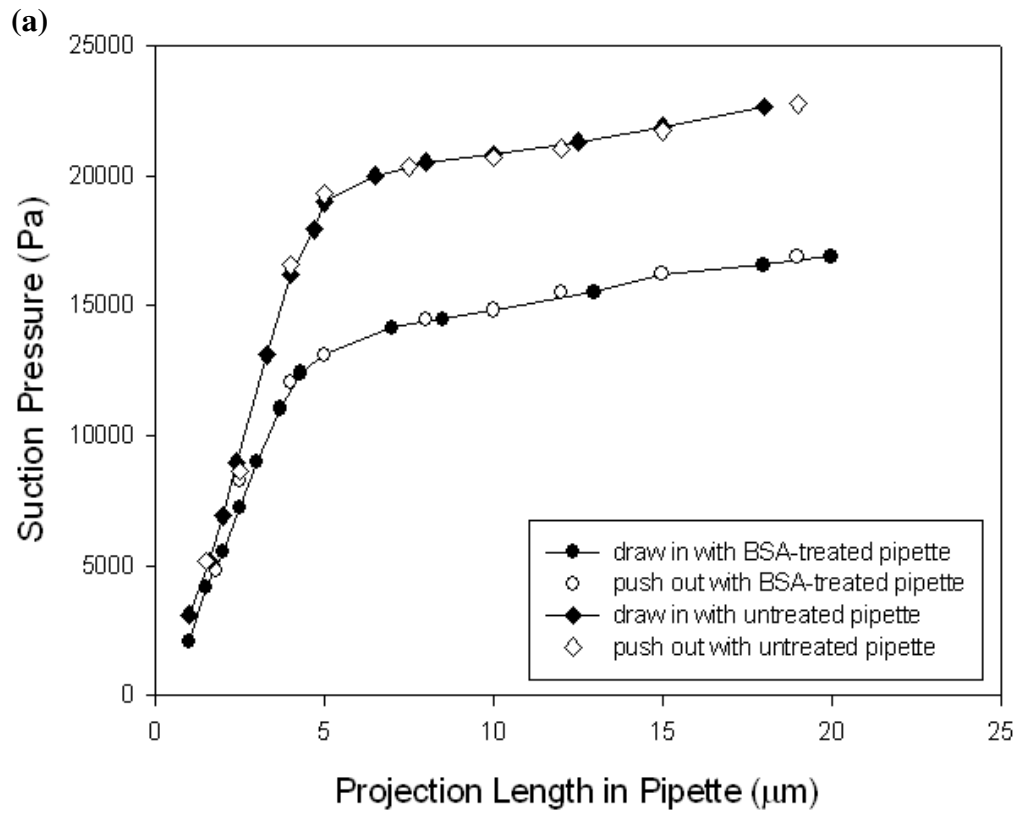
*Acinetobacter venetianus* RAG-1 films:  $\gamma_o = 46.6$  mN/m;  $K = 3.3$  mN/m

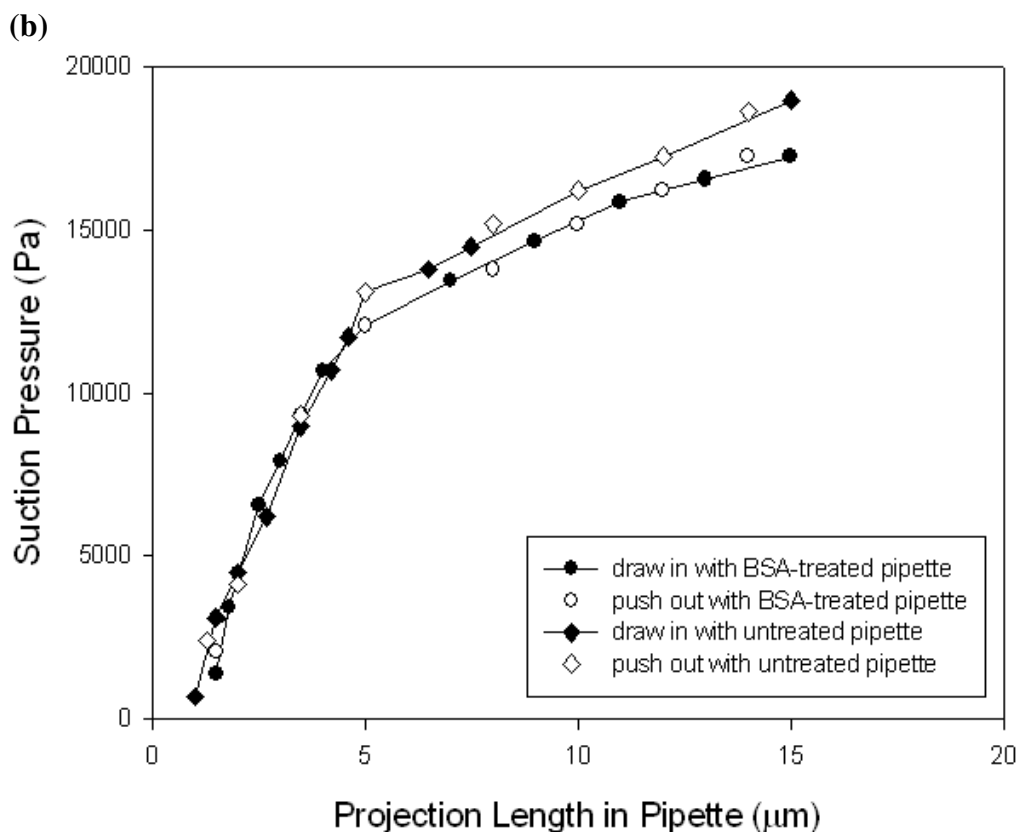
*Rhodococcus erythropolis* 20S-E1-c films:  $\gamma_o = 43.0$  mN/m;  $K = 5.6$  mN/m

The values for  $\gamma_o$  were noticeably lower than the IFT between distilled water and pure *n*-hexadecane (52 mN/m). This reduction may be due to the unavoidable release of surface active materials from the microbes (in trace amounts), despite efforts to eliminate these surfactants through repeated washing of the cells prior to emulsion formation. For the same preparation procedures, the equilibrium IFTs reported in our previous pendant drop study (~50 mN/m) were much closer to the

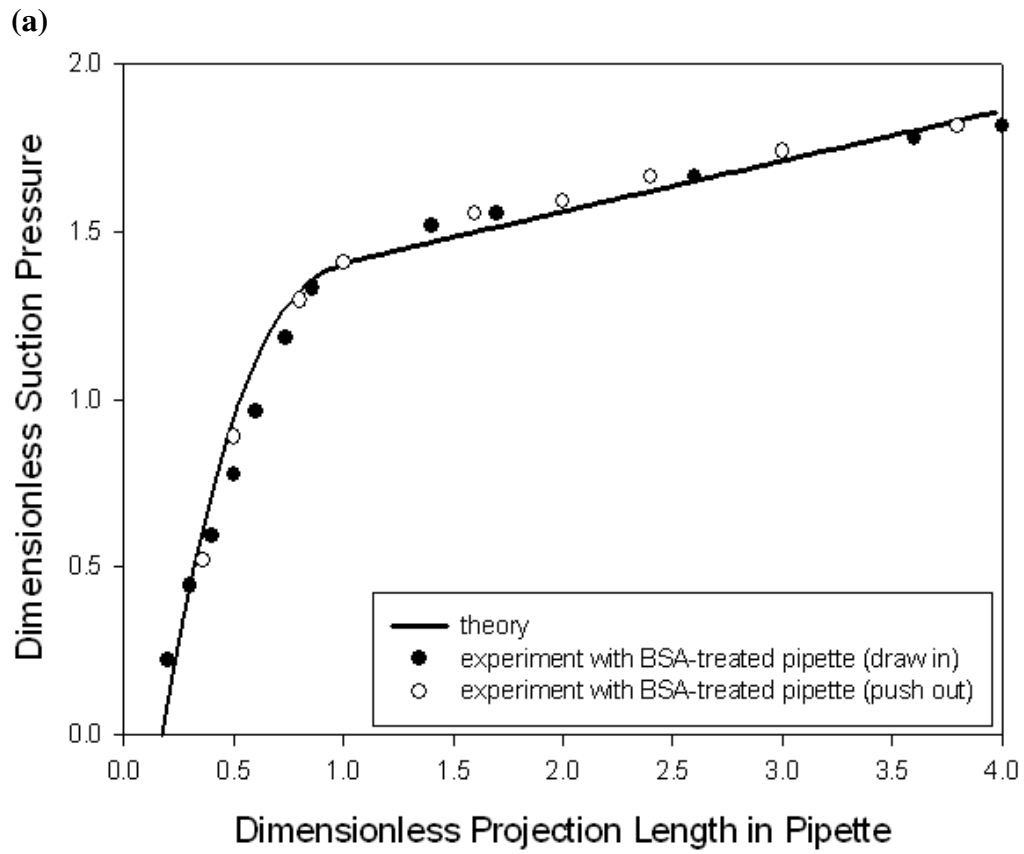
pure-liquids value (Table 4.1). This discrepancy, however, is not surprising as the results from Chapter 4 were derived from a macroscopic technique (pendant drop), while the present measurements were made directly on the surfaces of the emulsion drops. As demonstrated in an earlier investigation, in the presence of surfactants (particularly in small amounts), the equilibrium IFT can depend strongly on the method of measurement (Yeung *et al.*, 1998).

The dilational elastic moduli obtained above were somewhat surprising, as one would expect the *A. venetianus* RAG-1 microbes, given their surface fimbriae structures, to be more likely to interlink at the interface and result in a rigid structure; as such, the value of  $K$  for RAG-1 films should be larger than that for *R. erythropolis* 20S-E1-c films. On the other hand, the above values of  $K$  (3.3 mN/m for RAG-1 and 5.6 mN/m for 20S-E1-c) were remarkably similar to the ‘Maxwell spring constants’ obtained from our previous macroscopic study (3.5 mN/m and 7.6 mN/m, respectively; see Chapter 4). The clear difference between the two studies is that, whereas the macroscopic tension exhibited an exponential relaxation, the material properties appeared purely elastic at a length scale of less than 10 microns. These bacteria-adsorbed interfaces are perhaps another example of how rheological properties can depend on the length scale of the measurements (Liu *et al.*, 2006; Schmidt *et al.*, 2000).





**Figure 5.10:** Raw data of pipette suction (i.e. applied force) vs. droplet projection into pipette (i.e. resulting deformation). The interfaces were coated with (a) *A. venetianus* RAG-1 bacteria, or (b) *R. erythropolis* 20S-E1-c bacteria by mixing *n*-hexadecane and bacterial suspension with high cell concentration ( $2 \times 10^9$  CFU/mL for RAG-1 and  $10^9$  CFU/mL for 20S-E1-c). Dilational elasticity of the oil-water interface can be determined directly from such data.



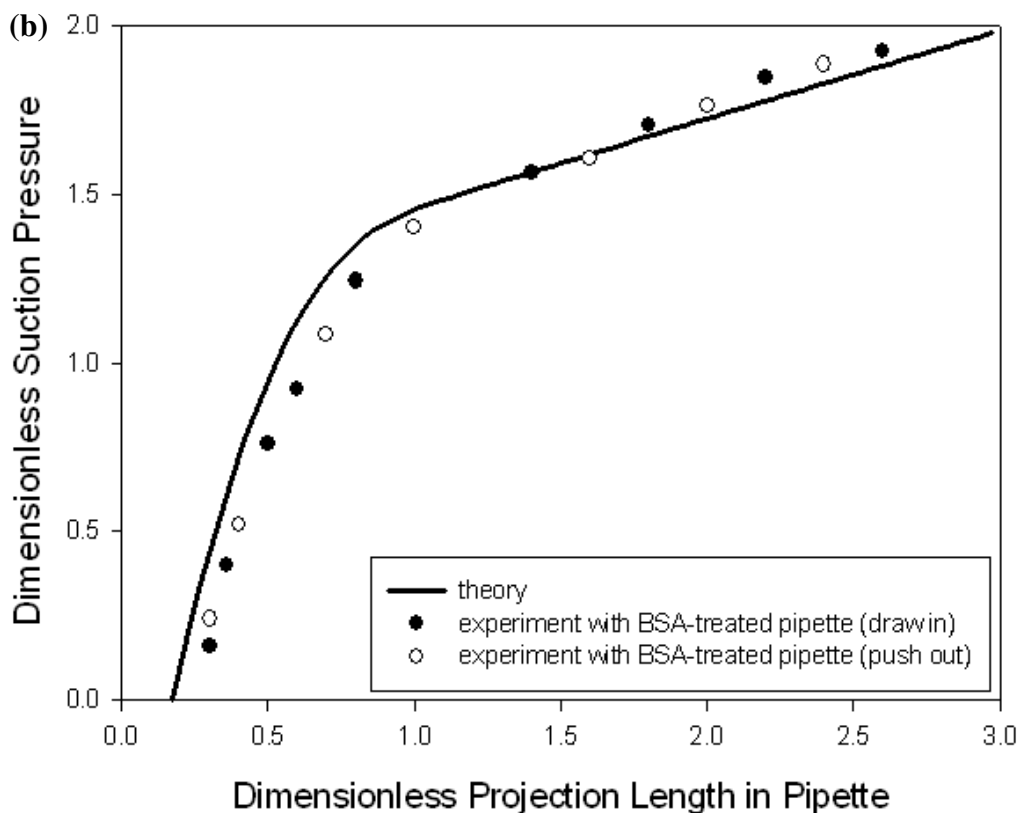


**Figure 5.11:** Fitting theoretical calculations to experimental data taken from Fig. 10. The two fitting parameters were the intrinsic interfacial tension  $\gamma_0$  and the dilational elastic modulus  $K$  (equation 5.2). The interfaces were coated with (a) *A. venetianus* RAG-1 bacteria, or (b) *R. erythropolis* 20S-E1-c bacteria by mixing *n*-hexadecane and bacterial suspension with high cell concentration ( $2 \times 10^9$  CFU/mL for RAG-1 and  $10^9$  CFU/mL for 20S-E1-c).

#### 5.4.6 Relation between elastic moduli and cell concentration in buffer

For the present systems, another striking difference between mm-scale and  $\mu\text{m}$ -scale interfacial properties can be seen from the variation of surface elastic moduli with cell concentration. In the previous mm-scale study (Chapter 4), the ‘Maxwell spring constants’ exhibited a monotonic decrease with cell concentrations (beginning with 3.5 mN/m and 7.6 mN/m at high cell concentrations, and falling to zero as the suspended cells were increasingly

diluted in the buffer). With the micropipette, the test procedures on single emulsion drops, as summarized in Figures 5.10 and 5.11, were repeated in aqueous buffers at *low* cell concentrations ( $5 \times 10^6$  CFU/mL for both RAG-1 and 20S-E1-c). Two important features about the experimental data were immediately evident:

- With much fewer cells in the buffer, only a portion of the oil phase could be emulsified; a significant amount of *n*-hexadecane remained phase separated as free oil. (This is in contrast to the situation at high cell concentrations, where all of the oil phase was emulsified as droplets.)
- For the oil that was emulsified in the aqueous phase,  $\Delta p$  vs  $L$  data on individual droplets were obtained. This  $\Delta p$  vs  $L$  data, which was obtained at low cell concentration, is in every respect indistinguishable from the data shown in Figure 5.6 (at high cell concentrations). A sample of the low cell concentration data is shown in Figure 5.8.

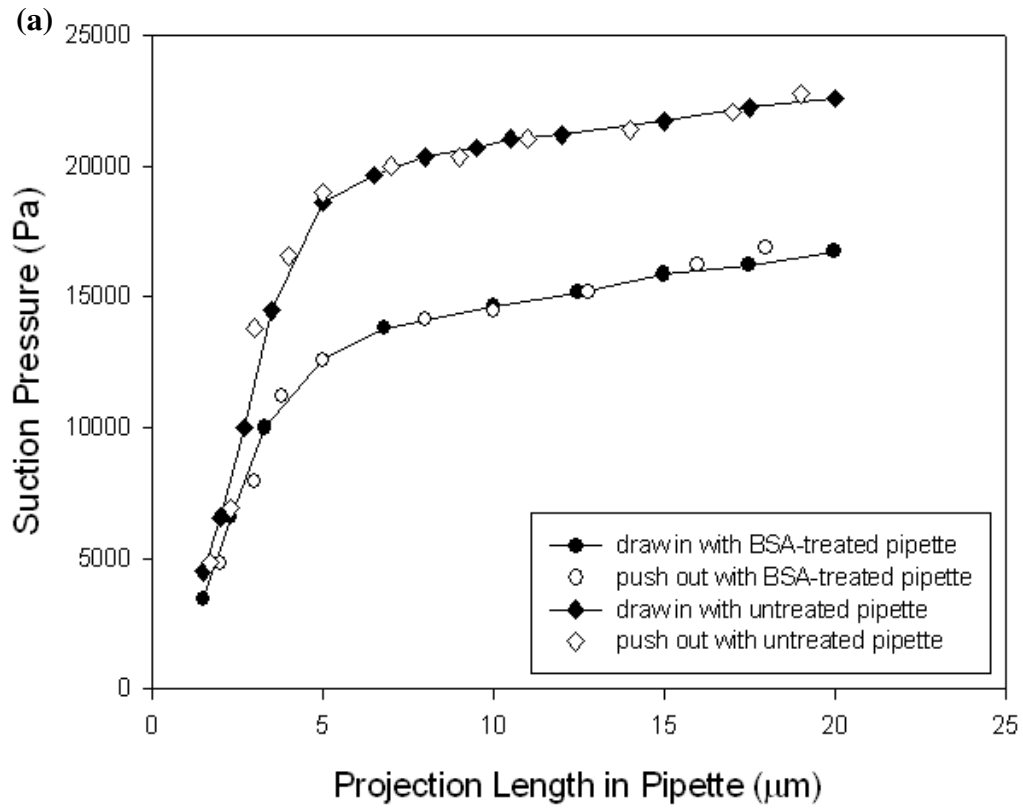
Based on more than ten individual measurements for each strain of bacteria, the average values of  $\gamma_o$  and  $K$  at low cell concentration were (Figures 5.12 and 5.13):

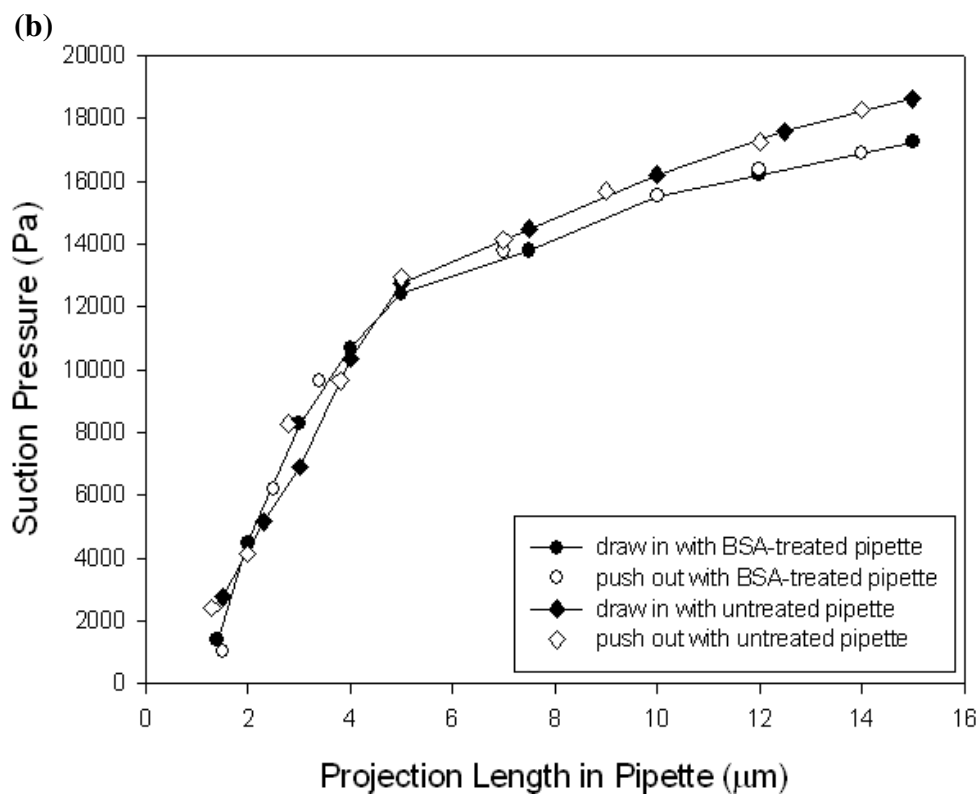
*Acinetobacter venetianus* RAG-1 films:  $\gamma_o = 47.5$  mN/m;  $K = 3.1$  mN/m

*Rhodococcus erythropolis* 20S-E1-c films:  $\gamma_o = 45.2$  mN/m;  $K = 5.4$  mN/m

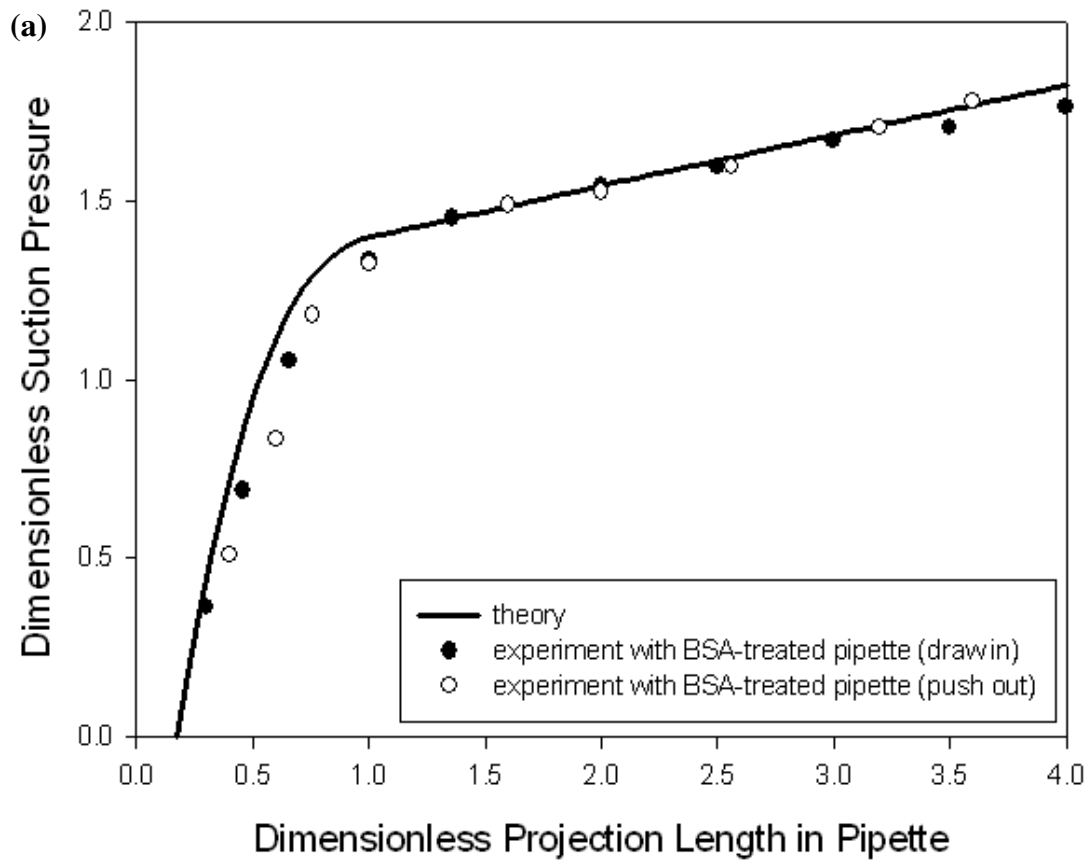
These values, which were determined at low cell concentration ( $5 \times 10^6$  CFU/mL), are practically the same as the values determined at high cell concentrations ( $2 \times 10^9$  CFU/mL for RAG-1 and  $10^9$  CFU/mL for 20S-E1-c). It appears that, on emulsion length scales, the adsorption of microbes onto the oil-water interface is

an “all-or-nothing” process: either the drop surface is fully covered with bacterial cells, or no emulsion is formed at all (resulting in hexadecane phase separating as “free oil”).





**Figure 5.12:** Raw data of pipette suction (applied force) vs. droplet projection into pipette (resulting deformation). The interfaces were coated with (a) *A. venetianus* RAG-1 bacteria, or (b) *R. erythropolis* 20S-E1-c bacteria by mixing *n*-hexadecane and bacterial suspension at low cell concentration ( $5 \times 10^6$  CFU/mL for both RAG-1 and 20S-E1-c). Dilational elasticity of the oil-water interface can be determined directly from such data.



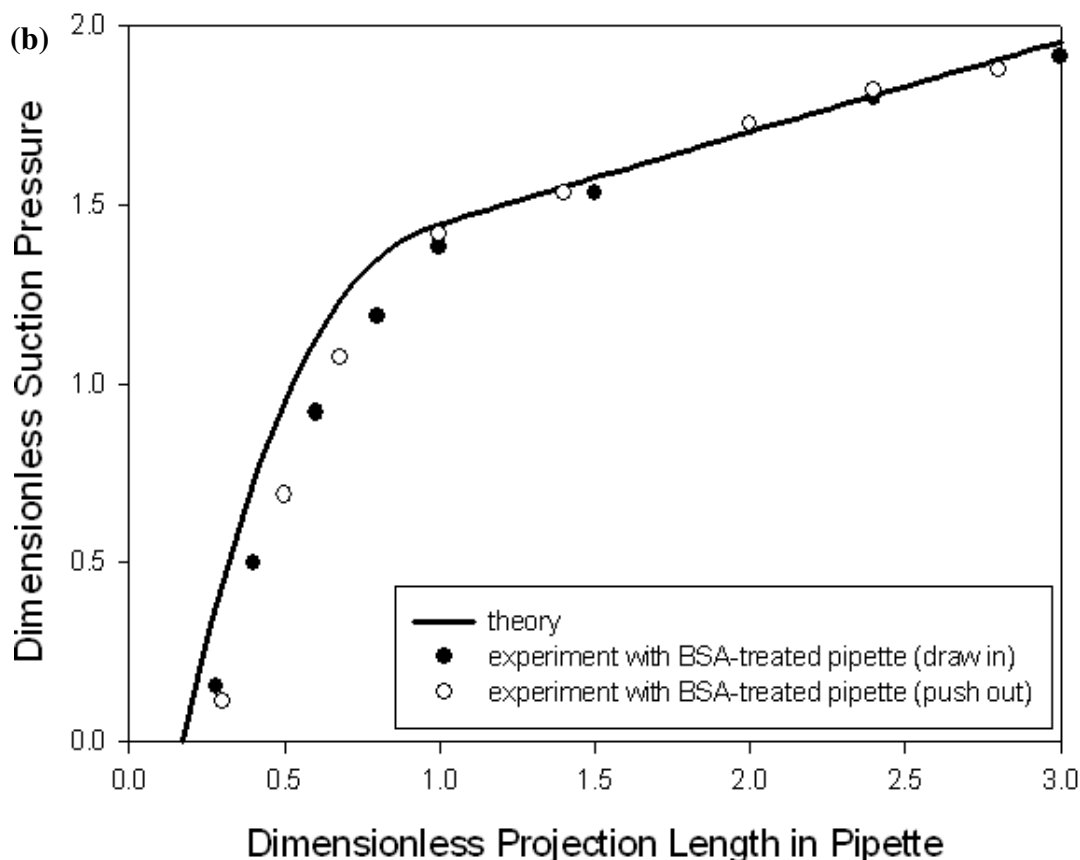


**Figure 5.13:** Fitting theoretical calculations to experimental data taken from Fig. 5.12. The two fitting parameters were the intrinsic interfacial tension  $\gamma_0$  and the dilational elastic modulus  $K$  (equation 5.2). The interfaces were coated with (a) *A. venetianus* RAG-1 bacteria, or (b) *R. erythropolis* 20S-E1-c bacteria, by mixing *n*-hexadecane and bacterial suspension at low cell concentration ( $5 \times 10^6$  CFU/mL for both RAG-1 and 20S-E1-c).

#### 5.4.7 Geometric analysis of bacterial cells at the interface in emulsion system

In this section, we now propose a 2-D geometric model on the packing of cells at the oil-water interfaces in the top emulsion layer and tried to explain the intriguing observations in the preceding section. The assumptions are as follows:

- For either strain, all the cells adsorbed at the oil/water interface are identical, which can be simplified to some specific shape. A RAG-1 cell would be perfectly spherical with a diameter of  $1.5 \mu\text{m}$ , while a 20S-E1-c

cell was perfectly rectangular with dimensions  $3\mu\text{m}\times 1\mu\text{m}$  lying on the interface (the shape and dimension are estimated from TEM image of single cell as shown in Figure 4.6). In addition, a single cell possesses uniform properties (e.g. hydrophobicity) on its surface.

- Either bacterial strain could form a close-pack *monolayer* at the interface, resembling a classic Langmuir-type adsorption (i.e. both bacterial films are comprised of single-layered cells). For 20S-E1-c, it does not matter the way that cells arrange on interface, as long as they could *fully* cover the interfacial surface. For RAG-1, since the bacterial cells were treated as “soft colloidal particles,” it was reasonable to assume that the cells were able to deform slightly (probably to hexagonal shapes) so that they could arrange easily to occupy all the space on the interface. It is also assumed that the fimbriae on the RAG-1 cells had no influence on their packing.
- The emulsion drops are treated as separate spherical particles and have uniform sizes. The diameter for RAG-1-coated oil drops is considered to be  $250\mu\text{m}$  and for 20S-E1-c to be  $270\mu\text{m}$ . These values are obtained from the particle size measurement with Mastersizer 2000 (Malvern Instruments Ltd., UK). It gives the actual particle size distribution curve for emulsion drops, and the size at volume weighted mean is chosen here as the representative drop size.

To test the model, we created oil-in-water emulsions by mixing 1 mL of *n*-hexadecane with 10 mL of bacterial suspension at high cell concentration ( $2\times 10^9$  CFU/mL for *A. venetianus* RAG-1 and  $10^9$  CFU/mL for *R. erythropolis*

20S-E1-c suspension). Here, high cell concentrations were chosen to ensure that all the oil would be emulsified, thus simplifying the calculations. As stated in Section 5.3.2, two layers of liquid would be observed in a bottle containing the oil-water mixture: a top creamy oil-in-water emulsion layer and a bottom water layer (still with suspended bacterial cells, but of a lower concentration), which is sketched in Figure 5.14.

In theory, the initial number of bacterial cells in suspension (here  $2 \times 10^{10}$  for RAG-1 and  $10^{10}$  for 20S-E1-c) should be equal to the total number of “unused” cells in the bottom layer plus the number of cells coating on the oil/water interfaces in the top layer. The number of non-adsorbed cells in the bottom layer could easily be determined by simply calibrating the volume of aqueous phase and the optical density, and by performing the dilution series test. The results were:

- for *A. venetianus* RAG-1,  $OD_{600} = 0.20$ , volume  $\approx 9.3$  mL, bacterial concentration  $\approx 2.2 \times 10^8$  CFU/mL, and the number of cells  $\approx 2.05 \times 10^9$  ;
- for *R. erythropolis* 20S-E1-c,  $OD_{600} = 0.32$ , volume  $\approx 9.0$  mL, bacterial concentration  $\approx 1.1 \times 10^8$  CFU/mL, and the number of cells  $\approx 0.99 \times 10^9$  .

Therefore, the number of bacterial cells in the top emulsion layer would roughly be  $18 \times 10^9$  for *A. venetianus* RAG-1 and  $9 \times 10^9$  for *R. erythropolis* 20S-E1-c.

Since we have known the actual number of cells in the emulsion phase, we are trying to check whether this number is consistent with the above geometric model for bacterial at the interface and the results for both strains are shown in Table 5-1.

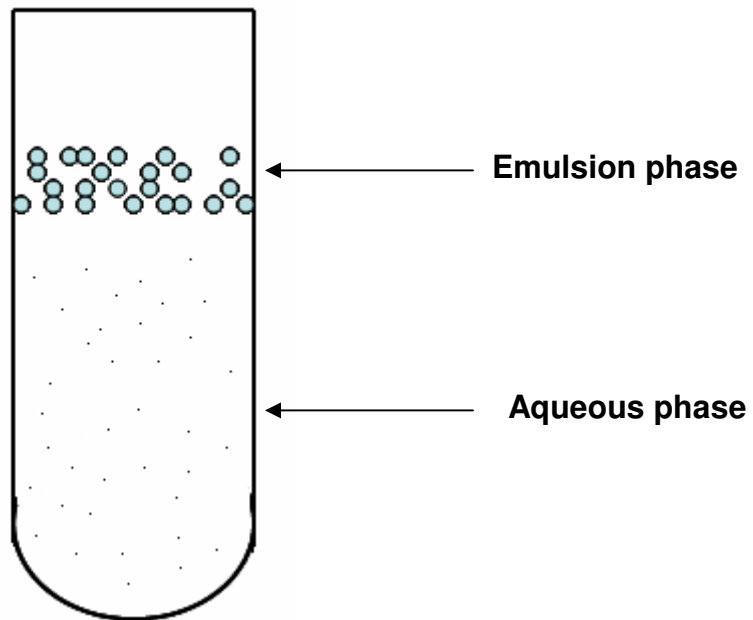


**Figure 5.14:** A sketch of the emulsion system. The initial number of bacterial cells should be equal to the number of non-adsorbed cells in the bottom aqueous phase, plus the number of cells that are adsorbed onto the oil/water interface in the top emulsion phase.

**Table 5.1:** Verification of the Geometric Model in the Emulsion System

	<i>A. venetianus</i> RAG-1	<i>R. erythropolis</i> 20S-E1-c
Emulsion drop size	Spherical with average diameter $d = 1.5\ \mu\text{m}$	rectangular with the side $3\ \mu\text{m} \times 1\ \mu\text{m}$ laid on the interfaces and with neglected cell thickness
Area of a single cell on interface	$A_{cell} = \pi\left(\frac{d}{2}\right)^2 = \pi \times \left(\frac{1.5 \times 10^{-6}}{2}\right)^2 = 1.767 \times 10^{-12}\ \text{m}^2$	$A_{cell} = a \times b = (3 \times 10^{-6}) \times 10^{-6} = 3 \times 10^{-12}\ \text{m}^2$
Total volume of oil drops	1mL	1mL
Volume of a single emulsion drop	$V = \frac{4}{3}\pi\left(\frac{D}{2}\right)^3 = \frac{4}{3}\pi\left(\frac{250 \times 10^{-6}}{2}\right)^3 = 8.181 \times 10^{-12}\ \text{m}^3$	$V = \frac{4}{3}\pi\left(\frac{D}{2}\right)^3 = \frac{4}{3}\pi\left(\frac{270 \times 10^{-6}}{2}\right)^3 = 1.031 \times 10^{-11}\ \text{m}^3$
Total number of emulsion drops	$\frac{1\text{mL}}{V} = \frac{10^{-6}\ \text{m}^3}{8.181 \times 10^{-12}\ \text{m}^3} = 122231$	$\frac{1\text{mL}}{V} = \frac{10^{-6}\ \text{m}^3}{1.031 \times 10^{-11}\ \text{m}^3} = 97087$
Total oil/water interfacial area	$A_{interface} = 4\pi\left(\frac{D}{2}\right)^2 \times 122231 = 4\pi\left(\frac{250 \times 10^{-6}}{2}\right)^2 \times 122231 = 24.0 \times 10^{-3}\ \text{m}^2$	$A_{interface} = 4\pi\left(\frac{D}{2}\right)^2 \times 97087 = 4\pi\left(\frac{270 \times 10^{-6}}{2}\right)^2 \times 97087 = 22.2 \times 10^{-3}\ \text{m}^2$
Total calculated number of bacterial cells in emulsion	$\frac{A_{interface}}{A_{cell}} = \frac{24.0 \times 10^{-3}\ \text{m}^2}{1.767 \times 10^{-12}\ \text{m}^2} = 13.6 \times 10^9$	$\frac{A_{interface}}{A_{cell}} = \frac{22.2 \times 10^{-3}\ \text{m}^2}{3 \times 10^{-12}\ \text{m}^2} = 7.4 \times 10^9$
Total actual number of bacterial cells in emulsion	$18 \times 10^9$	$9 \times 10^9$
Deviation	-25%	-18%

In both emulsion systems, since the deviation between the calculated and actual cell numbers are acceptable, it is in reasonable agreement with the geometric model which indicates the formation of a classic Langmuir-type monolayer at the interface; this is consistent with the observations at the millimetre scale with pendant drop shown in Chapter 4.

However, the deviation from this particular geometric model may be due to the several reasons:

- It was difficult to separate and measure the volumes of two layers. Initially, there were 11 mL of liquid in total (1 mL *n*-hexadecane was mixed with 10 mL bacterial suspension); the final volume was less than 11 mL due to the error in the measurement.
- The free bacterial cells in the upper emulsion layer were not included in the calculation. Since the upper layer was very cloudy with emulsion drops, we simply neglected the free bacteria in it and this can be a source of deviation.
- The estimation of cell sizes and emulsion drop sizes may not be accurate. In the first assumption, different parts of the cell surface may have different hydrophobicity, which means the attachment of a single cell may not be entirely onto the interface and this may affect the mass balance calculation.
- For 20S-E1-c, some cells may go to the oil phase and even form water-in-oil emulsions (Dorobantu *et al.*, 2004). Although only a very small

number of cells would do so, it still can be a factor which affects the calculation.

## 5.5 Conclusions

Hydrophobic bacteria, like colloidal solids, can function as emulsifiers by adsorbing onto the oil-water interface spontaneously and modifying their surface properties. In this study, two strains of hydrophobic bacteria (*Acinetobacter venetianus* RAG-1 and *Rhodococcus erythropolis* 20S-E1-c) were prepared in their stationary (i.e. non-dividing) phase in the absence of biosurfactants; these cells were then employed as emulsifiers to stabilize *n*-hexadecane droplets in aqueous environments. Microscope and micropipette techniques have been developed to study the general rheological behaviours of emulsion drop surfaces. These experiments involved simple and direct observations of bacterial films at interfaces, colloidal stability tests, and micron-scale stress-strain tests (from which interfacial tensions and surface elasticities were determined). In the direct microscopic observations, it was found that the *A. venetianus* RAG-1 on the interface could interlink with one another via the fimbriae and form a network which resisted in-plane shearing. In contrast, for the *R. erythropolis* 20S-E1-c cells, if the interface were disturbed by some forces, their smooth surfaces would likely facilitate free sliding between neighbouring cells; these observations were in agreement with the previous TEM photos and pendant drop study. In the colloidal stability tests, two bacteria-coated droplets were examined through direct contact. Both types of bacteria were seen to function as effective stabilizers,

although the RAG-1 film provided stronger resistance to droplet-droplet coalescence. In addition to creating steric barriers, the adsorbed bacteria also interacted with one another at the interface and gave rise to *higher order* rheological properties. In the micron-scale stress-strain experiments (a technique of directly probing the *in situ* mechanical properties of the emulsion drop surfaces), the bacterial films appeared purely elastic on length scales of ~10 microns. As an initial attempt to model the elastic behaviour of surface films, a two-parameter theoretical model was introduced and excellent agreement with experimental data was obtained. With this added elasticity provided by the bacteria, the phenomenon of capillary instability was eliminated. The result was in contrast to a previous macroscopic (i.e. mm-scale) study, which showed that stresses in similar adsorbed films could be relieved through internal relaxation. More strikingly, the surface elasticity was not affected by the cell concentration in the aqueous phase, which was in contrast to the previous results at the millimetre scale by pendant drop technique. Therefore, the rheological properties of bacteria-adsorbed interfaces appeared to be length scale-dependent. At the same time, the bacteria in the emulsion system were proven to form a classic Langmuir-type monolayer at the interface, which is consistent with the observations at the millimetre scale. These observations may be important for MEOR applications. In particular, with the creation of bacterial films and the elimination of capillary instability, the ability for emulsified droplets to plug porous channels is strongly enhanced.

## CHAPTER 6 PRELIMINARY STUDY ON EMULSION FLOW THROUGH A CONSTRICTED CHANNEL

### 6.1 Introduction

In Chapter 5, it was stated that, on the micrometre scale (i.e. the length scale which is relevant to the porous rock), hydrophobic bacteria can function as emulsifiers by adsorbing onto the oil-water interface spontaneously and modifying their surface properties. These emulsions occur in most microbial enhanced oil recovery processes and are involved in crude oil transportation (Sen, 2008). Therefore, a crucial aspect of MEOR process is to understand the mechanisms of removing oil from the rock pores with the formation of such emulsions; this requires detailed research of the physics in the bacteria-involved immiscible displacement processes. However, most studies in MEOR have concentrated on the bacterial transportation in the presence of two immiscible phases under experimental conditions of porous medium (e.g. sand packed column) (Reynolds *et al.*, 1989; Gannon *et al.*, 1991; Sarkar, 1994). Very little research has been carried out in the area of the effect of biosurfactants or bioemulsifiers on flow mechanics of emulsion system under laboratory scale experiments (Georgiou *et al.*, 1992; Banat, 1995; Bognolo, 1999). Furthermore, no attempt has been made in the literature to simulate macroemulsion flow performance by including the interfacial rheological properties of bacterial films at the oil-water interface. Therefore, there is a need for understanding the fundamental physics controlling the flow of a bacteria-stabilized emulsion in simple porous medium.

In Chapter 5, micropipette experiments were developed to quantify the surface elasticity of bacteria-adsorbed oil-water interfaces. In addition to determining intrinsic material properties, the micropipette is also an ideal model device for simulating flow through constricted channels in porous rocks (in microbial-enhanced oil recovery). In this part of the study, using micropipettes, controlled oil displacement experiments can be designed in which the surface of a hexadecane droplet (representing residual oil ganglia trapped in an oil well) is adsorbed with bacterial cells, while the pipette, with deliberately manipulated surface properties, can represent a constricted channel within the porous medium. In such experiments, the micropipettes would be lubricated using BSA proteins, which would simulate one of the surface properties encountered in MEOR applications.

## **6.2 Materials and Methods**

### **6.2.1 Sample preparation**

Bacterial culture and staining processes have been introduced in Section 3.1. Emulsion preparation was discussed in Section 3.2; we made emulsions with only high cell concentration for both bacterial strains.

### **6.2.2 Micropipette experiments setup**

We conducted experiments with pipettes containing truncated tips as shown in Figure 6.1. The detailed micropipette manufacturing process has been

introduced in Section 5.3.2., with less pulling voltage being required to obtain an abruptly decreasing tip from millimetres to a few microns.

In the experiment, the micropipette was connected with that Teflon tube that was full of emulsion. It was then mounted and put in a sample cell which initially contained about 30  $\mu\text{L}$  of an oil-in-water emulsion. The pushing pressure could be measured accurately using a pressure transducer (Omega Engineering, Stamford, CT) which was connected to the pipette and the syringe with a T-section. The emulsion drops would be pushed through the constricted channel one after another and the stress-strain behavior would be observed. Again, experiments would be conducted with untreated pipettes as well as pipettes pre-coated with BSA, which would simulate different surface properties of the porous medium.

### **6.3 Preliminary Results**

For clean oil/water interfaces (no microbes), as control tests with BSA-coated or uncoated pipettes, if pushed, the oil drops in the pipette would quickly coalesce on contact until finally a large oil drop was formed and pushed out of the pipette; the phenomena of capillary instability appeared during this process.

For RAG-1-coated oil drops flowing in untreated pipettes, the bacterial films showed very strong friction against the untreated glass surface. The oil drops went slowly under the pressure; more drops tended to gather and form a larger drop group and stuck in the pipette. When the pushing pressure increased to 5 psi, the RAG-1 film at the oil/water interface was torn (please recall the

paper-like films formed by RAG-1 cells), the oil in the emulsion group was squeezed out and the released “naked” oil became stable immediately (this was possible with the quick adsorption of free bacterial cells onto the oil/water interfaces); the “bacterial skins” remained and plugged the pipette. It was almost impossible to push those films out of the pipette with the syringe (Figure 6.2a).

For RAG-1-coated oil drops in the BSA-treated pipettes, much less pressure was needed to push the emulsion drops in the pipettes (the pressure was kept around 3 psi). Upon pushing, single emulsion drops or small interacting groups of drops easily connected and formed a larger drop group. The interconnected drops could go through the pipette tip one by one under pressure by keeping their integrity; the released emulsion drops still tended to interact with each other and form a group (Figure 6.2b). These phenomena were easy to explain with the cell surface properties as being stated in Section 4.3.4.

For 20S-E1-c-coated oil drops in untreated pipettes, the drops showed similar flow behaviour with RAG-1-coated drops in untreated pipettes: the bacterial films had strong friction against the pipette surface, the oil was squeezed out from the emulsion drops and the bacterial skins tended to plug the pipette (Figure 6.3a). The important message from Figure 6.3a is: it is the first time that we can observe the 20S-E1-c films at the oil/water interfaces. In the previous static experiments, we indicated the existence of such films from the modification of properties that they have displayed on the interface (Figure 4.5b). Since the 20S-E1-c films are soap film-like, we did not observe the wrinkles or sheets like

RAG-1 films. Here, the bacterial films shown in Figure 6.3a have provided the direct evidence for the previous discussions.

For 20S-E1-c-coated oil drops moving in the BSA-treated pipettes, it was much easier to push the oil drops out of the pipette (the pressure was around 2 psi). The oil drops can pass through the pipette tip one by one; those oil drops remained separate and did not interact with each other (Figure 6.3b). These observations can also be related to the smooth cell surface property that 20S-E1-c cell has (Section 4.3.4).

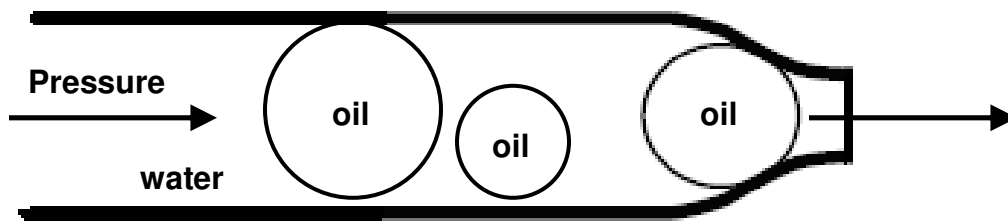


**Figure 6.1:** The actual experimental system; the tip of the micropipette is around 10  $\mu\text{m}$ .

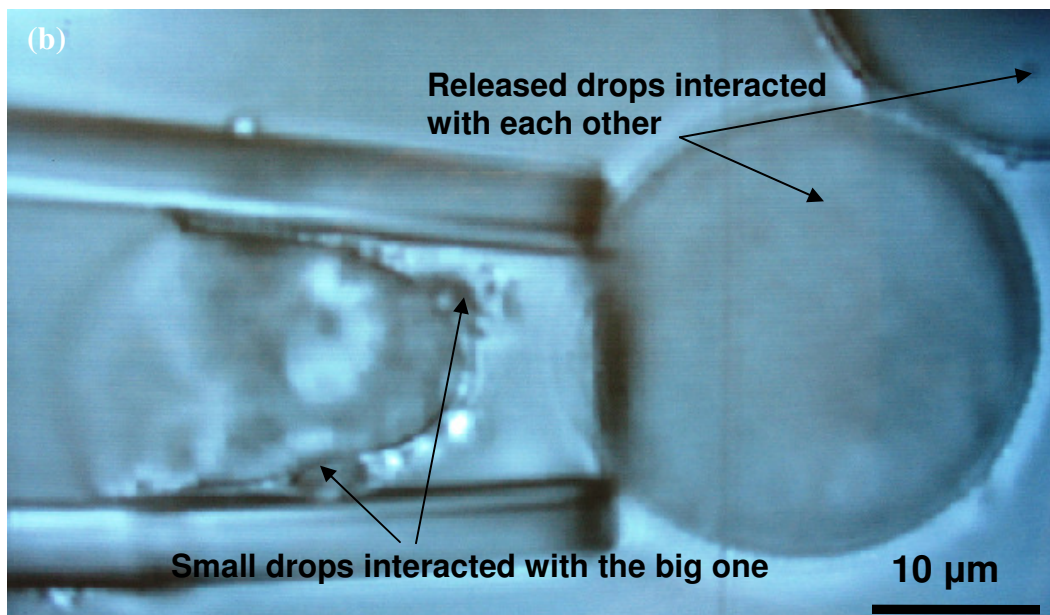
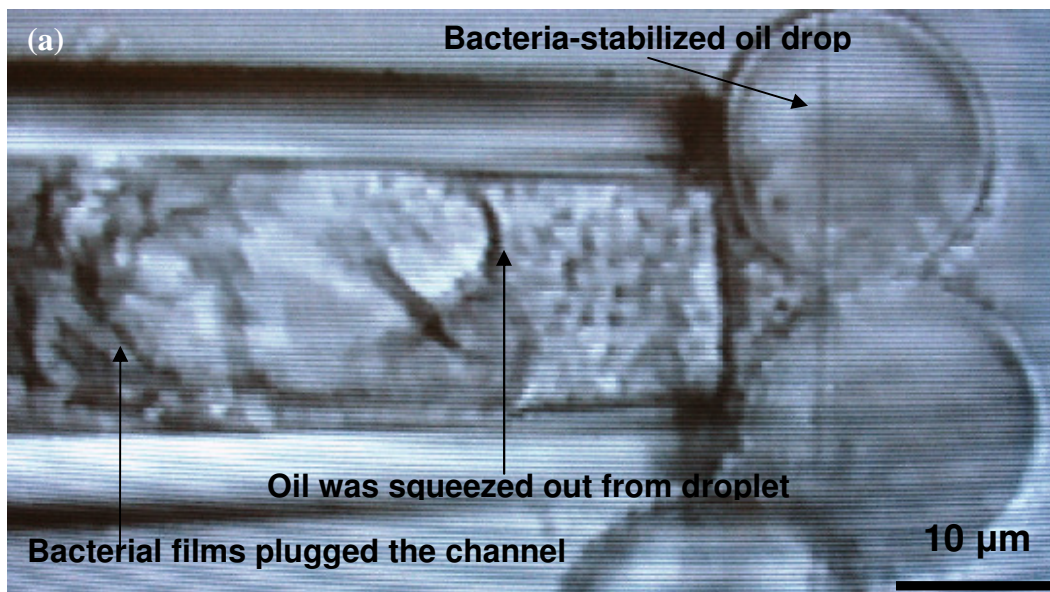


**Figure 6.2:** Behavior of oil drop coated with *A. venetianus* RAG-1 in an “oil displacement” experiment through a constricted channel. (a) The pipette was not pre-treated with BSA. The oil drops in the emulsion in the channel were squeezed out and they formed stable drops outside of the channel. The bacterial skins plugged the channel. (b) The pipette was pre-treated with BSA. The interconnected emulsion drops in channel can go through the pipette tip one by one under pressure and the released drops still intended to interact with each other.

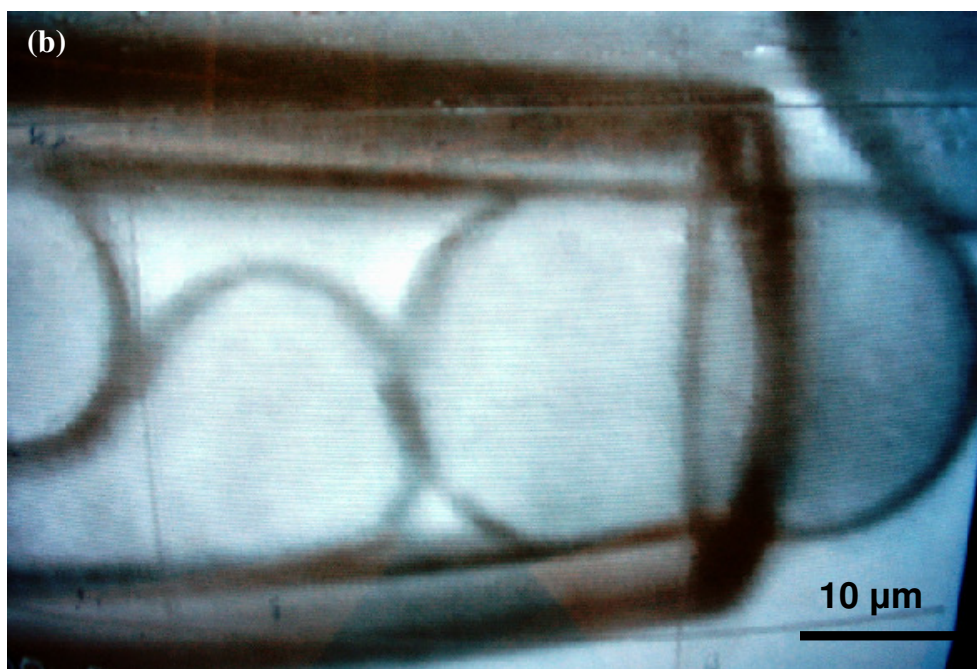
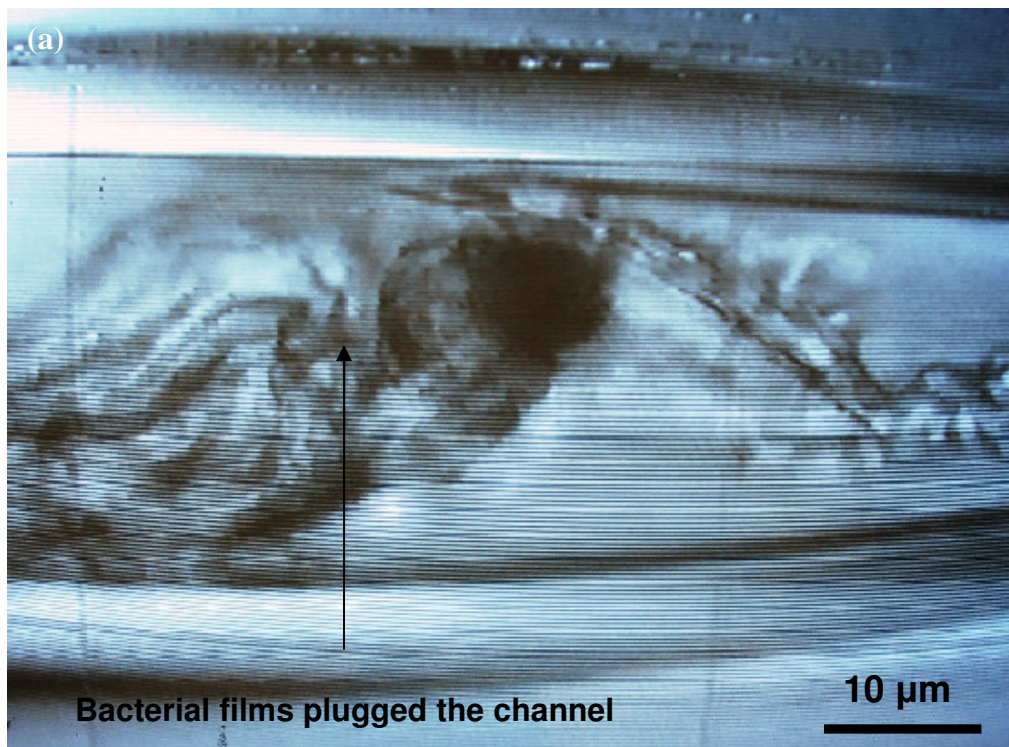


**Figure 6.3:** Behavior of oil drop coated with *R. erythropolis* 20S-E1-c in an “oil displacement” experiment through a constricted channel. (a) The pipette was not pre-treated with BSA. Bacterial films were seen to plug the channel. (b) The pipette was pre-treated with BSA. The emulsion drops in channel can go through the pipette tip one by one under pressure.

## 6.4 Conclusions

An oil displacement experiment was designed for hexadecane drops with bacterial cells adsorbed at surfaces. These experiments involved simple and direct observations of micron-scale emulsion drop flow behavior in a constricted channel. The qualitative results can be correlated with the interfacial rheological properties from the previous obtained static experiments and can be explained by the cell surface ultrastructures.

The experimental results have indicated that two factors are crucial in determining the bacterial involved oil displacement process in porous medium: the properties of interfacial bacterial films (ultimately the cell surface properties) and the surface properties of porous medium. In general, the RAG-1 films can facilitate the formation of a three-dimensional oil drop network via the fimbriae on cell surfaces, which would be easier to plug the pores. A lubricated pore surface would help eliminate the pore plugging phenomena.

However, these are only preliminary observations from a simple oil displacement experiment. More detailed flow experiments need be designed to obtain insights in the fundamental physics controlling the flow of such bacteria-stabilized emulsion in porous medium. Quantitative results need to be drawn from the micropipette experiments regarding the force that is added to the flow and the flow behaviours. More correlations need to be made between the interfacial rheological properties and the flow situation. At the same time, parameters regarding the pore surface properties must be further considered. Currently, it is assumed that the interior of glass surface was characterized by

simple and uniform properties. In real porous rocks, these surface properties may deviate significantly from these assumptions. For example, the hydrophobicity of the rock may vary along the channel, which would likely affect the flow of oil drops. In addition, some porous medium may be characterized by additional properties, such as complex geometry, grain composition, permeability, non-uniform temperature and corrosion (Sadhukhan *et al.*, 2007; Hassanien and Elaiw, 2007). It is important to design experiments and develop theoretical models that incorporate more complex situations for the porous medium as they may interact with the bacterial films and play crucial roles in the mechanical behavior of emulsion drops in the flow. For example, the hydrophobicity of the interior of glass surface can be manipulated using silanizing chemicals.

## CHAPTER 7 SUMMARY AND RECOMMENDATIONS

The mechanical properties of bacterial films formed at oil/water interfaces can have profound relevance to applications in the petroleum industry — such as microbial enhanced oil recovery (MEOR) and bioremediation — in which large oil/water interfacial areas are involved. As outlined in the Introduction, the objectives of this research were to develop techniques to explore the behaviour of bacterial film coatings on individual oil drops and to quantify their material properties on the millimetre- and micrometre scales. In what follows, the main contributions of this study are outlined and recommendations for future studies are discussed.

### 7.1 Summary of contributions

The pendant drop technique was applied to examine, both qualitatively and quantitatively, the mechanical properties of bacterial films formed at the oil-water interface when a droplet of model oil (*n*-hexadecane) was in contact with an aqueous bacterial suspension. This is considered a “macro-scale” technique as the sizes of the oil droplets were typically several millimetres (as dictated by the capillary constant). Dynamic response of the oil drop surfaces was observed in stress-strain experiments in which a drop was subjected to step up/step down area perturbations and the interfacial responses were recorded and analysed. Using such a technique, *high order* interfacial properties, such as surface elasticity and internal stress relaxation, were determined.

To explore interfacial properties on the micrometer scale, the micropipette technique was developed to directly examine the *in situ* behaviour of single emulsion drops. As such, phenomena due to the “smallness” of the emulsion drops (giving rise, for example, to large surface area-to-volume ratios) could accurately be reflected by such unique experiments. Unlike the pendant drop technique, which relied on gravity as the external force applied to the oil drop, individual emulsion drops were deformed here by micron-scale suction pipettes. Through precise control of the pipette suction pressures, it was possible to carry out controlled stress-strain experiments on the micrometer (i.e. emulsion) scale. Using such a method, the elastic behaviour of bacterial films was quantified, for the first time, directly at the surfaces of individual emulsion drops. A two-parameter constitutive model was introduced to represent the interfacial elasticity of the bacterial films; excellent agreement was seen between the theoretically-predicted behaviours (based on the Young-Laplace equation) and experimental observations. As such, we have developed a means of quantifying the interfacial mechanical properties of emulsion drops *in situ*.

In addition to determining intrinsic material properties, the micropipette was also applied as a model device for simulating flow through constricted channels in porous rocks (in microbial-enhanced oil recovery). Controlled oil displacement experiments were designed in which the surface of a hexadecane droplet (representing residual oil ganglia trapped in an oil well) was adsorbed with bacterial cells, while the pipette, with deliberately manipulated surface properties, represented a constricted channel within the porous medium.

Preliminary results in such experiments have shown that the material properties of the bacterial films at the oil/water interfaces and the surface properties of porous mediums are two crucial parameters in understanding the two-phase flow properties in porous medium.

This was the first study detailing the surface rheology of bacterial films formed at oil/water interfaces. In regard to MEOR (microbial-enhanced oil recovery) applications, such rheological properties are expected to be crucial in understanding the passage of small bacteria-coated oil droplets through constricted channels (e.g. in porous rocks; Preliminary results shown in Chapter 6). It was interesting to note that the two bacterial strains employed in this study revealed two classes of material properties which were due to differences in cell-cell interactions at the interface (i.e. whether the cells would interlock or slide freely past one another); TEM images of the surface structures of the bacteria appeared to support such a conjecture. With respect to IFT measurement at different length scales, these techniques gave the same conclusions that the bacterial cells would not lower the oil/water equilibrium interfacial tension, which agreed with theoretical prediction. However, some rheological properties of bacteria-adsorbed interfaces appeared to be length scale-dependent: the bacterial films appeared purely elastic in micron-scale stress-strain experiments (Chapter 4), while millimetre-scale studies (Chapter 5) indicated that stresses in similar adsorbed films could be relieved through internal relaxation. More strikingly, the cell concentration in the aqueous phase affected interfacial rheological properties only on the millimetre scale.

## 7.2 Recommendations for future work

In this project, all the experiments were conducted at room temperature and one atmosphere (the so-called the “standard” conditions). However, many industrial processes involving bacteria operate at temperatures and pressures that differ from standard conditions. For example, since oil reservoirs are often subjected to elevated temperature and pressure conditions, successful microbial strains for MEOR should be able to adapt to such environments and their behaviours can be quite different from those in our experiments (Premuzic and Lin, 1991; Behlulgil and Mehmetoglu, 2002). Also, *in situ* bioremediation must overcome the inhibitory effects of seasonal variations such as the rainy and winter seasons (Ko *et al.*, 2007). Therefore, it is important to adapt the pendant drop and micropipette techniques to study the thermomechanical and pressure-dependent properties of bacterial films under different temperatures and pressures.

In this study, bacterial surfaces have been shown either to be smooth or covered with “hairy” filaments. We can mimic these structures by making “model colloids,” which are created, for example, by grafting macromolecules (polysaccharides or proteins of known molecular weights) onto polystyrene or silica nanoparticles of different shapes; these colloids would adsorb readily onto oil-water interfaces. Then, the surface properties of these polymer-conjugated surfaces can be characterized through measurements of zeta potential, hydrodynamic radius, contact angle, etc. We may also devoid the bacterial cell surface fimbriae (through low shear agitation, sonication, mutation, etc) and investigate the oil-water interfacial properties with these “modified” cells. The

results can be compared to those properties brought by the normal bacterial cells and silica particles. In all these trials, for oil-water interfaces adsorbed with such modified cells or model colloids, interfacial rheological measurements can be performed using pendant drop technique (with the aqueous colloidal suspension being the dispersed phase, and hexadecane the continuous phase) and then switching to micropipette technique (with hexadecane as the dispersed droplet and the aqueous colloidal suspension as the surrounding medium). Following the experimental approach developed in this study, using the pendant drop, we may begin experiments with static response (control test), followed by step and oscillatory responses; we may then look for evidence of *higher order* interfacial properties such as dilational elasticity and signs of in-plane shear resistance. With micropipettes, we can observe the interactions between model colloids and determine the interfacial material properties by conducting experiments similar to those discussed in Chapter 5. Force-based experiments using the microcantilever (Moran *et al.*, 1999, 2000) may also be useful. As such, the results can be compared to the current results obtained in this study and would become a valuable component of the knowledge base in the petroleum industry.

## BIBLIOGRAPHY

Abend, S., Bonnke, N., Gutschner, U., Lagaly, G., Stabilization of emulsions by heterocoagulation of clay minerals and layered double hydroxides, *Colloid and Polymer Science*, **276**, 730-737, (1998)

Acevedo, S., Ranaudo, M.A., Escobar, G., Gutierrez, X., Dynamic interfacial tension measurement of heavy crude oil-alkaline systems: The role of the counterion in the aqueous phase, *Fuel*, **78**, 309-317, (1998)

Adamson, A.W., *Physical Chemistry of Surfaces*, 2<sup>nd</sup> Ed., Interscience Publishers, John Wiley & Sons, New York, 1967

Adamson, A.W., *Physical Chemistry of Surfaces*, John Wiley & Sons, New York, NY, USA, 1-6, 47-98, (1976)

Aitken M.D., Characteristics of phenanthrene degrading bacteria isolated from soils contaminated with PAHs, *Canadian Journal of Microbiology*, **44**, 743-752, (1998)

Akit, J., Cooper, D.G., Manninen, K.I., Zajic, J.E., Investigation of potential biosurfactan production among phytopathogenic Corynebacterai and related soil microbes, *Current Microbiology*, **6**, 145-150, (1981)

Alexander, M., *Biodegradation and Bioremediation*, Academic Press, New York, (1994)

Allen, P.G., Francy, D.S., Duston, K.L., Thomas, J.M., Ward, C.H., Biosurfactant production and emulsification capacity of subsurface microorganisms, In: *Preprints: Soil Decontamination Using Biological Processes*, Karlsruhe, Germany, 58-66, (1992)

Andreas, J.M., Hauser, E.A., Tucker, W.B., Boundary tension by pendant drops, *The Journal of Physical Chemistry*, **42(8)**, 1001-1019, (1938)

Arashiro, E.Y., Demarquette, N.R., Use of pendant drop method to measure interfacial tension between molten polymers, *Material Research*, **2**, 23-32, (1999)

Aske, N., Orr, R., Sjoblom, J., Dilational elasticity moduli of water-crude oil interfaces using the oscillating pendant drop, *Journal of Dispersion Science and Technology*, **23(6)**, 809-825, (2002)

Atlas, R.M., Cerniglia, C.E., Bioremediation of petroleum pollutants, *Bioscience*, **45(5)**, 332-338, (1995)

Atlas, R.M., Microbial hydrocarbon degradation-bioremediation of oil spills, *Journal of Chemical Technology and Biotechnology*, **52(2)**, 149-156, (1991)

Atlas, R.M., Unterman, R., Bioremediation, In *Manual of industrial microbiology and biotechnology*, Demain, A.C., Davis, J.E. (Eds.), 666–681, 2<sup>nd</sup> edition, ASM Press, Washington, (1999)

Aveyard, R., Binks, B.P., Clint, J.H., Emulsions stabilized solely by colloidal particles, *Advances in Colloid and Interface Science*, **100-102**, 503-546, (2003)

Banat, I.M., Biosurfactants production and possible uses in microbial enhanced oil recovery and oil pollution remediation: a review, *Bioresource Technology*, **51**, 1-12, (1995)

Barclay, C.D., Biodegradation and sorption of polyaromatic hydrocarbons by *Phanaerochaete chrysosporium*, *Applied Microbiology and Biotechnology*, **62**, 1188–1196, (1995)

Bartell, F.E., Neiderhauser, D.O., Film forming constituents of crude petroleum oils, *Fundamental Research on Occurrence and Recovery of Petroleum*, API, **57**, 1946-1947, (1949)

Beal, R., Betts, W.B., Role of rhamnolipid biosurfactants in the uptake and mineralization of hexadecane in *Pseudomonas aeruginosa*, *Journal of Applied Microbiology*, **89**, 158-168, (2000)

Becher, P., (Ed.), *Emulsions-Theory and Practice*, Oxford University Press, USA, (2001)

Beckman, J.W., The action of bacteria on mineral oil, *Industrial and Engineering Chemistry*, **4**, 23-26, (1926)

Behlulgil, K., Mehmetoglu, M.T., Bacteria for improvement of oil recovery: A laboratory study, *Energy Resources*, **24(5)**, 413-421, (2002)

Bell, K.S., Philp, J.C., Aw, D.W.J., Christofi, N., A review: the genus *Rhodococcus*, *Journal of Applied Microbiology*, **85(2)**, 195-210, (1998)

Berkman, S., Egloff, G., (Eds.), *Emulsions and Foams*, Reinhold Publishing Corp., New York, USA, (1941)

Beveridge, T.J., Graham, L.L., Surface layers of bacteria, *Microbiological Reviews*, **55(4)**, 684-705, (1991)

Beveridge, T.J., Pouwels, P.H., Margit, S., Kotiranta, A., Lounatmaa, K., Kari, K., Kerosuo, E., Haapasalo, M., Egelseer, E.M., Schocher, I., Sleytr, U.B., Morelli, L., Callegari, M.L., Nomellini, J.F., Bingle, W.H., Smit, J., Leibovitz, E., Lemaire, M., Miras, I., Salamiou, S., Béguin, P., Ohayon, H., Gounon, P., Matuschek, M., Sahm, K., Bahl, H., Grogono-Thomas, K., Dworkin, J., Blaser, M.J., Woodland, R.M., Newell, D.G., Kessel, M., Koval, S.F., Function of s-layers, *FEMS Microbiology Reviews*, **20(1-2)**, 99-149, (1997)

Beverung, C.J., Radke, C.J., Blanch, H.W., Protein Adsorption at the Oil/Water Interface: Characterization of Adsorption Kinetics by Dynamic Interfacial Tension Measurements, *Biophysical Chemistry*, **81**, 59-80, (1999)

Bhardwaj, A., Hartland, S., Study on build up of interfacial film at the crude oil/water interface, *Journal of Dispersion Science and Technology*, **19(4)**, 465-473 (1998)

Bikerman, J.J., *Surface Chemistry*, Academic Press, New York, (1958)

Binks, B.P., (Ed.), *Modern aspects of emulsion science*, The Royal Society of Chemistry, UK, (1998)

Binks, B.P., Lumsdon, S.O., Catastrophic phase inversion of water-in-Oil emulsions stabilized by hydrophobic silica, *Langmuir*, **16**, 2539-2547, (2000)

Binks, B.P., Particles as surfactants – similarities and differences, *Current Opinion in Colloid and Interface Science*, **7**, 21-41, (2002)

Biswas, B., Haydon, D.A., The rheology of some interfacial adsorbed films of macromolecules. I. Elastic and creep phenomena, *Proceedings of the Royal Society of London A*, **271**, 296-316, (1963); The rheology of some interfacial adsorbed films of macromolecules. II. Stress relaxation phenomena, **271**, 317-323, (1963)

Boesch, D.F., Butler, J.N., Cacchione, D.A., Geraci, J.R., Neff, J.M., Ray, J.P., Teal, J.M., An assessment of the long-term environmental effects of U.S. offshore oil and gas development activities: Future Research Needs, In: *Long-term Environmental Effects of Offshore Oil and Gas Development*, Boesch, D.F., Rabalais, N.N., (Eds.), 1-55, (1987)

Bognolo, G., Biosurfactants as emulsifying agents for hydrocarbons, *Colloids and Surfaces A*, **152(1-2)**, 41-52, (1999)

Bos, M.A., Vliet, T.V., Interfacial rheological properties of adsorbed protein layers and surfactants: a review, *Advances in Colloid and Interface Science*, **91**, 437-471, (2001)

Bouchez-Naitali, M., Blanchet, D., Bardin, V., Vandecasteele, J.P., Evidence for interfacial uptake in hexadecane degradation by *Rhodococcus equi*: the importance of cell flocculation, *Microbiology*, **147**, 2537-2543, (2001)

Bouriat, P., El Kerri, N., Graciaa, A., Lachaise, J., Properties of a two-dimensional asphaltene network at the water - Cyclohexane interface deduced from dynamic tensiometry, *Langmuir*, **20(18)**, 7459-7464, (2004)

Boussinesq, J., Sur l'existence d'une viscosite superficielle, dans la mince couche de transition separant un liquide d'un autre fluide contgu. *Annales de Chemie et de Physique*, Huiteme Serie, **24**, 349-357, (1913)

Boussinesq, J., Application des formules de viscosite superficielle a la surface d'une goutte liquide spherique, tombant lentement, d'un mouvement devenu uniforme, au sien d'une masse fluide indefinite en physique, *Huitieme Series*, **24**, 357-371, (1913)

Boyce, J.F., Schurch, S., Rotenberg, Y., Neumann, A.W., The measurement of surface and interfacial tension by the axisymmetric Drop Technique, *Colloids and Surfaces*, **9(4)**, 307-317, (1984)

Bredholt, H., Bruheim, P., Potocky, M., Eimhjellen, K., Hydrophobicity development, alkane oxidation, and crude-oil emulsification in a *Rhodococcus* species, *Canadian Journal of Microbiology*, **48(4)**, 295-304, (2002)

Brock, T.D., Madigan, M.T., (Eds.), *Biology of Microorganisms*, Prentice-Hall Inc., New Jersey, (1991)

Brooks, B.W., Richmond, H.N., Phase inversion in non-ionic surfactant – oil – water systems I: The effect of transitional inversion on emulsion drop sizes, *Chemical Engineering Science*, **49**, 1053-1065, (1994)

Bryant, R.S., Burchfield, T.E., Review of microbial technology for improving oil recovery, *SPE Reservoir Engineering*, **4**, 151-154, (1989)

Bryant, R.S., Douglas, J., Evaluation of microbial systems in porous media for EOR, *SPE Reservoir Engineering*, **3**, 489-495, (1988)

Busscher, H.J., Bos, R., van der Mei, H.C., Handley, P.S., Physicochemistry of microbial adhesion from an overall approach to the limits, In: *Physical Chemistry of Biological Interfaces*, Baszkin, A., Norde, W. (Eds.), Marcel Dekker, New York, 431-458, (2000)

Butt, H-J., Graf, K., Kappl, M., *Physicas and Chemistry of Interfaces*, Verlag GmbH & Co. KGaA, Weinheim, Germany, (2003)

Cairns, W.L., Cooper, D.G., Zajic, J.E., Wood, J.M., Kosaric, N., Characterization of *Nocardia amarae* as a potent biological coalescing agent of

water-oil emulsions, *Applied and Environmental Microbiology*, **43**, 362-366, (1982)

Carla, C. C. R., de Carvalho. M., Manuela, R., da Fonseca, T., The remarkable *Rhodococcus erythropolis*, *Applied Microbiological Biotechnology*, **67**, 715–726, (2005)

Caroff, M., Karibian, D., Structure of bacterial lipopolysaccharides, *Carbohydrate Research*, **338(23)**, 2431-2447, (2003)

Chappat, M., Some applications of emulsions, *Colloids and Surfaces A*, **91**, 57-77, (1994)

Cheng, P., Li, D., Boruvka, L., Rotenberg, Y., Neumann, A.W., Automation of axisymmetric drop shape analysis for measurement of interfacial tensions and contact angles, *Colloids and Surfaces*, **43(2-4)**, 151-167, (1990)

Cheng, P., Neumann, A.W., “Computational evaluation of axisymmetric drop shape analysis-profile (ADSA-P), *Colloids and Surfaces*, **62(4)**, 297-305, (1992)

Cirigliano, M.C., Carman, G.M., Isolation of a bioemulsifier from *Candida lipolytica*. *Applied and Environmental Microbiology*, **48**, 747-750, (1984)

Clayfield, E.J., Lumb, E.C., A theoretical approach to polymeric dispersant action I. Calculation of entropic repulsion exerted by random polymer chains terminally adsorbed on plane surfaces and spherical particles, *Journal of Colloid and Interface Science*, **22(3)**, 269-284, (1966); A theoretical approach to polymeric dispersant action II. Calculation of the dimensions of terminally adsorbed macromolecules, **22(3)**, 285-293, (1966)

Clayton, W., *The Theory of Emulsions*, Churchill, London, 92-98, (1954)

Cohen, R., Exerowa, D., Surface forces and properties of foam films from rhamnolipid biosurfactants, *Advances in Colloid and Interface Science*, **134–135**, 24–34, (2007)

Cookson, J.T., *Bioremediation Engineering: Design and Application*, McGraw-Hill, New York, (1994)

Cooper, D., Goldenberg, B.G., Surface-active agents from two *Bacillus* species, *Applied and Environmental Microbiology*, **53(2)**, 224-229, (1987)

Cooper, D.G., Akit, J., Kosaric, N., Surface activity of the cells and extracellular lipids of *Corynebacterium fascians* CF15, *Journal of Fermentation Technology*, **60**, 19-24, (1982)

Cooper, D.G., Paddock, D.A., Production of a biosurfactant from *Torulopsis bombicola*, *Applied and Environmental Microbiology*, **47**, 173-176, (1984)

Cooper, D.G., Paddock, D.A., *Torulopsis bombicola* and surface activity, *Applied and Environmental Microbiology*, **46**, 1426-1429, (1983)

Cowell, C., Li-In-On, R., Vincent, B., Reversible flocculation of sterically-stabilised dispersions, *Journal of the Chemical Society: Faraday transactions I*, **74**, 337-347, (1978)

Craig, L., Pique, M.E., Tainer, J.A., Type IV pilus structure and bacterial pathogenicity, *Nature Reviews Microbiology*, **2(5)**, 363-378, (2004)

Davies, J.T., Rideal, E.K. *Interfacial Phenomena*, 2<sup>nd</sup> edition, Academic Press, New York, (1963)

Davis, H.T., Factors determining emulsion type: Hydrophile—lipophile balance and beyond, *Colloids and Surfaces A*, **91**, 9-24, (1994)

Desouky, S.M., Abdel-Daim, M.M., Sayyouh, M.H., Dahab, A.S., Modelling and laboratory investigation of microbial enhanced oil recovery, *Journal of Petroleum Science and Engineering*, **15**, 309-320, (1995)

Dobbie, J.W., Evans, R., Gibson, D.V., Smitham, J.B., Napper, D.H., Enhanced steric stabilization, *Journal of Colloid and Interface Science*, **45(3)**, 557-565, 1973

Doble, M., Kumar, A., (ed.), *Biotreatment of Industrial Effluents*, Elsevier, (2005)

Dodd, C.G., The rheological properties of films at crude petroleum-water interfaces, *The Journal of Physical Chemistry*, **64**, 544-550, (1960)

Dorobantu, L.S., Yeung, A., Foght, J.M., Gray, M.R., Stabilization of oil-water emulsion by hydrophobic bacteria, *Applied and Environmental Microbiology*, **70(10)**, 6333-6336, (2004)

Duguid, J.P., Old, D.C., In: *Bacterial Adherence*, Beachey, E.H., (Ed.), Chapman & Hall, London, 185-217, (1980)

Dworkin, M., Falkow, S., Rosenberg, E., Schleifer, K.H., Stackebrandt, E., (Eds. ), *The Prokaryotes*, Springer, New York, (2006)

Edwards, D.A., Wasan, D.T., Brenner, H., *Interfacial Transport Processes and Rheology*, Butterworth-Heinemann, Boston, MA, USA, (1991)

Ehrlich, R., Viscous coupling in two-phase flow in porous media and its effects on relative permeabilities, *Transport in Porous Media*, **11**, 201-218, (1993)

Eley, D.D., Hey, M.J., Lee, M.A., Rheological studies of asphaltene films adsorbed at the oil/water interface, *Colloids and Surfaces*, **24**, 173-182, (1987)

Enever, R.P., Correlation of phase inversion temperature with kinetics of globule coalescence for emulsions stabilized by a polyoxyethylene alkyl ether, *Journal of Pharmaceutical Science*, **65(4)**, 517-520, (1976)

Ese, M.H., Yang, X., Sjöblom, J., Film forming properties of asphaltenes and resins: A comparative Langmuir-Blodgett study of crude oils from North Sea, European continent and Venezuela, *Colloid and Polymer Science*, **276**, 800-809, (1998)

Evan, E., Skalak, R., *Mechanics and Thermodynamics of Biomembranes*, CRC, Boca Raton, (1980)

Evans, D.F., Wennerstrom, H., *The colloidal Domain: Where Physics, Chemistry, Biological and Technology Meet*, VCH, New York, 445, (1994)

Evans, E., Needham, D., Physical properties of surfactant bilayer membranes: thermal transitions, elasticity, rigidity, cohesion and colloidal interactions, *The Journal of Physical Chemistry*, **91(16)**, 4219-4228, (1987)

Evans, E.A., Skalak, R., *Mechanics and Thermodynamics of Biomembranes*, CRC Press, Boca Raton, (1980)

Fang, J., Joos, P., Lunkenheimer, K., Van Uffelen, M., Study of the modulus of elasticity by linear compression of an adsorbed layer, *Colloids and Surfaces A*, **97**, 271-278, (1995)

Finkle, P., Draper, H.D., Hildebrand, J.H., The theory of emulsification, *Journal of the American Chemical Society*, **45**, 2780-2788, (1923)

Finnerty, W.R., The biochemistry of microbial alkane oxidation: new insights and perspectives, *Trends in Biochemical Sciences*, **2**, 73-75, (1977)

Floodgate, G.G., The formation of oil emulsifying agents in hydrocarbonclastic bacteria, In: *Microbial Ecology*, Loutit, M.W., Miles, J.A.R. (Eds.), Springer-Verlag, Berlin, 82-85, (1978)

Foght, J.M. *Identification of the bacterial isolates comprising the environment Canada freshwater and cold marine standard inocula, using 16SrRNA gene sequencing and analysis*. Manuscript report EE-164, Environmental Protection Service, Environment Canada, Ottawa, ON, (1999)

Fordham, S., On the calculation of surface tension from measurements of pendant drops, *Proceedings of the Royal Society of London A*, **194**, 1-16, (1948)

Freer, E.M., Radke, C.J., Relaxation of asphaltenes at the toluene/water interface: diffusion exchange and surface rearrangement, *The Journal of Adhesion*, **80(6)**, 481-496, (2004)

Freer, E.M., Svitova, T., Radke, C.J., The role of interfacial rheology in reservoir mixed wettability, *Journal of Petroleum Science and Engineering*, **39(1-2)**, 137-158, (2003)

Freer, E.M., Wong, H., Radke, C.J., Oscillating drop/bubble tensiometry: effect of viscous forces on the measurement of interfacial tension, *Journal of Colloid and Interface Science*, **282 (1)**, 128-132, (2005)

Freer, E.M., Yim, K.S., Fuller, G.G., Radke, C.J., Shear and dilatational relaxation mechanisms of globular and flexible proteins at the hexadecane/water interface, *Langmuir*, **20 (23)**, 10159-10167, (2004)

Friberg, S., (Ed.), *Food Emulsions*, Marcel Dekker, New York, 1976

Gannon, J. T., Manilal, V. B., Alexander, M., Relationship between cell surface properties and transport of bacteria through soil, *Applied and Environmental Microbiology*, **57(1)**, 190-193, (1991)

Georgiou, G., Lin, S.C., Sharma, M.M., Surface-active compounds from microorganisms, *Biotechnology*, **10(1)**, 60-65, (1992)

Gibson, D.T. (Ed.), *Microbial Degradation of Organic Compounds*, Marcel Dekker, New York, (1984)

Giordano, R.M., Slattery, J.C., Effect of interfacial viscosities upon displacement in capillaries with special application to tertiary oil recovery, *AIChE Journal*, **29(3)**, 483-492, (1983)

Girault, H.H., Schiffrin, D.J., Smith, B.D.V., Drop image processing for surface and interfacial tension measurements, *Journal of Electroanalytical Chemistry*, **137(2)**, 207-217, (1982)

Gould, R.F., In: *Contact angle, Wettability and Adhesion*, Advances in chemistry series, American Chemical Society, Washington, **43**, (1964)

Graciaa, A., Lachaise, J., Marion, G., Schechter, R.S., A study of the required hydrophile-lipophile balance for emulsification, *Langmuir*, **5 (6)**, 1315-1318, (1989)

Gray. N.C.C., Steward, A.L., Cairns, W.L., Kosaric, N., Bacteria-induced de-emulsification of oil-in-water petroleum emulsions, *Biotechnology Letters*, **6**, 419-424, (1984)

Griffin, W.C., Classification of Surface-Active Agents by "HLB", *Journal of the Society of Cosmetic Chemists*, **1**, 311-318, (1949)

Guerra-Santos, L., Kappeli, O., Fiechter, A., *Pseudomonas aeruginosa* biosurfactant production in continuous culture with glucose as carbon source, *Applied and Environmental Microbiology*, **48(2)**, 301-305, (1984)

Gunde, R., Dawes, M., Hartland, S., Surface tension of wastewater samples measured by the drop volume method, *Environmental Science and Technology*, **26**, 1036-1040, (1992)

Gunning, W.T., Calomeni, E.P., A brief review of transmission electron microscopy and applications in pathology, *Journal of Histotechnology*, **23(3)**, 237-246, (2000)

Gutnick, D.L., Rosenberg, E., Oil tankers and pollution: a microbiological approach, *Annual Review of Microbiology*, **31**, 379-396, (1977)

Han, D.K., Yang, C.Z., Zhang, Z.Q., Lou, Z.H., Chang, Y.I., Recent development of enhanced oil recovery in China, *Journal of Petroleum Science and Engineering*, **22(1-3)**, 181-188, (1999)

Hancock, I., In: *Microbial Cell Surface Analysis: Structural and Physicochemical Methods*, Mozes, N., Handley, P.S., Busscher, H.J., Rouxhet, P.G., (Eds.), VCH Publishers, New York, 21-59, (1991)

Handley, P.S., Carter, P.L., Fielding, J., *Streptococcus salivarius* strains carry either fibrils or fimbriae on the cell surface, *Journal of Bacteriology*, **157(1)**, 64-72, (1984)

Handley, P.S., Carter, P.L., Wyatt, J.E., Hesketh, L.M., Surface structures (peritrichous fibrils and tufts of fibrils) found on *Streptococcus sanguis* strains may be related to their ability to coaggregate with other oral genera, *Infection and Immunity*, **47(1)**, 217-227, (1985)

Handley, P.S., In: *Microbial Cell Surface Analysis: Structural and Physicochemical Methods*, Mozes, N., Handley, P.S., Busscher, H.J., Rouxhet, P.G., (Eds.), VCH Publishers, New York, 63-86, (1991)

Harayama, S., Polycyclic aromatic hydrocarbon bioremediation design, *Current Opinion in Biotechnology*, **8**, 268–273, (1997)

Hassanien, I.A., Elaiw, A.M., Variable permeability effect on buoyancy-induced inclined boundary layer flow in a saturated porous medium with variable wall temperature, *Heat and Mass Transfer*, **43(12)**, 1241-1247, (2007)

Heller, W., Pugh, T.L., “Steric Protection” of Hydrophobic Colloidal Particles by Adsorption of Flexible Macromolecules, *The Journal of Chemical Physics*, **22(10)**, 1778, (1954)

Hesselink, F.Th., Density distribution of segments of a terminally adsorbed macromolecule, *The Journal of Physical Chemistry*, **73(10)**, 3488-3490, (1969); Theory of the stabilization of dispersions by adsorbed macromolecules. I. Statistics of the change of some configurational properties of adsorbed macromolecules on the approach of an impenetrable interface, **75(1)**, 65-71, (1971)

Hesselink, F.Th., Vrij, A., Overbeek, J.Th.G., Theory of the stabilization of dispersions by adsorbed macromolecules. II. Interaction between two flat particles, *The Journal of Physical Chemistry*, **75(14)**, 2094-2103, (1971)

Hiemenz, P.C., *Principles of Colloid and Surface Chemistry*, 2<sup>nd</sup> Ed., Marcel Dekker Inc., New York, (1986)

Holliger, C., Gaspard, S., Glod, G., Heijman, C., Schumacher, W., Schwarzenbach, R.P., Vazquez, F., Contaminated environments in the subsurface and bioremediation: organic contaminants, *FEMS Microbiology Reviews*, **20(3-4)**, 517-523, (1997)

Hommel, R.K., Formation and physiological role of biosurfactants produced by hydrocarbon-utilizing microorganisms, *Biodegradation*, **1**, 107-110, (1990)

Hunter, R.J., *Foundations of Colloid Science*, Volume 1. Clarendon Press, Oxford, (1986)

Hunter, R.J., *Foundations of Colloid Science*, Volume I and II, Oxford University Press, USA, (1995)

Hunter, R.J., *Zeta Potential in Colloidal Science*, Academic Press, New York, (1981)

Iguchi, T., Takeda, I., Ohsawa, H., Emulsifying factor of hydrocarbon produced by a hydrocarbon-assimilating yeast, *Agricultural and Biological Chemistry*, **33**, 1657-1658, (1969)

Illarionova, V.I., Shishkanova, N.V., Haferburg, D., Finogenova, T.V., Emulsifying activity of yeast grown on normal alkane, *Microbiology*, **53(3)**, 336-339, (1984)

Inoue, S., Ito, S., Sophorolipids from *Torulopsis bombicola* as microbial surfactants in alkane fermentations, *Biotechnology Letters*, **4**, 3-8, (1982)

Israelachvili, J., *Intermolecular & Surface Force*, 2<sup>nd</sup> Ed., Academic Press, London, (1992)

Israelachvili, J., The science and applications of emulsions — an overview, *Colloids and Surfaces A*, **91**, 1-8, (1994)

James, A.M., The electrical properties and topochemistry of bacterial cells, *Advances in Colloid and Interface Science*, **15(3)**, 171-221, (1982)

James, M., In: *Microbial Cell Surface Analysis: Structural and Physicochemical Methods*, Mozes, N., Handley, P.S., Busscher, H.J., Rouxhet, P.G., (Eds.), VCH Publishers, New York, 221-262, (1991)

Janshekar, H., in *Microbes and Oil Recovery*, (eds.) Zajic, J.E., Donaldson, E.C., Bioresource Publishers, El Paso TX, (1985) PennWell Books, Tulsa, Okla, (1983)

Jenneman, G.E., Knapp, R.M., McInerney, M.J., Meznie, D.E., Revus, D.E., Experimental studies of *in situ* microbial enhanced oil recovery, *Society of Petroleum Engineers Journal*, **24**, 33-37, (1984)

Jenneman, G.E., McInerney, M.J., Knapp, R.M., Clark, J.B., Feero, J.M., Revus, D.E., Menzie, D.E., A halotolerant, biosurfactant-producing *Bacillus* species potentially useful for enhanced oil recovery, *Developments in Industrial Microbiology*, **24**, 485-492, (1983)

Jezequel, R., Menot, L., Merlin, F-X, Prince, R.C., Natural cleanup of heavy fuel oil on rocks: an *in situ* experiment, *Marine Pollution Bulletin*, **46**, 983-990, (2003)

Johnson, M.J., Utilization of hydrocarbon by microorganisms, *Chemistry and Industry (London)*, **36**, 1532-1537, (1964)

Jones, T.J., Neustadter, E.L., Whittingham, K.P., Water-in-crude oil emulsion stability and emulsion destabilization by chemical demulsifiers, *The Journal of Canadian Petroleum Technology*, **17 (2)**, 100-108, (1978)

Kabalnov, A.S., Shchukin, E.D., Ostwald ripening theory: applications to fluorocarbon emulsion stability, *Advances in Colloid and Interface Science*, **38**, 69-97, (1992)

Kaplan, N., Rosenberg, E., Exopolysaccharides distribution of and bioemulsifier production by *Acinetobacter calcoeticus* BD4 and BD413, *Applied and Environmental Microbiology*, **44**, 1335-1341, (1982)

Khire, J.M., Kham, M.I., Microbially enhanced oil recovery (MEOR): Part 1. Importance and mechanism of MEOR, *Enzyme and Microbial Technology*, **16(2)**, 170-172, (1994); Microbially enhanced oil recovery (MEOR): Part 2. Micobes and the subsurface environment for MEOR, **16(3)**, 258-259, (1994)

Kim, S., Foght, J.M., Gray, M.R., Selective transport and accumulation of alkanes by *Rhodococcus erythropolis* S+14He, *Biotechnology and Bioengineering*, **80(6)**, 650-659, (2002)

Kimbler, O.K., Reed, R.L., Silberberg, I.H., Physical characteristics of natural films formed at crude oil-water interfaces, *Society of Petroleum Engineers Journal*, **6**, 153-165, (1966)

Ko, I., Kim, K.W., Lee, C.H., Lee, K.P., Effect of scale-up and seasonal variation on biokinetics in the enhanced Bioremediation of petroleum hydrocarbon-contaminated soil, *Biotechnology and Bioprocess Engineering*, **12(5)**, 531-541, (2007)

Koma, D., Hasumi, F., Yamamoto, E., Ohta, T., Chun, S-Y, Kubo, M., Biodegradation of long-chain n-paraffins from waste oil of car engine by *Acinetobacter* sp., *Journal of Bioscience and Bioengineering*, **91(1)**, 94-96, (2001)

Koronelli, T.V., Komarova, T.I., Denisov, Y.V., The chemical composition of *Pseudomonas aeruginosa* peptidoglycolipid and its role in the process of hydrocarbon assimilation, *Microbiology*, **52**, 767-769, (1983)

Kozlovsky, A., Metzger, Z., Eli, I., Cell surface hydrophobicity of *Actinobacillus actinomycetemcomitans* Y<sub>4</sub>, *Journal of Clinical Periodontology*, **14(6)**, 370-372, (1987)

Kwok, D.Y., Vollhardt, D., Miller, R., Li, D., Neumann, A.W., Axisymmetric drop shape analysis as a film balance, *Colloids and Surfaces A*, **88**, 51-58, (1994)

Lagaly, G., Reese, M., Abend, S., Smectites as colloidal stabilizers of emulsions. I. Preparation and properties of emulsions with smectites and non-ionic surfactants, *Applied Clay Science*, **14**, 83-103, (1999)

Langevin, D., Influence of interfacial rheology on foam and emulsion properties, *Advances in Colloid and Interface Science*, **88**, 209–222, (2000)

Langwaldt, J.H., Puhakka, J.A., On-site biological remediation of contaminated groundwater: a review, *Environmental Pollution*, **107(2)**, 187-197, (2000)

LaPlace, P.S., Sur l'action capopparie, Supplément au Dixième Livre du Traité Mécanique Céleste, Tome quatrième. Imprimeur-Libraire pour les Mathematiques, quai des Augustins, **71**, 1-65, (1805); LaPlace, P.S., On capillary attraction. Supplement to the Tenth Book of the Mécanique Céleste, **4** (Translated by N. Bowditch), Chelsea Publishing Company, Bronx, New York, 685-1018, (1966)

Lazar, I., Donaldson, E.C. (eds.), *Microbial Enhancement of Oil Recovery – Recent Advances, MEOR Field trials carried out over the world during the last 35 years*, Elsevier, (1991)

Leahy, J.G., Khalid, Z.M., Quintero, E.J., Jones-Meehan, J.M., Heidelberg, J.F., Batchelor, P.J., Colwell, R.R., The concentrations of hexadecane and inorganic nutrients modulate the production of extracellular membrane-bound vesicles, soluble protein, and bioemulsifier by *Acinetobacter venetianus* RAG-1 and *Acinetobacter* sp. strain HO1-N, *Canadian Journal of Microbiology*, **49**, 569–575, (2003)

Lee, S.K., Lee., S.B.V., Isolation and characterization of a thermo tolerant bacterium *Ralstonia* sp. strain PHS1 that degrades benzene, toluene, ethyl benzene, and o-xylene, *Applied Microbiology and Biotechnology*, **56**, 270–275, (2001)

Lee, W. K., Bani-Jaber, A., McGuire, J., Daeschel, M. A., Il-Hyun Jung, Interfacial tension kinetics of nisin and b-casein at an oil-water interface, *Korean Journal of Chemical Engineering*, **17(2)**, 179-183, (2000)

Lehnert, S., Tarabishi, H., Leuenberger, H., Investigation of thermal phase inversion in emulsions, *Colloids and Surfaces A*, **91**, 227-235, (1994)

Levine, S., Bowen, B.D., Partridge, S.J., Stabilization of emulsions by fine particles I. Partitioning of particles between continuous phase and oil/water interface, *Colloids and Surfaces*, **38**, 325-343, (1989)

Li, D., Lu, S., Liu, Y., Wang, D., The effect of biosurfactant on the interfacial tension and adsorption loss of surfactant in ASP flooding, *Colloids and Surfaces A*, **244**, 53-60, (2004)

Li, M., Xu, M., Ma, Y., Wu, Z., Christy, A.A., Interfacial film properties of asphaltenes and resins, *Fuel*, **81**, 1847-1853, (2002)

Lin, S.C., Biosurfactants: recent advances. *Journal of Chemical Technology & Biotechnology*, **66(2)**, 109-120, (1996)

Lin, S.Y., Hwang, H.F., Measurement of Low Interfacial Tension by Pendant Drop Digitization, *Langmuir*, **10(12)**, 4703-4709, (1994)

Liu, J., Gardel, M.L., Kroy, K., Frey, E., Hoffman, B.D., Crocker, J.C., Bausch, A.R., Weitz, D.A., Microrheology Probes length scale dependent rheology, *Physical Review Letters*, **96(11)**, #118104, (2006)

Loglio, G., Tesei, U., Cini, R., Surface compressional modulus of surfactant solutions – Time domain method of measurement, *Physical Chemistry Chemical Physics*, **81(11)**, 1154-1156, (1977)

Long, J., Osmond, D.W.J., Vincent, B., The equilibrium aspects of weak flocculation, *Journal of Colloid and Interface Science*, **42(3)**, 545-553, (1973)

Lucassen, J., Van den Tempel, M., Dynamic Measurements of Dilational Properties of a Liquid Interface, *Chemical Engineering Science*, **27(6)**, 1283-1291, (1972)

Madigan, M.T., Martinko, J.M. *Brock Biology of Microorganisms*, 11<sup>th</sup> edition, Pearson Prentice Hall, Upper Saddle River NJ, 143-144, (2006)

Madigan, M.T., Martinko, J.M., Parker, J., *Brock Biology of Microorganisms*, Prentice-Hall Inc., Upper Saddle River, NJ, (2000)

Mahinpey, N., Ambalae, A., Asghari, K., *In situ* combustion in enhanced oil recovery (EOR): A review, *Chemical Engineering Communications*, **194(8)**, 995-1021, (2007)

March, G.C., Napper, D.H., The thermodynamic limit to the flocculation stability of sterically stabilized emulsions, *Journal of Colloid and Interface Science*, **61(2)**, 383-387, (1977)

Masliyah, J.H., *Electrokinetic Transport Phenomena*, AOSTRA Technical Publication Series #12, Alberta Oil Sands Information Services, Calgary, (1994)

McInerney, M.J., Knapp, R.M., Chisholm, J.L., Bhupathiraju, V.K., Coates, J.D., Use of indigenous injected microorganisms for enhanced oil recovery, in *Microbial Biosystems: New Frontiers*, Proceedings of the 8<sup>th</sup> International Symposium on Microbial Ecology, Bell, C.R., Brylinsky, M., Johnson-Green, P. (ed.), Atlantic Canada Society for Microbial Ecology, Halifax, Canada, (1999)

Menon, V.B., Wasan, D.T. A review of the factors affecting the stability of solids-stabilized emulsions, *Separation Science and Technology*, **23(12)**, 2131-2142, (1988)

Meufeld, R.J., Zajic, J.E., Gerson, D.F., Cell surface measurements in hydrocarbon and carbohydrate fermentations, *Applied and Environmental Microbiology*, **39(3)**, 511-517, (1980)

Midmore, B.P., Preparation of a novel silica-stabilized oil/water emulsion, *Colloids and Surfaces A*, **132**, 257-265, (1998)

Midmore, B.R., Effect of aqueous phase composition on the properties of a silica-stabilized w/o emulsion, *Journal of Colloid and Interface Science*, **213**, 352-359, (1999)

Midmore, B.R., Preparation of a novel silica-stabilized oil/water emulsion. *Colloids and Surfaces A*, **132**, 257-265, (1998)

Miller, R., Wüstneck, R., Krägel, J., Kretschmar, G., Dilational and shear rheology of adsorption layers at liquid interfaces, *Colloids and Surfaces A*, **111**, 75-118, (1996)

Mills, M.A., Bonner, J.S., McDonald, T.J., Page, C.A., Autenrieth, R.L., Intrinsic bioremediation of a petroleum-impacted wetland, *Marine Pollution Bulletin*, **46**, 887–899, (2003)

Mitani Y., Meng X.Y., Kamagata Y., Tamura, T., Characterization of LtsA from *Rhodococcus erythropolis*, an enzyme with glutamine amidotransferase activity, *Journal of Bacteriology*, **187 (8)**, 2582–2591, (2005)

Mittal, K.L., Kumar, P., (Eds.), Emulsions, foams, and thin films, In: *Foam and Emulsion Stability: Interfacial Rheology and Thin Liquid Film Phenomena*, Marcel Dekker, NY, USA, 1-31, (2000)

Mohammed, R.A., Bailey, A.I., Luckham, P.F., Taylor, S.E., Dewatering of crude oil emulsions - 1. Rheological behaviour of the crude oil—water interface, *Colloids and Surfaces A*, **80(2-3)**, 223-235, (1993)

Mohammed, R.A., Bailey, A.I., Luckham, P.F., Taylor, S.E., The effect of demulsifiers on the interfacial rheology and emulsion stability of water-in-crude oil emulsions, *Colloids and Surfaces A*, **91**, 129-139, (1994)

Mollet, H., Grubenmann, A., (Eds.), *Formulation Technology - Emulsions, Suspensions, Solid Forms*, WILEY-VCH, Federal Republic of Germany, (2001)

Moran, K., Yeung, A., Czarnecki, J., Masliyah, J., Micron-scale tensiometry for studying density-matched and highly viscous fluids – with application to bitumen-in-water emulsions, *Colloids and Surfaces A*, **174**, 147-157, (2000)

Moran, K., Yeung, A., Masliyah, J., Measuring interfacial tensions of micrometer-sized droplets: A novel micromechanical technique technique, *Langmuir*, **15 (24)**, 8497-8504, (1999)

Morris, E.J., Ganeshkumar, N., Song, M., McBride, B.C., Identification and preliminary characterization of a *Streptococcus sanguis* fibrillar glycoprotein, *Journal of Bacteriology*, **169(1)**, 164-171, (1987)

Moses, V., Springham, D.G., *Bacteria and the Enhancement of Oil Recovery*, Applied Science Publishers, London, (1982)

Mozes, N., Rouxhet, P.G., Methods for measuring hydrophobicity of microorganisms, *Journal of Microbiological Methods*, **6(2)**, 99-112, (1987)

Mulligan, C., Cooper, D.G., Neufeld, R.J., Selection of microbes producing biosurfactants in media without hydrocarbons, *Journal of Fermentation Technology*, **62(4)**, 311-314, (1984)

Napper, D.H., Steric stabilization, *Journal of Colloidal and Interface Science*, **58(2)**, 390-407, (1977)

Nessbitt, W.E., Doyle, R.E., Taylor, K.G., Hydrophobic interactions and the adherence of *Streptococcus sanguis* to hydroxylapatite, *Infection and Immunity*, **38(2)**, 637-644, (1982)

Neufeld, R.J., Zajic, J.E., Gerson, D.F., Growth characteristics and cell partitioning of *Acinetobacter* on hydrocarbon substrates, *Journal of Fermentation Technology*, **61**, 315-321, (1983)

Neufeld, R.J., Zajic, J.E., The surface activity of *Acinetobacter venetianus* sp. 2CA2, *Biotechnology and Bioengineering*, **26(9)**, 1108-1113, (1984)

Neustadter, E.L., Whittingham, K.P., Graham, D.E., Interfacial Rheological Properties of Crude Oil/Water Systems, Shah, D.O., (Ed.), *Surface Phenomenon in Enhanced Oil Recovery*, Plenum Press, New York, NY, USA, 307-326, (1979)

Ottweill, R.H., in *Nonionic Surfactants*, Schick, M.J., (ed.), Marcel Dekker, New York, Chapter 19, (1967)

Panchal, C.J., Zajic, J.E., Isolation of emulsifying agents from a species of *Corynebacterium*, *Developments in Industrial Microbiology*, **19**, 569-576, (1978)

Pembrey, R.S., Marshall, K.C., Schneider, E.P., Cell surface analysis techniques: What do cell preparation protocols do to cell surface properties? *Applied and Environmental Microbiology*, **65(7)**, 2877-2894, (1999)

Perry, J.J., Microbial Metabolism of Cyclic Hydrocarbons and Related Compounds, *Critical Reviews in Microbiology*, **5**, 387-412, (1977)

Pickering, S.U., Emulsions, *Journal of the Chemical Society*, **91**, 2001-2021, (1907)

Pierce, B.E., Leboffe, M.J., *Exercises for the Microbiology Laboratory*, Morton Publishing Company, Colorado, USA, (1999)

Pines, O., Bayer, E.A., Gutnick, D.L., Localization of emulsan-like polymers associated with the cell surface of *Acinetobacter calcoaceticus*, *Journal of Bacteriology*, **154(2)**, 893-905, (1983)

Pines, O., Guthick., D., Role of emulsan in growth of *Acinetobacter Venetianus* RAG-1 on crude oil, *Applied and Environmental Microbiology*, **51(3)**, 661-663, (1986)

Pirnik, M.P., Microbial oxidation of methyl branched alkanes, *Critical Reviews in Microbiology*, **5**, 413-422, (1977)

Plateau, J., Recherche's Experimental et Theoriques sur les figures d'equilibre d'une masse liquide sans pesanteur, 8<sup>e</sup> Serie. "Annales de Chimie et de Physique, Quatrieme Serie", **17**, 260-276, (1869); Plateau, J., Experimental and Theoretical Researches into the Figures of Equilibrium of a Liquid Mass without Weight, Eight Series. Phil. Mag., Fourth Series, **38**, 445-455. (1869)

Premuzic, E.T., Lin, M.S., Interaction between thermophilic microorganisms and crude oils – recent developments, *Resources Conservation and Recycling*, **5(2-3)**, 277-284, (1991)

Raiders, R.A., Knapp, R.M., McInerney, M.J., Microbial selective plugging and enhanced oil recovery, *Journal of Industrial Microbiology*, **4(3)**, 215-230, (1989)

Ramamohan, T.R. and Slattery, J.C., Effects of surface viscoelasticity in the entrapment and displacement of residual oil, *Chemical Engineering Science*, **26**, 241-263, (1984)

Ramos, A.L.de, Redner, R.A., Cerro, R.L., Surface tension from pendant drop curvature, *Langmuir*, **9(12)**, 3691-3694, (1993)

Ramsden, W., Separation of Solids in the Surface-Layers of Solutions and 'Suspensions' (Observations on Surface-Membranes, Bubbles, Emulsions, and Mechanical Coagulation) -- Preliminary Account, *Proceedings of the Royal Society of London*, **72**, 156-164, (1903)

Rapp, P., Bock, H., Wray, V., Wagner, F., Formation, isolation and characterization of trehalose dimycolates from *Rhodococcus erythropolis* grown on n-alkanes, *Journal of General Microbiology*, **115**, 491-503, (1979)

Reddy, P.G., Singh, H.D., Pathak, M.G., Shagat, S.D., Baryah, J.N., Isolation and functional characterization of hydrocarbon emulsifying and solubilizing factors produced by a *Pseudomonas* species, *Biotechnology and Bioengineering*, **25(2)**, 387-401, (1983)

Reisberg, J., Doscher, T.M., Interfacial Phenomenon in Crude-Oil-Water Systems, *Producers Monthly*, **21(1)**, 43-50, (1956)

Reisfeld, A., Rosenberg, E., Gutnick, D., Microbial degradation of crude oil: factors affecting the dispersion in sea water by mixed and pure cultures, *Applied Microbiology*, **24**, 363-368, (1972)

Reynolds, P. J., Sharma, P., Jenneman, G. E., McInerney, M., J., Mechanism of microbial movement in subsurface materials, *Applied and Environmental Microbiology*, **55(9)**, 2208-2286, (1989)

Roe, R.J., Bachetta, V.L., Wong, P.M.G., Refinement of pendant drop method for the measurement of surface tension of viscous liquid, *The Journal of Physical Chemistry*, **71(13)**, 4190-4193, (1967)

Ron, E.Z., Rosenberg, E., Biosurfactants and oil bioremediation, *Current Opinion in Biotechnology*, **13**, 249-252, (2002)

Rosenberg, E., Exploiting microbial growth on hydrocarbons-new markets, *Trends in Biotechnology*, **11**, 419-424, (1993)

Rosenberg, E., Navon-Venezia, S., Ziber-Rosenberg, I., Ron, E.Z., Rate limiting steps in the microbial degradation of petroleum hydrocarbons, in: *Soil and Aquifer Pollution*, Rubin, H. (Ed.), Berlin-Heidelberg: Springer-Verlag, 159-172, (1998)

Rosenberg, E., Ron, E.Z., Surface-active polymers of *Acinetobacter*, In: *Biopolymers from Renewable Sources*, Kaplan, D. (Ed.), Springer-Verlag, Berlin, 281-291, (1998)

Rosenberg, M., Bacterial adherence to hydrocarbons: a useful technique for studying cell surface hydrophobicity, *FEMS Microbiology Letters*, **22(2)**, 289-295, (1984)

Rosenberg, M., Bayer, E.A., Delarea J., Rosenberg, E., Role of thin fimbriae in adherence and growth of *Acinetobacter calcoaceticus* RAG-1 on hexadecane, *Applied and Environmental Microbiology*, **44(4)**: 929-937, (1982)

Rosenberg, M., Doyle, R.J., (Eds.), Microbial cell surface hydrophobicity: history, measurement and significance, In: *Microbial Cell Surface Hydrophobicity*, 1-37, ASM, Washington, (1990)

Rosenberg, M., Gutnik, D., Rosenberg, E., Adherence of bacteria to hydrocarbons: a simple method for measuring cell-surface hydrophobicity, *FEMS Microbiology Letters*, **9**, 29-33, (1980)

Rosenberg, M., Rosenberg, E., Bacterial adherence at the hydrocarbon-water interface, *Oil and Petrochemical Pollution*, **2(3)**, 155-162, (1985)

Ross, S., Morrison, I.D., *Colloidal Systems and Interfaces*, John Wiley & Sons, New York, 1988

Rotenberg, Y., Boruvka, L., Neumann, A.W., Determination of surface tension and contact angle from the shapes of axisymmetric fluid interfaces, *Journal of Colloid and Interface Science*, **93**, 169-183, (1983)

Roy, P.K., Singh, H.D., Bhagat, S.D., Baruah, J.N., Characterization of hydrocarbon emulsification and solubilization occurring during the growth of *Endomycopsis lipolytica* on hydrocarbons, *Biotechnology and Bioengineering*, **21**, 955-974, (1979)

Russel, W.B., Saville, D.A. and Schowalter, W.R., *Colloidal Dispersions*, Cambridge University Press, Cambridge, (1989)

Rutter, P.P., Vincent, B., In: *Microbial Adhesion and Aggregation*, Marshall, K.C., (Ed.), Springer-Verlag, Berlin, 21-38, (1984)

Sadhukhan, S., Dutta, T., Tarafdar, S., A bidisperse ballistic deposition model for simulating porous media: the effect of grain size, composition and relaxation, *Journal of Statistical Mechanics – Theory and Experiment*, Art. No. **P06006**, (2007)

Sanders, S., Masliyah, J.H., *Characteristics and Demulsification of Solids-Stabilized Emulsion: A Literature Survey and Summary*, Report to OSLO Project Group, Department of Chemical Engineering, University of Alberta, (1990)

Sar, N., Rosenberg, E., Emulsifier production by *Acinetobacter calcoaceticus* strains, *Current Microbiology*, **9(6)**, 309-313, (1983)

Sarkar, A. K., Georgiou, G., Sharma, M. M., Transport of bacterial in porous media: I. An experimental investigation, *Biotechnology and Bioengineering*, **44**, 489-497, (1994)

Schmidt, F. G., Hinner, B., Sackmann, E., Microrheometry underestimates the values of the viscoelastic moduli in measurements on F-actin solutions compared to macrorheometry, *Physical Review E*, **61(5)**, 5646-5653, (2000)

Scriven, L.E., Dynamics of a fluid interface: equations of motion for Newtonian surface fluids, *Chemical Engineering Science*, **12**, 98-108, (1960)

Sen, R., Biotechnology in petroleum recovery: The microbial EOR, *Progress in Energy and Combustion Science*, **34**, 714– 724, (2008)

Sharma, V.P., Pandey, B.P., A review of the modern techniques applied in research and development of enhanced oil recovery. 1. Chemical processes, *Research and Industry*, **31(2)**, 115-123, (1986)

Shinoda, K, Saito, H., The stability of O/W type emulsions as a function of temperature and the HLB of emulsifiers: The emulsification by PIT-method, *Journal of Colloid and Interface Science*, **30**, 258-267, (1969)

Skinner, F.K., Rotenberg, Y., Newman, A.W., Contact angle measurements from the contact diameter of sessile drops by means of a modified axisymmetric drop shape analysis, *Journal of Colloid and Interface Science*, **130(1)**, 25-34, (1989)

Slattery, J.C., Interfacial effects in the entrapment and displacement of residual oil, *AIChE Journal*, **20(6)**, 1145-1154, (1974)

Slattery, J.C., *Interfacial Transport Phenomena*, Springer-Verlag, New York, (1990)

Smith, A.L., (Ed.), *Theory and Practice of Emulsion Technology*, Academic Press, New York, (1976)

Snellman, E.A., Sullivan, E.R., Colwell, R.R., Purification and properties of the extracellular lipase, LipA, of *Acinetobacter* sp. RAG-1, *European Journal of Biochemistry*, **269 (23)**, 5771–5779, (2002)

Spiecker, P.M., Kilpatrick, P.K., Interfacial rheology of petroleum asphaltenes at the oil-water interface, *Langmuir*, **20**, 4022-4032, (2004)

Stauffer, C.E., The Measurement of Surface Tension by the Pendant Drop Technique, *The Journal of Physical Chemistry*, **69(6)**, 1933-1938, (1965)

Stoddart, P.R., Brack, N., Physical techniques for cell surface probing and manipulation, In: *Nanoscale Structure and Properties of Microbial Cell Surfaces*, Ivanova, E.P., (Ed.), Nova Science Publishers, New York, 1-58, (2006)

Strassner, J.E., Effects of pH on Interfacial Films and Stability of Crude Oil-Water Emulsions, *Journal of Petroleum Technology*, **20**, 303-312, (1968)

Suci, P.A., Frølund, B., Quintero, E.J., Weiner, R.M., Geesey, G.G., Adhesive extracellular polymers of *Hyphomonas* MHS-3: interactions of polysaccharides and proteins, *Biofouling*, **9(2)**, 95-114, (1995)

Surzhko, L.F., Utilization of oil in soil and water by microbial cells, *Microbiology*, **64**, 330-334, (1995)

Susnar, S.S., Chen, P., del Rio, O.I., Neumann, A.A., Surface tension response to area changes using axisymmetric drop shape analysis, *Colloids and Surfaces A*, **116**, 181-194, (1996)

Susnar, S.S., Hamza, H.A., Neuman, A.W., Pressure dependence of interfacial tension of hydrocarbon-water systems using axisymmetric drop shape analysis, *Colloids and Surfaces A*, **89**, 169-180, (1993)

Sutherland, I.W., Biofilm exopolysaccharide: a strong and sticky framework, *Microbiology*, **147(1)**, 3-9, (2001)

Sztukowski, D.M., Yarranton, H.W., Rheology of asphaltene-toluene/water interfaces, *Langmuir*, **21**, 11651-11658, (2005)

Tadros, T.F. and Vincent, B., *Encyclopedia of Emulsion Technology*, Volume I, Marcel Dekker Inc., New York, (1983)

Tambe, D.E., Sharma, M.M., The effect of colloidal particles on fluid-fluid interfacial properties and emulsion stability. *Advances in Colloid and Interface Science*, **52**, 1-63, (1994)

van der Mei, H.C., Busscher, H.J., On the difference between water contact angles measured on partly dehydrated and on freeze-dried oral streptococci, *Journal of Colloid and Interface Science*, **136(1)**, 297-300, (1990)

van der Mei, H.C., Rosenberg, M., Busscher, H.J., In: *Microbial Cell Surface Analysis: Structural and Physicochemical Methods*, Mozes, N., Handley, P.S., Busscher, H.J., Rouxhet, P.G., (Eds.), VCH Publishers, New York, 263-287, (1991)

Van Hamme, J.D., Singh, A., Ward, O.P., Recent advances in petroleum microbiology, *Microbiology and Molecular Biology Reviews*, **67**, 503-549, (2003)

Van Hammer, J.D., Singh, A., Ward, O.P., Recent advances in petroleum microbiology, *Microbiology and Molecular Biology Reviews*, **67(4)**, 503-549, (2003)

Van Loosdrecht, M.C., Lyklema, J., Norde, W., Schraa, G., Zehnder, A.J., The role of bacterial cell wall hydrophobicity in adhesion, *Applied and Environmental Microbiology*, **53(8)**, 1893-1897, (1987); Electrophoretic mobility and hydrophobicity as a measured to predict the initial steps of bacterial adhesion, **53(8)**, 1898-1901, (1987)

Van Loosdrecht, M.C.M., Lykelma, J., Norde, W., Schraa, G., Zehnder, A.J.B., The role of bacterial cell wall hydrophobicity in adhesion, *Applied and Environmental Microbiology*, **53(8)**, 1893-1897, (1987)

Van Oss, C.J., Gillman, C.F., Phagocytosis as surface phenomenon. 1. Contact angle and phagocytosis of non-opsonized bacteria, *Journal of the Reticuloendothelial Society*, **12(3)**, 283-292, (1972)

Vanechoutte, M. Oil-degrading *Acinetobacter* strain RAG-1 and strains described as "*Acinetobacter venetianus* sp. nov." belong to the same genomic species, *Research in Microbiology*, **150**, 69-73, (1999)

Vincent, B., The effect of adsorbed polymers on dispersion stability, *Advances in Colloid and Interface Science*, **4(2-3)**, 193-277, (1974)

Wagner, F., Behrendt, U., Kretschmer, A., Lang, S., Syltatk, C., Production and chemical characterization of surfactants from *Rhodococcus erythropolis* and *Pseudomonas* sp. MUB on hydrocarbons, In: *Microbial Enhance Oil Recovery*, (Eds.) Zajic, J.E. and Donaldson, E.C., PennWell Books, Tulsa, Okla, 55-60, (1983)

Walstra, P., Principles of emulsion formation, *Chemical Engineering Science*, **48**, 333-349, (1993)

Ward, A.J.I., Regan, L.H., Pendant drop studies of adsorbed films of bovine serum albumin: I. Interfacial tensions at the isooctane/water interface, *Journal of Colloid and Interface Science*, **78(2)**, 389-394, (1980)

Watanabe, K., Microorganisms relevant to bioremediation, *Current Opinion in Biotechnology*, **12**, 237-241, (2001)

Weekamp, A.H., Jacobs, T., Cell Wall-Associated Protein Antigens of *Streptococcus salivarius*: Purification, Properties, and Function in Adherence, *Infection and Immunity*, **38(1)**, 233-242, (1982)

Wicken, A.J., In: *Bacterial Adhesion: Mechanisms and Physiological Significance*, Savage, D.C., Fletcher, M., (Eds.), Plenum Press, New York, 45-70, (1985)

Wilde, P.J., Interfaces: their role in foam and emulsion behaviour, *Current Opinion in Colloids and Interface Science*, **5**, 176-181, (2000)

Wu, X., Investigating the Stability Mechanism of Water-in-Diluted Bitumen Emulsions through Isolation and Characterization of the Stabilizing Materials at the Interface, *Energy fuels*, **17(1)**, 179-190, (2003)

Yan, N., Gray, M.R., Masliyah, J.H., On water-in-oil emulsions stabilized by fine solids, *Colloids and Surfaces A*, **193**, 97-107, (2001)

Yan, N., Masliyah, J.H., Characterisation and demulsification of solids-stabilized oil-in-water emulsions, Part 1-Partitioning of clay particles and preparation of emulsions. *Colloids and Surfaces A*, **96**, 229-242, (1995)

Yarranton., H.W., Sztukowski, D.M., Urrutia, P., Effect of interfacial rheology on the model emulsion coalescence, I. Interfacial rheology, *Journal of Colloid and Interface Science*, **310**, 246-252, (2007)

Yen, T.F., *Microbial enhanced oil recovery: principle and practice*, CRC Press, Boca Raton, FL, (1990)

Yeung, A., Dabros, T., Czarnecki, J., Masliyah, J., On the interfacial properties of micrometre-sized water droplets in crude oil, *Proceedings of the Royal Society of London A*, **455**, 3709-3723, (1999)

Yeung, A., Dabros, T., Masliyah, J., Czarnecki, J., Micropipette: a new technique in emulsion research, *Colloids and Surfaces A*, **174**, 169-181, (2000)

Yeung, A., Dabros, T., Masliyah, J., Does equilibrium interfacial tension depend on method of measurement? *Journal of Colloid and Interface Science*, **208(1)**, 241-247, (1998)

Yeung, A., Zhang, L.C., Shear effects in interfacial rheology and their implications on oscillating pendant drop experiments, *Langmuir*, **22 (2)**, 693-701, (2006)

Young, T., An essay on the cohesion of fluids, *Philosophical Transactions of the Royal Society of London*, **95**, 65-87, (1805)

Zajic, J.E., Supplisson, B., Emulsification and degradation of "Bunker C" fuel oil by microorganisms, *Biotechnology and Bioengineering*, **14**, 331-343, (1972)

Zhai, Z., Efrima, S., Chemical and physical aspects of macroemulsions stabilized by interfacial colloids, *The Journal of Physical Chemistry*, **100**, 11019-11028, (1996)

Zhang, L.Y., Xu, Z., Masliyah, J.H., Langmuir and Langmuir-Blodgett Films of Mixed Asphaltene and a Demulsifier, *Langmuir*, **19(23)**, 9730-9741, (2003)

Zosim, Z., Gutnick, D., Rosenberg, E., Properties of hydrocarbon-in-water emulsions stabilized by *Acinetobacter* RAG-1 emulsan, *Biotechnology and Bioengineering*, **24(2)**, 281-292, (1982)

## APPENDIX A GROWTH CURVE FOR BACTERIA STRAINS

**Figure A.1:** Growth curve for *Acinetobacter venetianus* RAG-1.

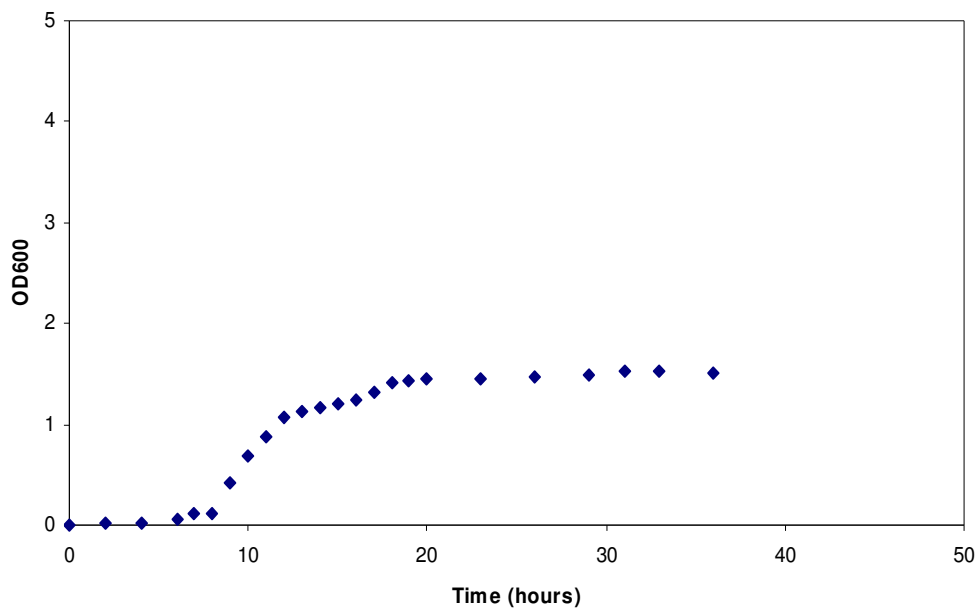
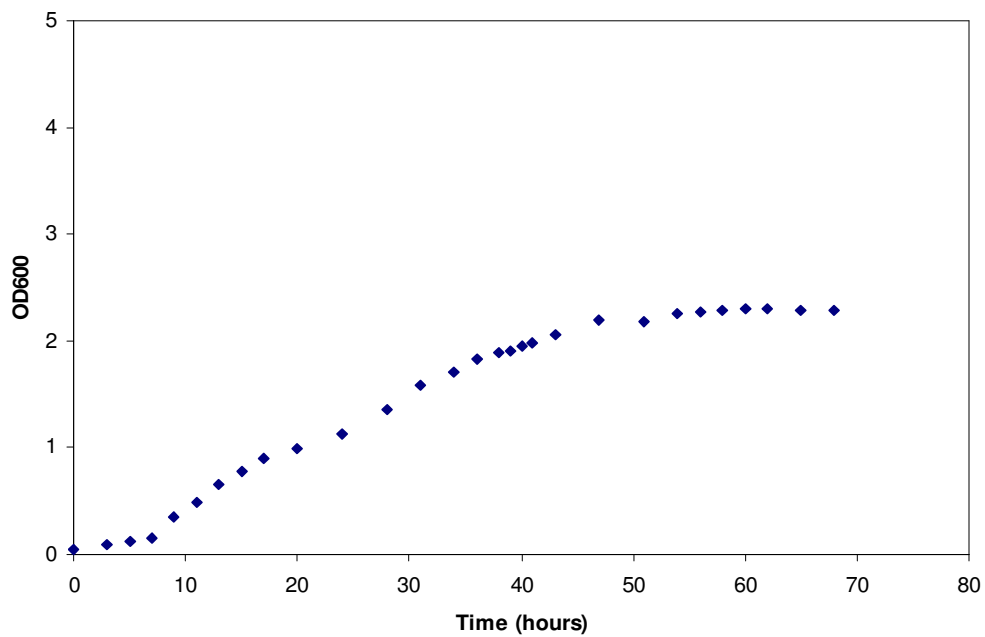


**Figure A.2:** Growth curve for *Rhodococcus erythropolis* 20SE1-c.



## APPENDIX B COLONY FORMATION UNIT VS. OD<sub>600</sub> FOR BACTERIA STRAINS

**Table B.1:** Colony formation unit (CFU/ml) versus OD<sub>600</sub> for *Acinetobacter venetianus* RAG-1.

OD <sub>600</sub>	CFU/ml
1.200	$2 \times 10^9$
0.850	$8 \times 10^8$
0.200	$2 \times 10^8$
0.050	$5 \times 10^7$
0.005	$5 \times 10^6$

**Table B.2:** Colony formation unit (CFU/ml) versus OD<sub>600</sub> for *Rhodococcus erythropolis* 20SE1-c.

OD <sub>600</sub>	CFU/ml
1.200	$10^9$
1.050	$9 \times 10^8$
0.650	$4 \times 10^8$
0.300	$10^8$
0.050	$2 \times 10^7$
0.005	$5 \times 10^6$

## APPENDIX C THEORETICAL EXPLANATION FOR THE REASON WHY BACTERIA CANNOT LOWER OIL/WATER IFT

We can roughly estimate of surfactant concentration at an interface as follows. We begin with the famous *Gibbs adsorption relation*, which states that a small change in the interfacial tension  $\gamma$  (N/m), due to the presence of surfactants at the interface, is

$$d\gamma = -\Gamma \cdot d\mu_{\text{surf}} . \quad (\text{C.1})$$

In eqn D.1,  $\Gamma$  (mol/m<sup>2</sup>) is the surface concentration of the adsorbed molecules, and  $\mu_{\text{surf}}$  (J/mol) is the “chemical potential” of the surfactants at the interface. In the bulk liquid, let the surfactants be at a concentration  $c$  (mol/m<sup>3</sup>) and have a chemical potential  $\mu_{\text{bulk}}$  (J/mol).

We now assume the surfactant solution is sufficiently dilute that it behaves more or less ideally (i.e., the dissolved molecules behave collectively as an “ideal gas”); the resulting bulk chemical potential is given by

$$\mu_{\text{bulk}} = \mu_0 + RT \ln c \quad (\text{C.2})$$

where  $\mu_0$  is some reference potential,  $R$  is the gas constant (8.314 J/mol·K), and  $T$  is the absolute temperature. At equilibrium, the chemical potentials in the bulk and at the interface must be equal, i.e.,

$$\mu_{\text{surf}} = \mu_{\text{bulk}} . \quad (\text{C.3})$$

Combining equations C.1–3, we get

$$\Gamma = -\frac{1}{RT} \frac{d\gamma}{d \ln c} . \quad (\text{C.4})$$

From eqn D.4, we conclude that the surface concentration of the adsorbed molecules is of order

$$\Gamma \sim \Delta\gamma/RT \quad (\text{C.5})$$

where  $\Delta\gamma$  is the change in interfacial tension due to a unit change in  $\ln c$  .

Assuming  $\Delta\gamma$  to be roughly 10 mN/m, we have, based on equation C.5, about  $10^{18}$  adsorbed molecules per  $\text{m}^2$ . This means every surfactant occupies roughly an area of  $1 \text{ nm}^2$  at the interface.

Bacteria, even when densely packed, cannot build up high enough surface densities (and hence chemical potentials) to significantly alter the interfacial tension.

Reduction of IFT is a colligative phenomenon. It can be argued from the Gibbs adsorption relation that, for the IFT to be lowered by any appreciable amount, there must be of order  $10^6$  adsorbed ‘entities’ on every  $\mu\text{m}^2$  of interfacial area. Colloidal particles are usually too large to satisfy such a requirement.

## APPENDIX D MATLAB CODE FOR DETERMINATION OF MICRON-SCALE SURFACE ELASTICITY AND IN SITU INTERFACIAL TENSION

```

*****
% Numerical solution of the relation between P and L in the micropipette
experiments
% The effect of surface elasticity on the pressure change in the pipette
*****

clc;

R0=3;                                     % R0/Rp=3,
assume Rp=1
K=0;                                       % elastic coefficient
gama=gama0+K[(A1+A2)/A0-1]                % assume gama0=1, K is how many times of
gama0

V0=4/3*pi*R0^3;                           % the initial volume of the oil drop
in water
A0=4*pi*R0^2;                             % the initial interfacial area of the oil drop
in water

L0=R0-sqrt(R0^2-1);                       % the initial value of the length in the
pipette
V20=0.05;                                 % the initial value of volume in the
pipette

h=optimset;h.Display='off';

% Define the "blank boxes" for the geometry of the oil drop and pressure change
during the suck process

RR1=[];
VV1=[];
AA1=[];
VV2=[];
RR2=[];
AA2=[];
tao11=[];
tao22=[];
PP=[];

```

```

% Conduct the following loop for each known length <Rp=1
% Get all the geometry of the oil drop and the pressure change in the pipette

for L=L0:0.05:1;

    f=inline(['r1.*(1-sqrt(1-1/(r1.^2)))-' num2str(L)],'r1');
    R1=abs(fsolve(f,L0,h));

    *****% Kown L, solve R1*****

    tao1=sqrt(1-1/(R1^2));
    % Get cos(thita1)
    V1=pi*R1^3/3*(1-sqrt(1-1/(R1^2)))^2*(2+sqrt(1-1/(R1^2)));
    % Get the volume in the pipette
    A1=2*pi*R1^2*(1-sqrt(1-1/(R1^2)));
    % Get the area in the pipette
    V2=V0-V1;

    ***** % From volume conservation, get the volume outside of the
    pipette*****

    f=inline(['pi*r2.^3/3*(1+sqrt(1-1/(r2.^2)))^2*(2-sqrt(1-1/(r2.^2)))-'
    num2str(V2)],'r2');
    R2=abs(fsolve(f,R0,h));
    % Known the volume, solve R2
    tao2=-sqrt(1-1/(R2^2));
    % Get cos(theta2)
    A2=2*pi*R2^2*(1+sqrt(1-1/(R2^2)));
    % Get the interfacial area outside of the pipette

    ***** % The geometry of the oil drop is totally known in the elongation
    process*****

    P=2*(1+K*((A1+A2)/A0-1))*(1/R1-1/R2);    % Get the pressure change in
    pipette

    *****% Save all the data for each step of L*****

    RR1=[RR1 R1];
    VV1=[VV1 V1];
    AA1=[AA1 A1];
    VV2=[VV2 V2];
    RR2=[RR2 R2];
    AA2=[AA2 A2];
    tao11=[tao11 tao1];
    tao22=[tao22 tao2];

```

```

PP=[PP P];

end
plot(L0:0.05:1,PP)
XLABEL('L/Rp');
YLABEL('deltaP*Rp/gama0')

for L=1.05:0.05:6

*****% For each known length > Rp=1(beyond hemisphere), get all the
geometry of the oil drop and the pressure change in the pipette *****

V2=V0+1/3*pi*pi*L;

f=inline(['pi*r2.^3/3*(1+sqrt(1-1/(r2.^2)))^2*(2-sqrt(1-1/(r2.^2)))-'
num2str(V2)],'r2');
R2=abs(fsolve(f,R0,h));

tao2=-sqrt(1-1/(R2^2));
A2=2*pi*R2^2*(1+sqrt(1-1/(R2^2)));

P=2*(1+K*((2*pi*L+A2)/A0-1))*(1-1/R2);

VV2=[VV2 V2];
tao22=[tao22 tao2];
RR2=[RR2 R2];
PP=[PP P];
end

*****% Output
data*****

RR1
VV1
AA1
tao11
VV2
AA2
RR2
tao22

*****% Output
figures*****

plot(0.05:0.05:1,RR1)
figure;

```

```
plot(0.05:0.05:1,RR2)
figure;
plot(0.05:0.05:1,VV1)
figure;
plot(0.05:0.05:1,VV2)
figure;
plot(0.05:0.05:1,tao11)
figure;
plot(0.05:0.05:1,tao22)
figure;
plot(L0:0.05:1,PP)
XLABEL('L/Rp');
YLABEL('deltaP*Rp/gama0')
```